

Alaska Park Science

National Park Service
U.S. Department of the Interior
Alaska Region



Understanding and Preparing for Alaska's Geohazards



Alaska Park Science

Volume 18, Issue 1
August 2019

Editorial Board:

Leigh Welling
Debora Cooper
Jim Lawler
Jennifer Pederson Weinberger

Guest Editor: Chad Hults

Managing Editor: Nina Chambers

Design: Nina Chambers

Contact *Alaska Park Science* at:
akr_alaska_park_science@nps.gov

Alaska Park Science is the semi-annual science journal of the National Park Service Alaska Region. Each issue highlights research and scholarship important to the stewardship of Alaska's parks.

Publication in *Alaska Park Science* does not signify that the contents reflect the views or policies of the National Park Service, nor does mention of trade names or commercial products constitute National Park Service endorsement or recommendation.

Cape Krusenstern
National Monument

Bering Land Bridge
National Preserve

Denali National
Park and Preserve

Lake Clark National
Park and Preserve

Katmai National
Park and Preserve

Aniakchak National
Monument and Preserve

Kenai Fjords
National Park

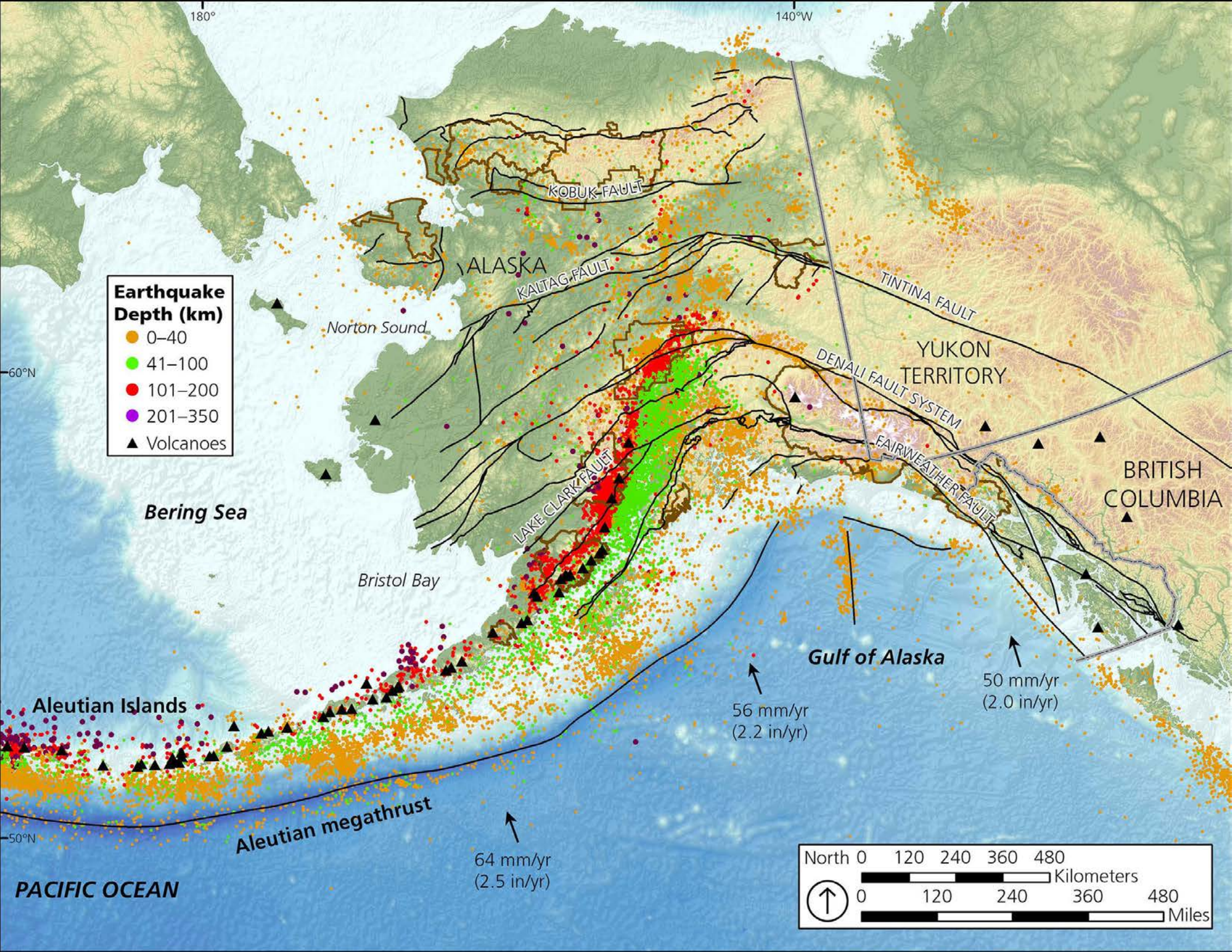
Yukon-Charley Rivers
National Preserve

Wrangell-St Elias National
Park and Preserve

Glacier Bay National
Park and Preserve

Table of Contents

Geohazards in Alaska's National Parks C. Hults, D. Capps, and E. Bilderback.....	1	Risk and Recreation in a Glacial Environment: Understanding Glacial Lake Outburst Floods at Bear Glacier in Kenai Fjords National Park D. Kurtz and G. Wolken.....	39	Spring Breakup on the Yukon: What Happens When the Ice Stops S. Lindsey	71
The 2015 Taan Fiord Landslide and Tsunami B. Higman, M. Geertsema, D. Shugar, P. Lynett, and A. Dufresne	7	Geohazard Risk Reduction along the Denali National Park Road D. Capps, D. A. Anderson, and M. McKinley ..	45	Coastal Dynamics in Bering Land Bridge National Preserve and Cape Krusenstern National Monument L. M. Farquharson, R. M. Buzard, D. H. Mann, and B. M. Jones	77
Catastrophic Glacier Collapse and Debris Flow at Flat Creek, Wrangell-St. Elias National Park and Preserve M. Jacquemart and M. Loso	17	Volcanic Hazards in Alaska's National Parks K. Mulliken, K. Wallace, C. Cameron, and C. Waythomas	53	Addressing Earthquake and Tsunami Hazards in Alaska Parks M. West, I. Dickson, and L. Gardine	85
An Initial Assessment of Areas Where Landslides Could Enter the West Arm of Glacier Bay, Alaska and Implications for Tsunami Hazards J. A. Coe, R. G. Schmitt, and E. K. Bessette-Kirton	27	Volcanic Ash Resuspension from the Katmai Region K. L. Wallace and H. F. Schwaiger.....	63		



Geohazards in Alaska's National Parks

Chad Hults, Denny Capps, and Eric Bilderback,
National Park Service

Geohazards are geologic processes that may pose a risk to people and our infrastructure. They include landslides, tsunamis, ice-dam floods, glacier calving, earthquakes, and volcanic eruptions—all of which occur in Alaska parks. In this issue of *Alaska Park Science*, we explore these geohazards: how they happen, where they could happen, and how we might mitigate their impacts.

Citation:

Hults, C., D. Capps, and E. Bilderback. 2019. Geohazards in Alaska's national parks. *Alaska Park Science* 18(1):1-5.

Alaska is the most geologically active part of North America. Active plate tectonics creates the high topographic relief and aggressive erosion by gravity, glaciers, rivers, and weathering creates unstable slopes. Southcentral Alaska overlies the subduction zone of the Pacific Plate where earthquakes are frequent and often high magnitude (Figure 1). Plate tectonics along with isostatic rebound result in rapidly uplifting mountains. For example, the Wrangell-St. Elias and Glacier Bay areas are uplifting at a rate of more than 0.75 inches (2 cm) a year (Larsen et al. 2004). *Geohazards* include earthquakes, landslides, rockfall, debris flows, glacier outburst floods, ice and snow avalanches, river erosion and deposition, and other hazards associated with geological processes. The active tectonics and extreme climatic processes combine to make geohazards common in Alaska.

Much of the mystique of Alaska is its essence of wilderness where the land is expected to be wild and unpredictable. The awe-inspiring landscape, harsh climate, and obvious forces of nature make it an exciting tourist destination. As such, geohazards are expected as a part of life, or even a badge of honor, for those who can overcome their challenges. With the expectation of Alaska being wild, it is often hard to justify diverting valuable resources to study a process that occurs infrequently. Furthermore, because Alaska's parks have so many types of geohazards, it can appear futile to attempt managing the potential risk.

It is often the case in the remote Alaska parks that geohazard events unfold without notice. For example, the massive Taan Inlet landslide and tsunami in Wrangell-St. Elias National Park and Preserve was not noticed until researchers detected it on seismometers and confirmed it by satellite imagery days later ([Higman and others, this issue](#)). No people were present, so no one was at risk. Only a remote airstrip was destroyed by the tsunami. Without exposure to a geohazard, there is no risk. However, events like this are occurring more frequently in Alaska parks, so it is important to recognize the nexus where infrastructure or people are exposed to geohazards.

In this issue of *Alaska Park Science*, the scientists that study geohazards present where they may occur, what we know about the processes influencing them, and what can be done to improve safety and resiliency. After reading these articles, a reader will better understand the state of the science for geologic and climatic processes that cause geohazards. Geohazards exist with or without resources, infrastructure, or people present. The hazard level is a function of the frequency of events and their magnitudes. Risk is a function of the probability of a geohazard, but also exposure levels, vulnerability, and resiliency. Although the exact timing of most geohazards is hard to determine, the areas at risk can be identified (mapped) and our vulnerabilities to these hazards can be assessed. Only with this

Figure 1. Map showing earthquake epicenters for earthquakes greater than magnitude 3.0 since 1889 (<http://www.aeic.alaska.edu>). Major faults (young and old) are shown as black lines, and active volcanoes are shown as black triangles. The Pacific Plate motion relative to the North American plate is shown with arrows.

knowledge can we manage our exposure and develop resilient systems to protect people and infrastructure from geohazards.

People are generally poor at assessing the risk of low-frequency events, even if they potentially pose catastrophic consequences. It is often the case that while hazards are recognized by geologists, the extent of a geohazard is understood only after catastrophic events. The National Park Service's (NPS) mission includes preserving naturally occurring geologic processes. The NPS also has a responsibility to protect people as well as park resources. The NPS policy states: "The U. S. Geological Survey and elsewhere, and with local, state, tribal, and federal disaster management officials, to devise effective geologic hazard identification and management strategies" (NPS 2006, Section 4.8.1.3). While the NPS is charged with unimpaired preservation of naturally occurring geologic processes and scenery, risk reduction is also a central management strategy. This *Alaska Park Science* issue was created to highlight the state of the knowledge about geohazards as a park management issue and to better inform decision makers and the public.

Geohazards in Alaska's Parks

Geohazards are present in every park in Alaska (Table 1). Some parks were formed due to geohazards; for example Aniakchak National Monument was created after the 1931 eruption of Aniakchak, and Katmai National Monument was created after the 1912 eruption of Novarupta ([Wallace and Schwaiger, this issue](#)). The NPS also manages the National Natural Landmarks program that includes landmarks formed by geohazards ([Mulliken and others, this issue](#)).

For each type of geohazard in Alaska, there are government agencies developed to study, evaluate, and warn the public about geohazards. For some

geohazards, there are robust monitoring systems in place that can provide early warning to help save lives. For example, the Alaska Volcano Observatory conducts studies to understand the eruptive histories and the potential hazards of active volcanoes. They have a monitoring system of seismometers, infrasound microphones, and satellite data that geophysicists use to detect eruptions and send notifications through a widely available warning system. In contrast, there are other geohazards, like landslide-generated tsunamis that are less understood and are not actively monitored.

Landslide-generated tsunamis have occurred in Alaska parks and some have killed people, but the areas with landslide potential have yet to be mapped, so the risk to visitor safety from landslide-generated tsunamis is largely unknown. Although massive landslide events are low frequency, the warming climate appears to be increasing the frequency of these events ([Capps and others, this issue](#); [Coe and others, this issue](#); [Higman and others, this issue](#); [Jacquemart and Loso, this issue](#)). Therefore, the known history of landslide events may not be useful for quantifying the frequency and magnitude of future events. Particularly for large landslides, the historic record in Alaska goes back less than a century. Also, places prone to landslide-generated tsunamis are in steep fjords that have only recently been deglaciated. For example, Icy Bay was completely glaciated in the 1950s, yet a significant landslide-generated tsunami occurred only a couple decades after the Taan Inlet glacier retreated. The potential for landslide-generated tsunamis in these areas is increasing because recent deglaciation is debutting slopes; thawing high-altitude permafrost is reducing the shear strength of the rocks; and precipitation in the form of rain, rather than snow, is increasing pore pressures in the soils. In addition to these geologic processes, visitation rates are increasing, which is

increasing exposure to risk. Mapping areas prone to landslides and landslide-generated tsunamis, and a quantification of the exposure, vulnerabilities, and resiliency, are necessary to reduce the risks to infrastructure and lives.

Denali National Park and Preserve provides a good example of how increasing landslide frequency has led to management actions to reduce risk. Denali has a long history of landslides impacting the park road and steps have been taken to address those hazards ([Capps and others, this issue](#)). Recently, the frequency of landslides appears to be increasing, possibly due to thawing permafrost. In response, Denali, together with the Federal Highways Administration, U. S. Geological Survey, numerous academic institutions, consultants, and others, developed an unstable slope management program for the park road. They have quantified and are tracking over 140 unstable slopes and are beginning to systematically improve safety and resiliency of the highest ranking sites.

Visitor and employee safety has precedence in NPS policy (NPS 2006). It is important that employees are trained so that they are empowered and prepared to provide safe access and effective disaster response. The NPS has a robust incident command system with people ready to respond, but also need plans for each geohazard type. These management plans would generally include:

- Identifying the geohazard (historic events or features).
- Mapping areas of potential geohazards.
- Understanding the processes that lead to the geohazard or its initiation.
- Quantifying the frequency and magnitude of a geohazard event.

Table 1. General exposure levels of Alaska parks to geohazards. These preliminary estimates are based on the likely presence of a significant magnitude and frequency of the geohazard events and the coincidence of the geohazards with park infrastructure and people.

Park	Landslide	Tsunami	Glacial Lake Outburst Flood	Volcano	Earthquake	River Breakup	River Erosion	Coastal Erosion
Sitka NHP	Moderate	High	No	Low	High	No	Moderate	Moderate
Glacier Bay NP&Pres	High	High	Moderate	No	High	No	Low	Low
Klondike Gold Rush NHP	High	Moderate	Moderate	No	Moderate	No	High	Low
Wrangell-St Elias NP&Pres	High	High	Moderate	High	High	Low	Moderate	Moderate
Kenai Fjords NP	High	High	High	Low	High	No	Moderate	Low
Aniakchak NM	Moderate	High	No	High	High	No	Moderate	Moderate
Katmai NP&Pres	Moderate	High	Low	High	High	No	Moderate	Moderate
Lake Clark NP&Pres	Moderate	Moderate	Low	High	Moderate	Low	Moderate	Moderate
Denali NP&Pres	High	No	Low	Low	High	Low	Moderate	No
Yukon-Charley Rivers NPres	Moderate	No	No	No	Low	High	High	No
Gates of the Arctic NP&Pres	Moderate	No	No	No	Low	Low	Moderate	No
Noatak NPres	Moderate	No	No	No	Low	Low	Moderate	No
Kobuk Valley NP	Low	No	No	No	Low	Low	High	No
Cape Krusenstern NM	Low	Low	No	No	Low	Low	Low	High
Bering Land Bridge NPres	Low	Low	No	No	Low	Low	Moderate	High

NHP=National Historical Park; NM=National Monument; NP=National Park; NP&Pres=National Park and Preserve; NPres=National Preserve

- Developing monitoring/detecting tools.
- Conducting a vulnerability assessment of the threatened infrastructure or people.
- Creating plans for avoiding and responding to geohazards.
- Educating employees and visitors of the geohazards in the parks.

Only through knowledge of potential geohazards are we able to reduce their risks. Newly accessible technologies like interferometric synthetic aperture radar (InSAR), light detection and ranging (LiDAR), structure from motion, and repeat high-resolution satellite imagery make identifying and mapping areas prone to geohazards easier, and makes monitoring geohazards more cost-effective. With accessible technologies, the areas prone to geohazards are identifiable and monitorable (for example, see [Kurtz and Wolken, this issue](#)).

Alaska's active tectonics and warming climate are not slowing down. Processes like volcanic eruptions ([Mulliken and others, this issue](#)) or earthquakes ([West and others, this issue](#)) are deep-Earth processes that are not influenced by humans; however, climate change is increasing the frequency of landslides ([Capps and others, this issue](#); [Coe and others, this issue](#); [Higman and others, this issue](#)), storms hitting the Arctic coast ([Farquharson and others, this issue](#)), and changing the timing and dynamics of river breakup ([Lindsey, this issue](#)).

Government Agencies Monitoring, Studying, and Warning about Geohazards

National Park Service, Geohazards
(Geologic Resources Division)

<https://www.nps.gov/subjects/geohazards/index.htm>

EARTHQUAKES

Alaska Earthquake Center

<https://earthquake.alaska.edu/>

The Alaska Earthquake Center is dedicated to reducing the impacts of earthquakes, tsunamis and volcanic eruptions in Alaska. We provide definitive earthquake information to the public, emergency managers, scientists and engineers.

Alaska Seismic Hazards Safety Commission

<http://seismic.alaska.gov>

People and references to connect with Alaska-specific resources.

U.S. Geological Survey seismic hazard map

<https://earthquake.usgs.gov/hazards/hazmaps>

The seismic hazard map estimates the probability of strong ground shaking and underpins most building codes. Though currently lagging behind the lower 48, the 2007 effort is slated for update in the next few years.

Federal Emergency Management Agency earthquake resources

<https://www.fema.gov/earthquake>

Starting point for developing risk mitigation plans, rapid visual screening, and grant opportunities.

TSUNAMIS

National Oceanic and Atmospheric Administration, National Weather Service, Pacific Tsunami Warning Center

<https://ptwc.weather.gov/>

The Pacific Tsunami Warning Center provides warnings for Pacific basin teletsunamis (tsunamis that can cause damage far away from their source) to almost every country around the Pacific rim and to most of the Pacific island states.

Alaska tsunami hazard maps and publications

<http://dggs.alaska.gov/pubs/keyword/tsunami>

Published as a joint effort between several state and federal entities, these products details potential tsunami hazards in most coastal Alaska communities—though notably most of the parks are not included.

VOLCANOES

U.S. Geological Survey, University of Alaska Fairbanks Alaska Volcano Observatory

<https://avo.alaska.edu/>

AVO objectives: (1) To conduct monitoring and other scientific investigations in order to assess the nature, timing, and likelihood of volcanic activity;(2) To assess volcanic hazards associated with anticipated activity, including kinds of events, their effects, and areas at risk; and (3) To provide timely and accurate information on volcanic hazards, and warnings of impending dangerous activity, to local, state, and federal officials and the public.

U.S. Geological Survey Volcano Hazards Program

<https://volcanoes.usgs.gov/index.html>

Volcanic Activity Notification (VAN) System

<https://volcanoes.usgs.gov/vns2/>

LANDSLIDES

U.S. Geological Survey Landslide Hazard Program

<https://www.usgs.gov/natural-hazards/landslide-hazards>

The primary objective of the National Landslide Hazards Program is to reduce long-term losses from landslide hazards by improving our understanding of the causes of ground failure and suggesting mitigation strategies.

Denali National Park and Preserve Landslides

<https://www.nps.gov/dena/learn/nature/landslides.htm>

RIVER BREAKUP

National Oceanic and Atmospheric Administration River Watch

<https://www.weather.gov/aprfc/riverwatchprogram>

Alaska-Pacific River Forecast Center (APRFC), it is time to coordinate a launch of a Riverwatch team with the State of Alaska DHS&EM. Riverwatch is a collaborative program between DHS&EM and the National Weather Service (NWS). National Weather Service (NWS) is responsible for monitoring ice breakup conditions throughout Alaska to assess flood threats and navigational hazards.

DISASTER RESPONSE

Division of Homeland Security and Emergency Management

<https://www.ready.alaska.gov/>

The mission of the Division of Homeland Security and Emergency Management is to lead the way in homeland security and emergency management to foster a prepared, resilient Alaska capable of meeting the needs of its communities and citizens in response to all-hazards events.

Geohazards themselves may not be manageable, but with increased knowledge and commitment, many of the risks to infrastructure, resources, and human safety are. Although every park in Alaska contains some type of geohazard, they don't occur everywhere. Where the nexus of geohazards and exposure exist, the NPS, together with other federal agencies and partners, has a role in gathering necessary data and communicating what we know to employees and the public. The articles in this issue of *Alaska Park Science* highlight some spectacular events that occurred in Alaska parks, describe the processes leading up to those events and discuss what we can do to reduce the risks associated with geohazards.

REFERENCES

- Larsen, C. F., R. J. Motyka, J. T. Freymueller, K. A. Echelmeyer, and E. R. Ivins. 2004. Rapid uplift of southern Alaska caused by recent ice loss. *Geophysical Journal International* 158: 1118–1133. doi:10.1111/j.1365-246X.2004.02356.x.
- National Park Service (NPS). 2006. Management Policies 2006: A guide to managing the National Park System. U.S. Department of the Interior, 168 p. Available at: <https://www.nps.gov/policy/mp/policies.html> (accessed June 20, 2019)



The 2015 Taan Fiord Landslide and Tsunami

Bretwood Higman, Ground Truth Trekking

Marten Geertsema, University of Northern British Columbia

Dan Shugar, University of Calgary

Patrick Lynett, University of Southern California

Anja Dufresne, Rheinisch-Westfälische Technische Hochschule Aachen University, Germany

On October 17, 2015, 180 million tons of rock slid into Taan Fiord generating a tsunami that stripped forest from 8 square miles and reached as high as 633 feet above the fjord, the fourth-highest tsunami ever recorded. Luckily, no one was near enough to be harmed. Cracking and shifting of the mountain for decades before the landslide could have provided warning, and similar conditions exist elsewhere in Alaska parks.

Citation:

Higman, B., M. Geertsema, D. Shugar, P. Lynett, and A. Dufresne. 2019. The 2015 Taan Fiord landslide and tsunami. *Alaska Park Science* 18(1): 6-15.

On October 17, 2015, 180 million tons of rock slid into Taan Fiord, an arm of Icy Bay, generating a tsunami that stripped forest from 8 square miles (20 square km) of Wrangell St.-Elias National Park and Preserve and reached as high as 633 feet (193 m) above the fjord, the fourth-highest tsunami ever recorded. It had almost no human impacts—nobody was near enough to be harmed, and the only damage to infrastructure was rocks scattered on a beach used for landing bush planes—good fortune that may not characterize similar events in the future.

Alaska parks are prone to events like this. Land-slides that generate large tsunamis most often happen in landscapes with retreating glaciers. In the last century, 10 of the 14 highest tsunamis in the world were in glaciated mountains and four were in Alaska parks, which include vast tracts of glaciated terrain (Table 1). Though landslides like this can happen at any time, these events are becoming more frequent—driven by climate change-induced glacial retreat and permafrost thaw. The Taan Fiord tsunami can help us understand subaerial landslide tsunami hazards and prepare for potential impacts.

Tsunamis from Landslides

Tsunamis are water waves generated by a sudden force (Bourgeois 2009), typically through either rapid displacement of the seafloor (during earthquakes or from submarine landslides), or through displacement and impact (by mountain landslides entering water, glacial ice collapses, or meteorite impacts).

Depending on the geometry, size, and speed of this force, the nature of the resulting tsunami wave can vary dramatically. Tsunamis caused by earthquakes are typically long-period waves, meaning they rise and fall gradually. They can impact areas as large as entire ocean basins, but with shorter runups (they run up from the coast to lower elevations), as happened with the Indian Ocean tsunami in 2004, and the Tohoku, Japan tsunami in 2011. These long-period tsunamis usually take up to a half-hour to inundate elevations less than twenty meters above the water. In contrast, tsunamis generated by subaerial landslides (as well as ice-calving and meteor impacts) are often much shorter-period, flooding the land more rapidly, and affect a smaller area. They crash ashore more like a wind wave, rising to their peak elevations within a few minutes at most. These tsunamis may reach several hundred meters above the water, but affect a much smaller area than their long-period cousins. Tsunamis generated by subaerial landslides are often confined to a few tens of kilometers around the landslide, both because shorter-period waves disperse energy more quickly and because they commonly are triggered in relatively confined bays and lakes.

Most of the research on tsunami impacts has focused on longer-period regional tsunamis—especially subduction zone earthquake tsunamis that produce some of the longest period waves. However, due to the differences outlined above, it is unclear how much of this work can be directly applied to tsunamis from subaerial landslides. The need

A geologist stands in front of a 16-foot (nearly 5 m) diameter boulder moved by the tsunami near where it reached its highest elevation (633 feet [193 m]). Photo courtesy of Ground Truth Trekking

Table 1. Tsunamis with runup of 50 m or greater in the past century. Ten out of 14 tsunamis (shaded) resulted from mountain landslides into fjords or lakes in glaciated terrain. Other cases have diverse causes: volcanic eruption (1980), landslide into artificial reservoir (1963), submarine delta failure (1964), and earthquake displacement (2004). (Table from Higman et al. 2018, originally modified from NGDC/WDS 2017.)

Year	Location	Water Body	Cause	Latitude	Longitude	Max Runup (m)
1958	Lituya Bay, Alaska, USA	Fjord	Subaerial landslide	58.672	-137.526	524
1980	Spirit Lake, Washington, USA	Lake	Volcanic landslide	46.273	-122.135	250
1963	Casso, Italy	Reservoir	Subaerial landslide	46.272	12.331	235
2015	Taan Fiord, Alaska, USA	Fjord	Subaerial landslide	60.2	-141.1	193
1936	Lituya Bay, Alaska, USA	Fjord	Subaerial landslide	58.64	-137.57	149
2017	Nuugaatsiaq, Greenland	Fjord	Subaerial landslide	71.8	-52.5	90
1936	Nesodden, Norway	Fjord	Subaerial landslide	61.87	6.851	74
1964	Cliff Mine, Alaska, USA	Fjord	Delta-front failure	61.125	-146.5	67
1934	Tafjord, Norway	Fjord	Subaerial landslide	62.27	7.39	62
1965	Lago Cabrera, Chile	Lake	Subaerial landslide	-41.8666	-72.4635	60
1967	Grewingk Lake, Alaska, USA	Lake	Subaerial landslide	59.6	-151.1	60
1946	Mt. Colonel Foster, British Columbia, Canada	Lake	Subaerial landslide	49.758	-125.85	51
2004	Labuhan, Indonesia	Open coast	Earthquake displacement	5.429	95.234	51
2000	Paatuut, Greenland	Fjord	Subaerial landslide	70.25	-52.75	50

to understand short-period landslide generated tsunamis was a major motivation for our study of the Taan Fiord event.

In Alaska, four giant tsunamis have been triggered by subaerial landslides in the past century: in Lituya Bay in 1938 and 1958 (Miller 1960); in Grewingk Lake in 1967 (Wiles and Calkin 1992); and in Taan Fiord in 2015 (Higman et al. 2018). Numerous landslides and

at least two smaller landslide tsunamis have occurred in Alaska recent years (e.g., Geertsema 2012, Coe et al. 2018, Gullufsen 2018).

Climate warming is likely driving an increase in the frequency of large landslides and promoting the growth of deep bodies of water where large tsunamis can form. Glaciers simultaneously erode the base of mountain slopes, impose stresses, and induce

fracturing, all of which increase the likelihood of slope failure. At the same time, glaciers fill the valley, preventing failure of lower slopes and supporting higher slopes to reduce the chance of slope collapse. When they retreat, whether due to changing climate or to regular glacial cycles, they remove that support, allowing slopes to sag and fractures to expand, making them vulnerable to failure. Furthermore, at higher elevations and in arctic and subarctic climates, permafrost is a significant contributor to the strength of some mountains, and thawing, or even warming of still-frozen permafrost, can greatly weaken those mountains. These factors are likely driving an increase in the frequency of large landslides. Additionally, glacial retreat is exposing new bodies of water that may be vulnerable to tsunamis. The events at Grewingk Lake, Taan Fiord, and a 2016 landslide tsunami in Cowee Creek near Juneau all occurred in bodies of water that didn't exist (because their basins were filled with ice) only a few decades before.

The Taan Fiord Landslide Tsunami

The Taan Fiord tsunami was preceded by a century of rapid glacial retreat (Koppes and Hallet 2006), decades of ground cracking and creep (Meigs et al. 2006), a month of above-average rain, and a few seconds of mild shaking from a distant earthquake (Higman et al. 2018). After crossing the toe of Tyndall Glacier and entering the water, it generated a violent wave that flattened about eight square miles (20 km²) of forest in Wrangell-St. Elias National Park and Preserve and adjacent private lands (Figure 1).

No one observed the slide or tsunami directly, but automatic seismic systems identified it within hours (using methods from Ekström and Stark 2013). Inversion of long-period waves arriving at nearby seismometers identified the general area and direction of the landslide. Days later, high-resolution satellite imagery revealed the landslide and tsunami

impacts, and tide gage data from more than 90 miles (~150 km) away at Yakutat showed small fluctuations in water level (4 inches or ~0.1 m) resulting from the tsunami. Months later, teams of scientists visited the site to document both the landslide and tsunami.

The landslide began as a rotational slide, likely following planes of weakness established decades earlier when failure initiated shortly after glacial retreat. Signs of active displacement are clearly visible in remote-sensed data extending back to the mid-1990s. A decade before catastrophic failure in 2015, Meigs and others (2006) noted ground-cracking and deformation, and aerial topographic surveys documented tens of meters of gradual motion (Higman et al. 2018).

After the failure in 2015, a portion of the slide block remained on the slope, still covered by jumbled, but still largely upright alder forest (Dufresne et al. 2018). However, most of the slide mass sped across the shoreline and terminus of Tyndall Glacier and entered Taan Fiord. Multibeam sonar and sub-bottom profiling show blocky deposits capped by more homogenous layered deposits filling the fjord bottom (Haeussler et al. 2018). A small portion of the landslide traveled across the fjord bottom and slid back up above the waterline on the far side of the fjord, forming 30-70 feet-high (10-20 m) debris hillocks. Several alluvial fans collapsed into deeper water as the slide moved along their fronts on its way down the fjord. These collapsed fans left no clear deposit—presumably because they were incorporated into the moving submarine slide mass.

The impact of the slide with the water generated one of the tallest tsunami waves in historical times. At one location, the wave reached 633 feet (193 m) above sea level. As it moved down the fjord, the wave stripped vegetation to varying heights that gradually diminished down-fjord. At the mouth of the fjord, 10

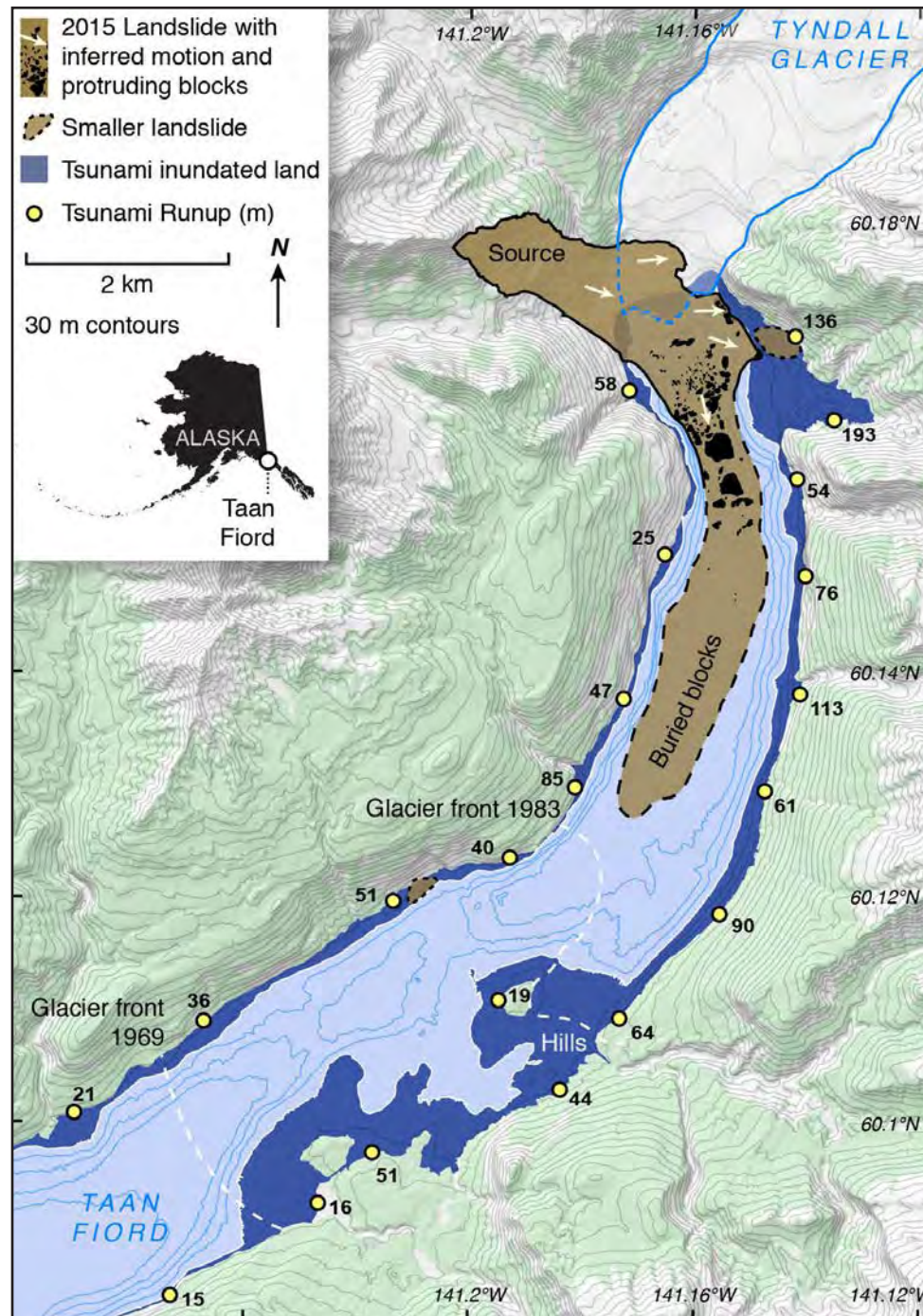


Figure 1. Taan Fiord landslide and tsunami. (Modified from Higman et al. 2018.)

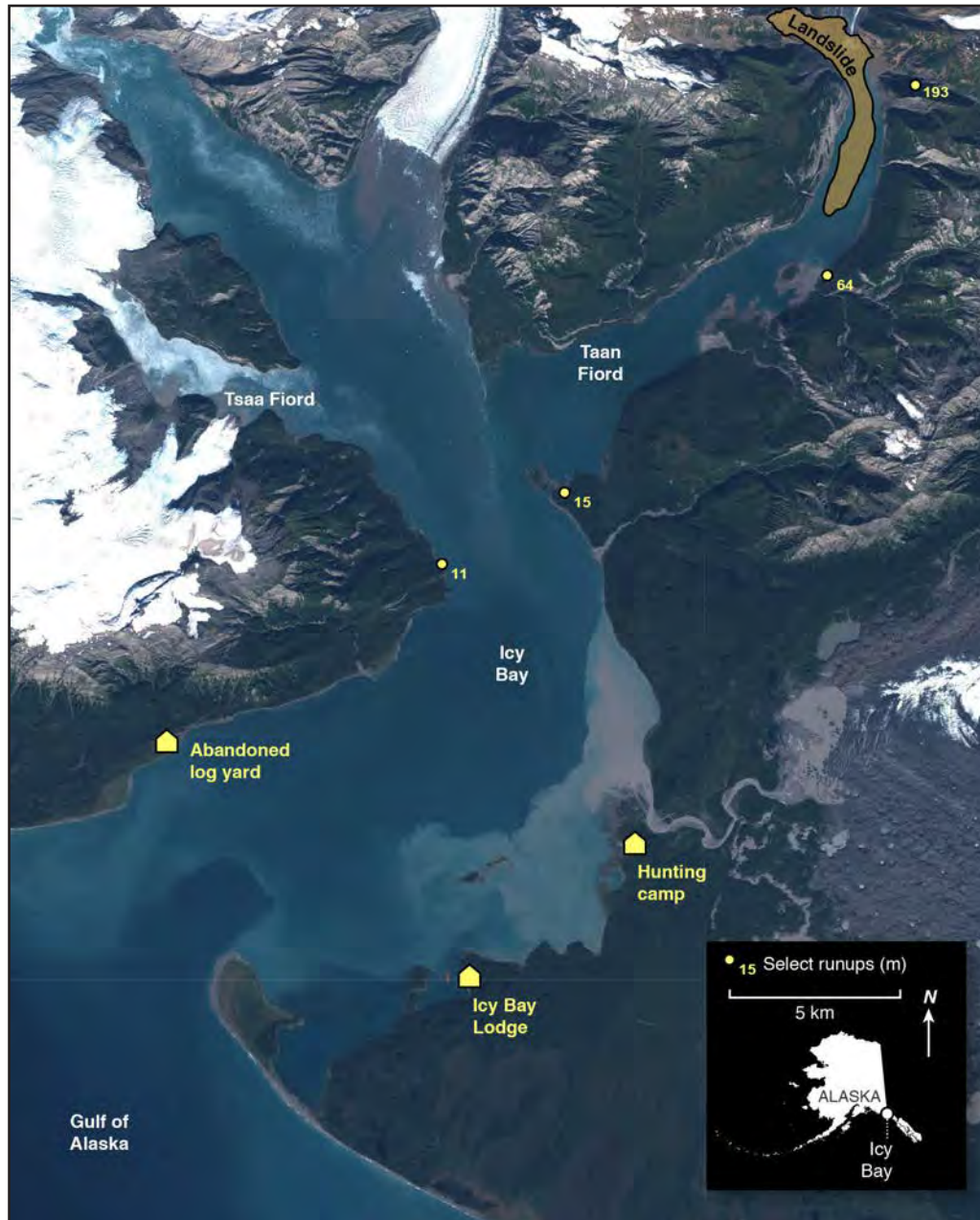


Figure 2. Icy Bay, Alaska. The landslide and tsunami occurred within Taan Fiord, and fortunately didn't impact any structures. The tsunami did have some impact outside the fjord, but did not reach coastal habitations. Yellow dots show how high the tsunami reached above water level (runup) in meters. Base-image: Sentinel 2, from 10 September 2018.

miles (16 km) from the landslide, the wave reached 50 feet (15 m), and dragged icebergs through moraine hills. Two-and-one-half-miles (4 km) farther, on a section of the west coast of Icy Bay that faces directly toward the mouth of Taan Fiord, the wave reached 36 feet (11 m) and toppled trees, but quickly diminished to below high tide as it spread out along the coast (Figure 2). The faint echo of the tsunami reached tide gages 80 and 250 miles (130 and 400 km) away where they recorded 40-minute-long oscillations of several inches in water level.

Potential for Future Disaster in Icy Bay

The Taan Fiord event provides warning that Icy Bay may see similar, potentially more deadly events in the future. Lituya Bay produced at least five giant tsunamis over the course of three centuries (Miller 1960) and Icy Bay could well rack up a similar record.

A century ago, Icy Bay was filled with glaciers (Russel 1893). It wasn't until the 1960s that four steep-walled fjords began to open at the head of the bay. The 2015 tsunami was the largest to occur in this narrow window of time, but it likely wasn't the only tsunami. At least two sites (see Figure 1) along the fjord have fresh landslide deposits extending into the ocean, and a ridge opposite the 2015 slide is laced with fissures that may produce future failures. Other fjords at the head of Icy Bay have steep slopes that haven't yet been surveyed for potential landslide hazards.

Adventure kayakers, trophy bear hunters, commercial and sport fishers, and even cruise ships visit Icy Bay (Figure 2). Though logging along its shore has ended, plans for a large-scale mine are being explored, potentially creating another vulnerable facility. When the tsunami occurred in October 2015, workers were present in Icy Bay Lodge just 20 miles (32 km) away, fortunately beyond damaging waves. However, many similar situations might have had

greater impact: A landslide might occur at a busy time of year; a small landslide or tsunami might impact a beach campsite; or a large landslide might occur in one of the other fjord arms of Icy Bay. Due to the geometry of the bay, a tsunami in a different arm would more directly impact the outer part of Icy Bay, where there is more human activity.

How an Event like the 2015 Landslide and Tsunami Might Play Out Elsewhere

Landslide Impacts

In addition to the complete destruction in the path of the slide, the 2015 Taan Fiord landslide reshaped the fjord bottom and far shoreline. The slide caused tens of meters of shallowing in some areas, while it eroded sections of the pre-landslide shoreline. Changes like this can render existing nautical charts unreliable and might mean that they need to be updated with new bathymetric surveys before large ships can return to waters impacted by similarly large landslides.

Tsunami Hazards to Vessels

The most dramatic hazard posed to vessels is the breaking tsunami wave in areas where the tsunami height is significant in comparison to the depth of the water. Runup of nearly 650 feet (200 m) shows that the Taan Fiord tsunami was likely about 300 feet (100 m) in height, and complex variability in the peak runup shows the wave had a very short period. A wave of such extreme amplitude and short wavelength would be likely to break even at fjord depths of hundreds of feet. Like all tsunami waves, it would also be prone to breaking in shallow water.

Even where the wave is not breaking, tsunamis can generate strong currents. In Taan Fiord, currents swept across shallow areas and low hills, sometimes carrying icebergs that left gouges in the soil surface (Figure 3), or were left stranded far above the tide. Ships carried in such currents would be vulnerable



Figure 3. Onshore tsunami impacts, including a 16 foot (5 m) transported boulder (a), boulder deposit (b), embedded gravel in a tree (c), iceberg keel-mark (d), and flattened forest (e). Photos courtesy of Ground Truth Trekking

to collisions that could rupture the hull, or they might be carried broadside into shoals where they could be rolled over. Smaller vessels might experience some of the same hazards as can be found in tidal rapids—strong eddy-lines and whirlpools that can capsize and sink boats. Finally, in troughs between waves vessels might ground on obstacles that would otherwise pose no threat.

It is possible to anticipate areas of potential hazard for vessels using tsunami models. One rough result has been published (not related to our study) that jointly models the landslide and tsunami (George et al. 2017). We are currently working to model the tsunami in more detail, using a numerical model tested against tectonic tsunamis (see video). However, modeling to simulate possible future events will be very sensitive to potential landslide locations, requiring many model runs to capture a range of possible scenarios. Also, while modeled tsunami runup has been widely validated, currents produced by tsunami flows are rarely directly documented, and tsunami models differ substantially in the results they produce (Lynett et al. 2012). Current velocity validation using natural indicators of previous tsunami flow, or using direct observations of tsunamis, are badly needed.

Not all Alaskan rockslides possess the same potential as the Taan Fiord event for generating giant waves that might endanger vessels. While most of the Taan landslide debris entered the fjord, in other cases, the percentages of debris deposited in water bodies may be minimal to non-existent. Figure 4 shows the 2012 Hubbard and Lituya landslides (Geertsema 2012). Even though some of the Hubbard landslide entered Disenchantment Bay, it was only a small proportion of the distal landslide deposit—thus the wave was very small—overtopping the beach by less than 6 feet (2 m). The Lituya slide, though very large, came to rest some 6 miles (10

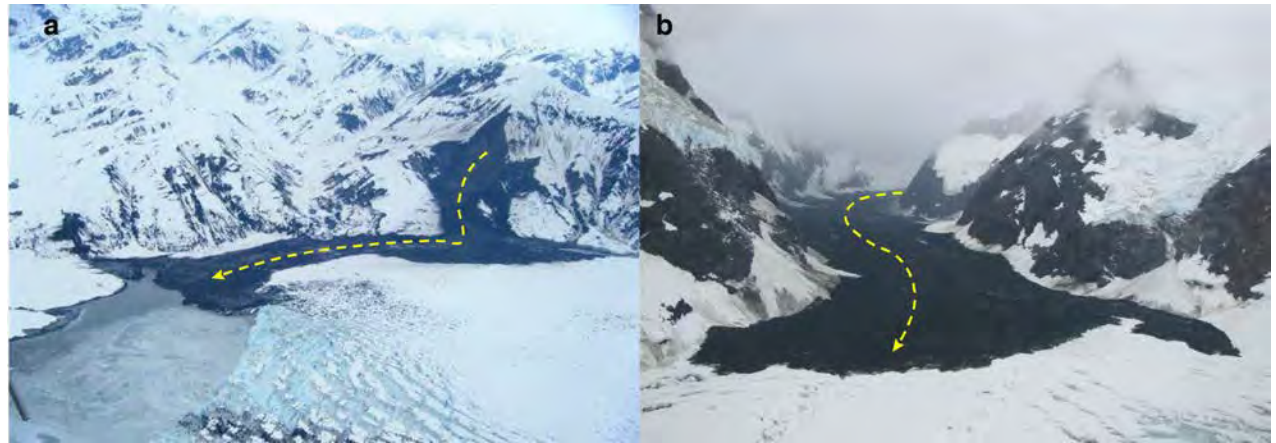


Figure 4. Contrasting Alaskan rock avalanches that happened in the spring of 2012. Only the distal portion of the Hubbard landslide (a) entered Disenchantment Bay in Wrangell-St. Elias National Park and Preserve, producing a tsunami that reached less than 6 feet (2 m) above high tide. The larger Lituya landslide (b) came to rest more than 6 miles (10 km) from tidewater in Glacier Bay National Park and Preserve, and thus produced no tsunami.

km) from tidewater. Nonetheless, the hazard from large landslide-generated waves will likely increase in the coming decades. Large landslides are on the increase in southeast Alaska (Coe et al. 2018), and as glaciers continue to migrate landwards, water bodies such as fjords and lakes will also grow landward toward steep, recently deglaciated terrain, increasing the potential for more landslides, more “direct hits” into water, and therefore more, and possibly larger landslide-generated tsunamis.

Onland Tsunami Hazards

Deforestation of the slopes above Taan Fiord demonstrates the destructive power of the tsunami (Figure 3). In most places, the forest was destroyed by the passing wave. The degree of destruction increased away from the limit of inundation, areas 60 feet (20 m) below that limit were typically so hard-hit that only a few torn roots and soil remnants remained, while trees near the limit were often toppled but still rooted. Some forest remained standing along steep slopes with runups of about 30 feet (10 m), and

patches of dense spruce forest at the mouth of the fjord survived where rafts of debris formed dams to protect them from the iceberg-laden flow.

The tsunami moved boulders up to 16 feet (5 m) in diameter where it was largest (Figure 3). In some areas where there was abundant loose sediment, deposits of everything from boulders to sand were so thick that they raised ground elevations by over 16 feet (5 m). Deposits were more typically 12-20 inches (30-50 cm) thick over areas as far as 6 miles (10 km) from the source. In contrast, one small island that used to support supra-tidal vegetation was scoured down such that now it is only a shoal emerging at low tide (location marked on Figure 5). Tree trunks that remained standing after the tsunami were scoured by strong sediment-laden currents that sometimes severely abraded the upstream side of trees, leaving them peppered with small rocks (Figure 3). Assuming these trees were originally circular in cross-section, some must have lost at least 4 inches (10 cm) of wood to achieve the scoured shape we observed.

A few sites showed that hills can provide significant protection from the worst tsunami impacts. An 800 foot (250 m) diameter hill that was surrounded but not overtopped by the tsunami had runups of over 160 feet (50 m) where the tsunami directly impacted it, but less than 65 feet (20 m) on the lee side (Figure 5). Even below the inundation line on the protected side of this hill, there were more rooted trees and intact soil than in less-protected areas. A structure built here or in analogous locations would likely fare better even than more exposed locations that are significantly farther from the tsunami source.

Where there was little loose sediment, the tsunami typically scoured the land down to bedrock, and left little in the way of deposits. Presumably what little sediment was available in these areas was transported offshore.

These impacts in Taan Fiord show that development should be sited outside areas of anticipated inundation, and evacuation routes are needed so that anyone within the flood zone can effectively flee. Additionally, some consideration should be given to sediment transport: rip rap boulders could be carried by a tsunami, increasing damage and recovery costs. Areas near stream deltas or other sediment sources might be buried by transported sediment. Ideally, new development in areas of potential tsunami inundation could be designed to maximize options for evacuation and minimize costs of reconstruction after an event.

Anticipating Future Events

Alaska's parks could do a lot to be better prepared for future events like this, whether in Icy Bay or anywhere else where steep glaciated mountains rise above deep water. Systematic field surveys of potential sources and remote analysis and monitoring of these sources for precursory movement could help identify likely landslide sites. Modeling based

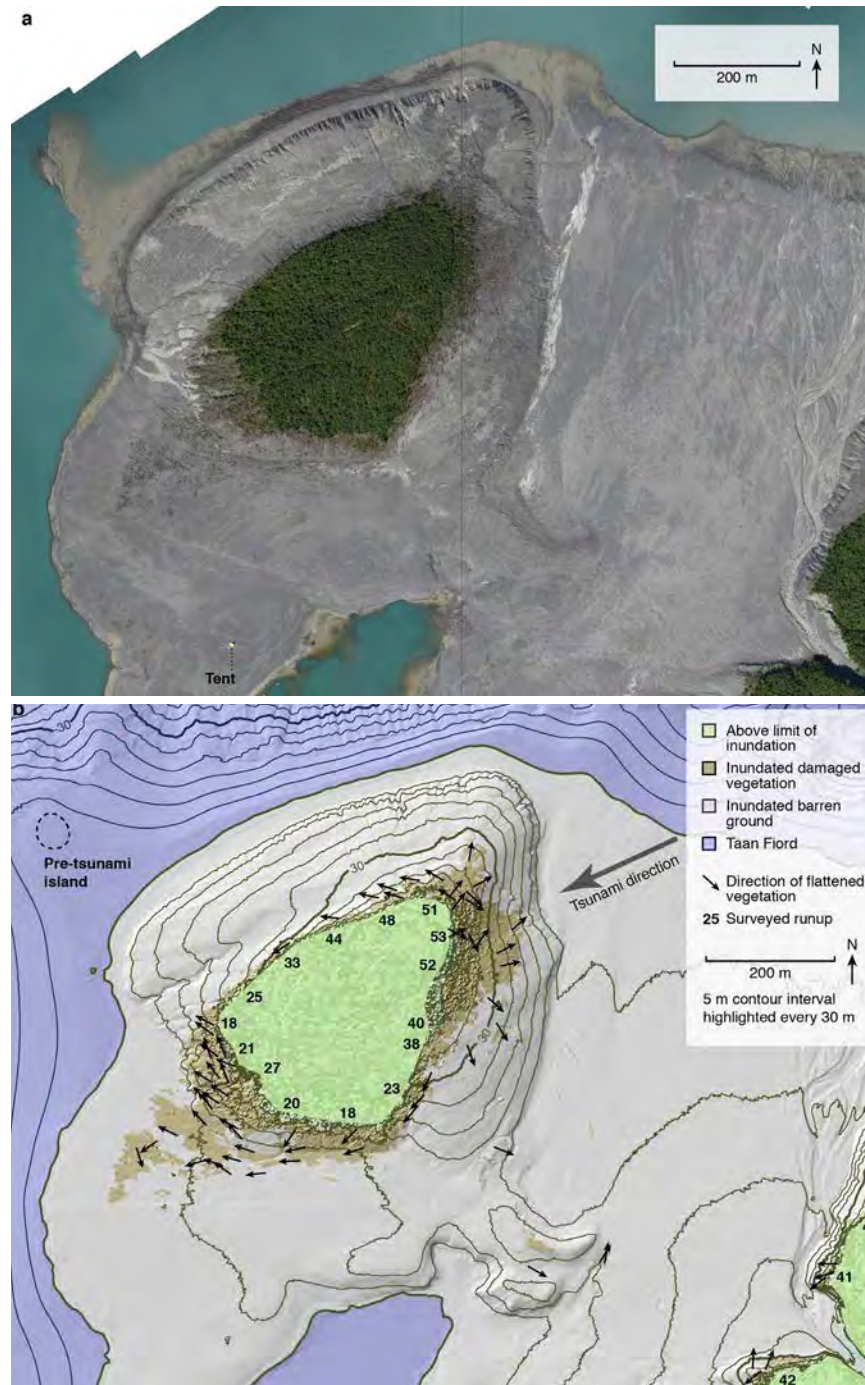


Figure 5. Runup was lower, and soil stripping less severe, where a small hill provided protection from the tsunami. Note the 23x15 foot (7 m x 4.5 m) yellow tent in a.

on potential sources can help outline areas of likely impact, with an emphasis on sites with known risk factors. These results could then be compared to areas of infrastructure development, popular tourist destinations, and ship course data (e.g., from Automatic Identification System (AIS) ship-tracking systems) to identify areas of particular vulnerability. A systematic analysis of this sort could inform park development planning and public education efforts that could reduce risk.

The Taan Fiord event could have been anticipated based on decades of precursory movement that preceded catastrophic failure, had such analysis been conducted prior to the failure. Acceleration revealed by active monitoring such as continuous GPS stations on the slide mass or satellite radar interferometry analysis can provide forewarning of imminent failure. The Taan Fiord event would have been a good candidate for active monitoring because precursory motion generated large, easily measured displacements (e.g., visible even in low-resolution Landsat imagery). Lodge operators and visitors might have been warned of the risk; tsunami modeling likely could have accurately shown the impacts would be potentially severe within the fjord, but would only extend a short way into the main bay. However, no such preparation was conducted and it's urgent that we learn from the 2015 event and take steps to assess and mitigate hazards in Icy Bay and elsewhere before another event happens.

See more about the scientific expedition in this [video](#).

REFERENCES

- Bourgeois, J. 2009.**
Geologic effects and records of tsunamis. *The Sea* 15: 53–91.
- Coe, J. A., E. K. Bessette-Kirton, and M. Geertsema. 2018.**
Increasing rock-avalanche size and mobility in Glacier Bay National Park and Preserve Alaska detected from 1984 to 2016 Landsat imagery. *Landslides* doi:10.1007/s10346-017-0879-7
- Dufresne, A., M. Geertsema, D. H. Shugar, M. Koppes, B. Higman, P. J. Haeussler, C. Stark et al. 2018.**
Sedimentology and geomorphology of a large tsunamigenic landslide, Taan Fjord, Alaska. *Journal of Sedimentology* 364: 302-318.
- Ekström, G. and C. P. Stark. 2013.**
Simple scaling of catastrophic landslide dynamics. *Science* 339: 1416–1419.
- Geertsema, M. 2012.**
Initial observations of the 11 June 2012 rock/ice avalanche, Lituya mountain, Alaska. in The First Meeting of International Consortium of Landslides Cold Region Landslides Network, Harbin, China 49–54. <https://doi.org/10.1016/j.sedgeo.2017.10.004>
- George, D. L., R. M. Iverson, and C. M. Cannon. 2017.**
New methodology for computing tsunami generation by subaerial landslides: Application to the 2015 Tyndall Glacier landslide Alaska. *Geophysical Research Letters* 44: 7276–7284.
- Gullufsen, K. 2018.**
Scientists discover rare ‘alpine tsunami’ occurred after massive 2016 rockfall near Juneau, Juneau Empire 14 Feb 2018. Available at: <https://www.juneauempire.com/news/scientists-discover-rare-alpine-tsunami-occurred-after-massive-2016-rockfall-near-juneau/> (accessed May 14, 2019)
- Haeussler, P. J., S. P. S. Gulick, N. McCall, M. Walton, R. Reece, C. Larsen, D. H. Shugar, M. Geertsema, J. G. Venditti, and K. Labay. 2018.**
Submarine deposition of a subaerial landslide in Taan Fjord, Alaska. *Journal of Geophysical Research-Earth Surface* 123(10): 2443-2463.
- Higman, Bretwood, Dan H. Shugar, Colin P. Stark, Göran Ekström, Michele N. Koppes, Patrick Lynett, Anja Dufresne et al. 2018.**
The 2015 landslide and tsunami in Taan Fjord, Alaska. *Scientific Reports* 8(1): 12993. doi:10.1038/s41598-018-30475-w
- Koppes, M. and B. Hallet. 2006.**
Erosion rates during rapid deglaciation in Icy Bay Alaska. *Journal of Geophysical Research* 111 no. F2. DOI:10.1029/2005JF000349.
- Lynett, P., J. Borrero, R. Weiss, S. Son, D. Greer, and W. Renteria. 2012.**
Observations and modeling of tsunami-induced currents in ports and harbors. *Earth and Planetary Science Letters* 327-328:68-74.
- Meigs, A., W. C. Krugh, K. Davis, and G. Bank. 2006.**
Ultra-rapid landscape response and sediment yield following glacier retreat Icy Bay, southern Alaska. *Geomorphology* 78: 207–221.
- Miller, D. J. 1960.**
Giant waves in lituya bay, Alaska. (US Government Printing Office Washington, DC).
- National Geophysical Data Center / World Data Service (NGDC/WDS). 2017.**
Global Historical Tsunami Database. National Geophysical Data Center, NOAA. doi:10.7289/V5PN93H7
- Russel, I. C. 1893.**
Malaspina Glacier. *The Journal of Geology* 1: 3.
- Wiles, G. C. and P. E. Calkin. 1992.**
Reconstruction of a debris-slide-initiated flood in the southern Kenai Mountains Alaska. *Geomorphology* 5: 535–546.



A young forest of alder and willow was flattened by the retreating tsunami about 140 feet (43 m) above the fjord and over 5 miles (8 km) from the source of the tsunami.
Photo courtesy of Ground Truth Trekking



Catastrophic Glacier Collapse and Debris Flow at Flat Creek, Wrangell-St. Elias National Park and Preserve

Mylène Jacquemart, University of Colorado Boulder
Michael Loso, National Park Service

Debris flows are common events in mountainous regions. At Flat Creek, we expected to find a very large debris flow or landslide. Instead, we found that an entire glacier had spontaneously detached off the mountainside, sending millions of cubic yards of ice and debris shooting down the valley in two catastrophic mass flows. Almost six years later, we are only just starting to piece together what actually happened.

Citation:

Jacquemart, M. and M. Loso. 2019. Catastrophic glacier collapse and debris flow at Flat Creek, Wrangell-St. Elias National Park and Preserve. *Alaska Park Science* 18(1): 16-25.

On July 15, 2015, Bucknell University geologist Jeff Trop was studying regional tectonics of the eastern Wrangell Mountains when his small aircraft happened to pass over a messy looking debris deposit on the south bank of the White River. The deposit, at the mouth of a small tributary valley known locally as Flat Creek, appeared large, recent, and out of character with the braided glacier stream deposits that dominate the area. Trop snapped some pictures (Figure 1), shared them with some colleagues, and in the process revealed yet another example (like the [Taan Fiord landslide tsunami](#)) of a landscape-altering geologic event. It had gone unnoticed for several years by park visitors and staff in our largest and, arguably, wildest park in the National Park System: Wrangell-St. Elias National Park and Preserve.

If anyone was close enough to witness the event that deposited the debris, they could easily have been killed. Luckily, no one was there to see it happen. Although, it actually didn't go *completely* unnoticed. Tom Vaden, a long-time seasonal resident at Solo Creek on the opposite side of the White River, remembered hearing and feeling a large shock from the direction of Flat Creek in mid-summer 2013. On later inspection, he found an impressive deposit, rich in ice and mud, burying white spruce forests almost to the White River. And Vaden also recalled an even larger mass flow coming down the same creek in 2015, just days after Trop took those fortuitous photos.

The scant evidence initially available—mainly anecdotal reports and a few scattered photographs—clearly demonstrated that some sort of debris-flow-like event had occurred at least twice on Flat Creek (Figure 2). Available satellite imagery helped narrow down the search, but it was up to U. S. Geological Survey (USGS) seismologist Kate Allstadt to confirm the timing. Seismometers near Barnard Glacier, 40 miles (65 km) SSE of Flat Creek, recorded the events because they shook the ground hard, just as resident Tom Vaden had described. In fact, the seismic data (Figure 3) tell us that there were two main slope failures: the first one was recorded on August 5, 2013 and a second one was recorded almost exactly two years later, on July 31, 2015. The second one was a very large detachment followed by two smaller events, all within half an hour of each other. And then, while we were just beginning to piece together the story in 2016, another event was witnessed.

National Park Service rangers Luke Wassink and Peter Christian were flying a routine hunting patrol on August 10, 2016, when they happened to be passing over the Flat Creek area. In an amazing coincidence, they looked down just in time to witness an icy debris avalanche flowing down the river channel at almost 25 mph (40 km/h). They caught the event on video, and quickly shared it with park geologist Mike Loso. The flow they recorded ([in a video available here](#)) is much smaller than the 2013 and 2015 events—a conclusion supported by the seismic data—but it's

Figure 1. This photo, taken 7 July 2015, marks the first time that geologists became aware of debris-flow activity at Flat Creek. We later determined, using additional historic photos and data from nearby seismometers, that the lumpy deposit in the mouth of the valley was deposited by a debris flow in August 2013.
Photo courtesy of Jeff Trop, Bucknell University

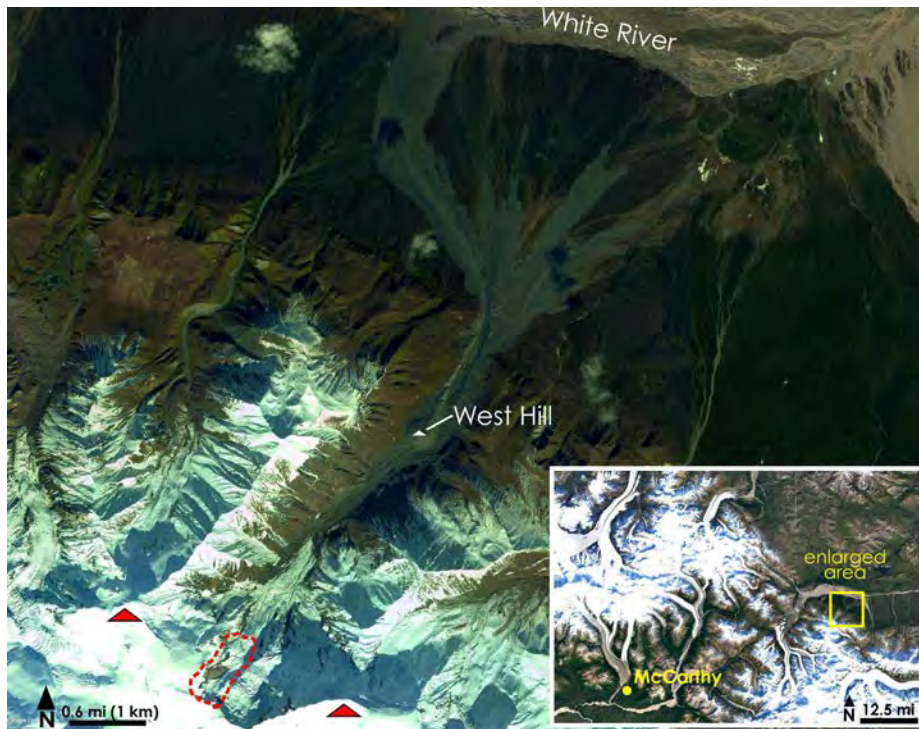


Figure 2. Location of Flat Creek within Wrangell-St. Elias National Park and Preserve. The inset shows that Flat Creek lies 50 miles (80 km) northeast of McCarthy and the Kennecott National Historic Landmark in the heart of the park. Flat Creek flows north into the eastward-flowing White River, shown at the top of the image. Two glaciated peaks (red triangles) form the headwaters of Flat Creek at the southwest end of the valley. The red dashed line shows the approximate boundary of the glacial source area for the debris flows; see Figure 4 for more detail. West Hill, partly visible in Figure 1, is also identified. Based on the height of West Hill, we preliminarily estimate that both debris flows must have been moving at a speed of approximately 70 mph (~110 km/h).

nevertheless a dramatic sight. The flow is extremely wet and it appears to be carrying more ice than mud. In this way, it seems to differ from the earlier events, which we assume based on their deposits, carried very large volumes of silt, sand, gravel, and even larger material. They had seemed, in other words, to be classic debris flows.

Debris flows are common processes in mountain regions, including those of Alaska's parks, where

large amounts of debris can accumulate in narrow stream valleys (Costa 1984). When the time is right, usually coincident with intense snowmelt or strong rainfall, much of the accumulated debris may be washed down the valley. Debris flows can be highly mobile and travel for long distances, especially when they come raging down steep streambeds. In his 1988 essay, *Los Angeles against the Mountains*, author John McPhee (1988) described a debris flow this way:

It was not a landslide, not a mudslide, not a rock avalanche, nor by any means was it the front of a conventional flood. In geology, it would be known as a debris flow. Debris flows amass in stream valleys and more or less resemble fresh concrete. They consist of water, mixed with a good deal of solid material, most of which is above sand size. Some of it is Chevrolet size.

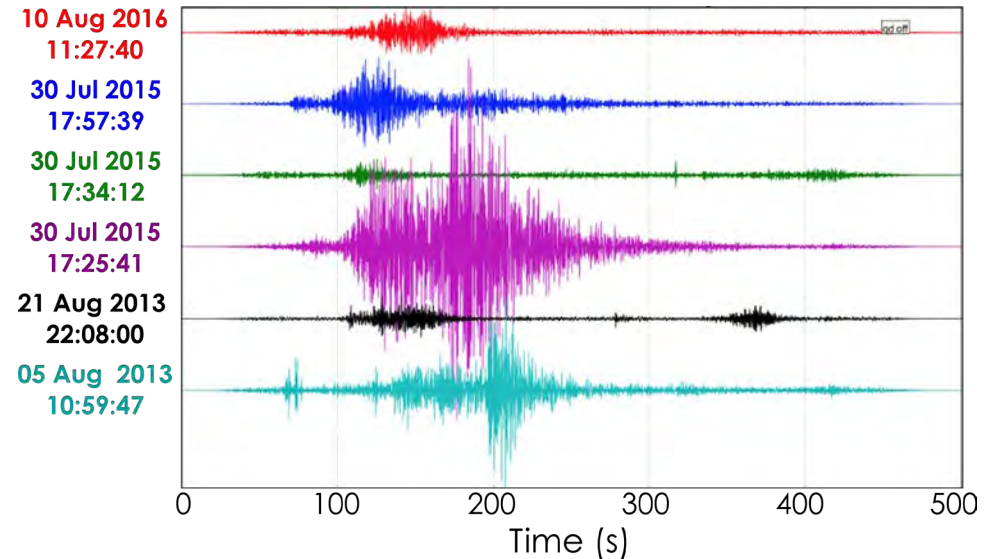


Figure 3. Records of ground motion from a seismometer at Barnard Glacier, about 40 miles (65 km) SSE of Flat Creek, confirm the timing (local Alaska time) of each debris flow identified in photos. In the long run, we hope that these data will also tell us something about the dynamics of the slides. Data Source: Kate Allstadt, USGS.

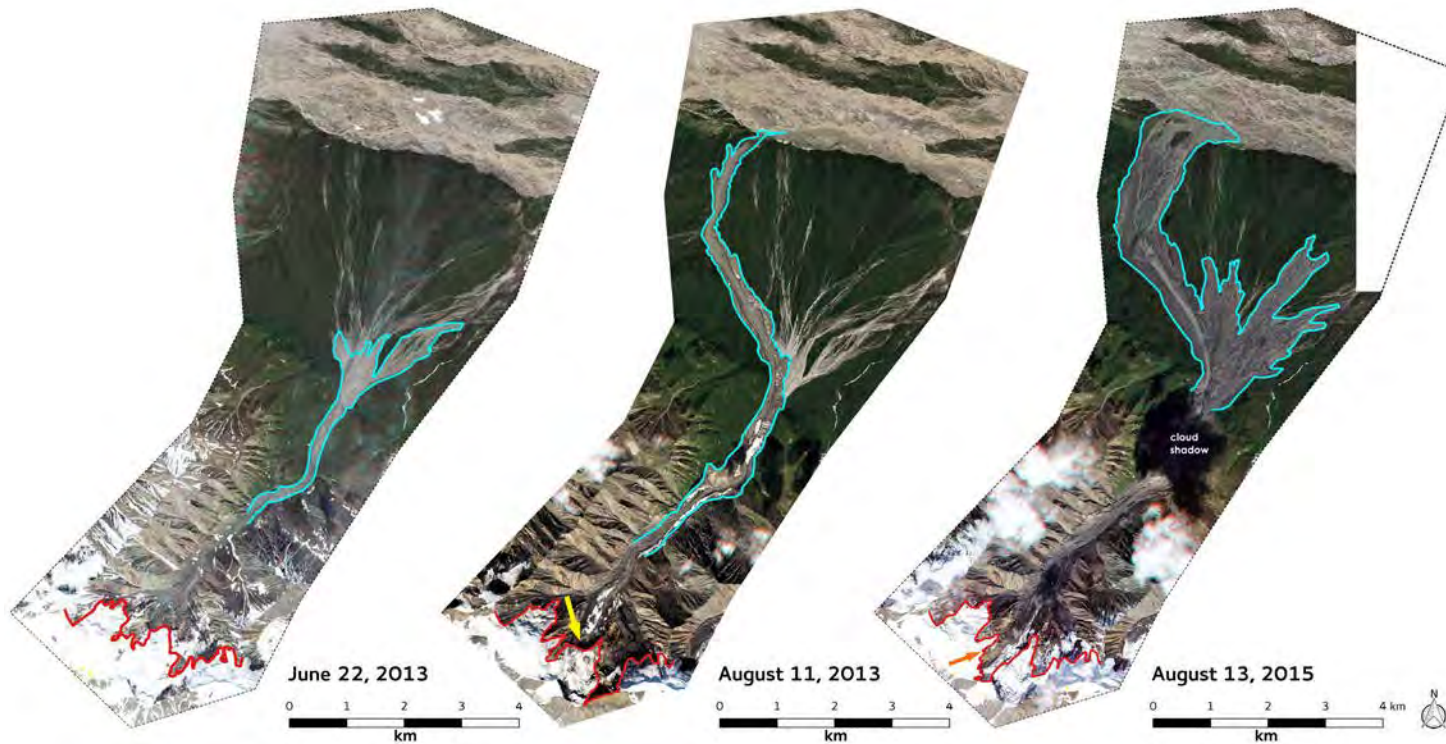


Figure 4. Sequential satellite images of Flat Creek reveal the destructive nature of the debris flows. Left panel (June 2013) shows the glacier (terminus outlined in red) and braided river deposits (outlined in light blue) in their “normal” state, mostly unchanged since at least 2010. In the middle panel (August 2013, after the first debris flow), a prominent tongue of the glacier (yellow arrow) has gone missing and a long, skinny debris-flow deposit is visible all the way down to the White River. Right panel (August 2015, after the large 2015 events) shows a vast debris deposit on the fan and much of the glacier missing (orange arrow).

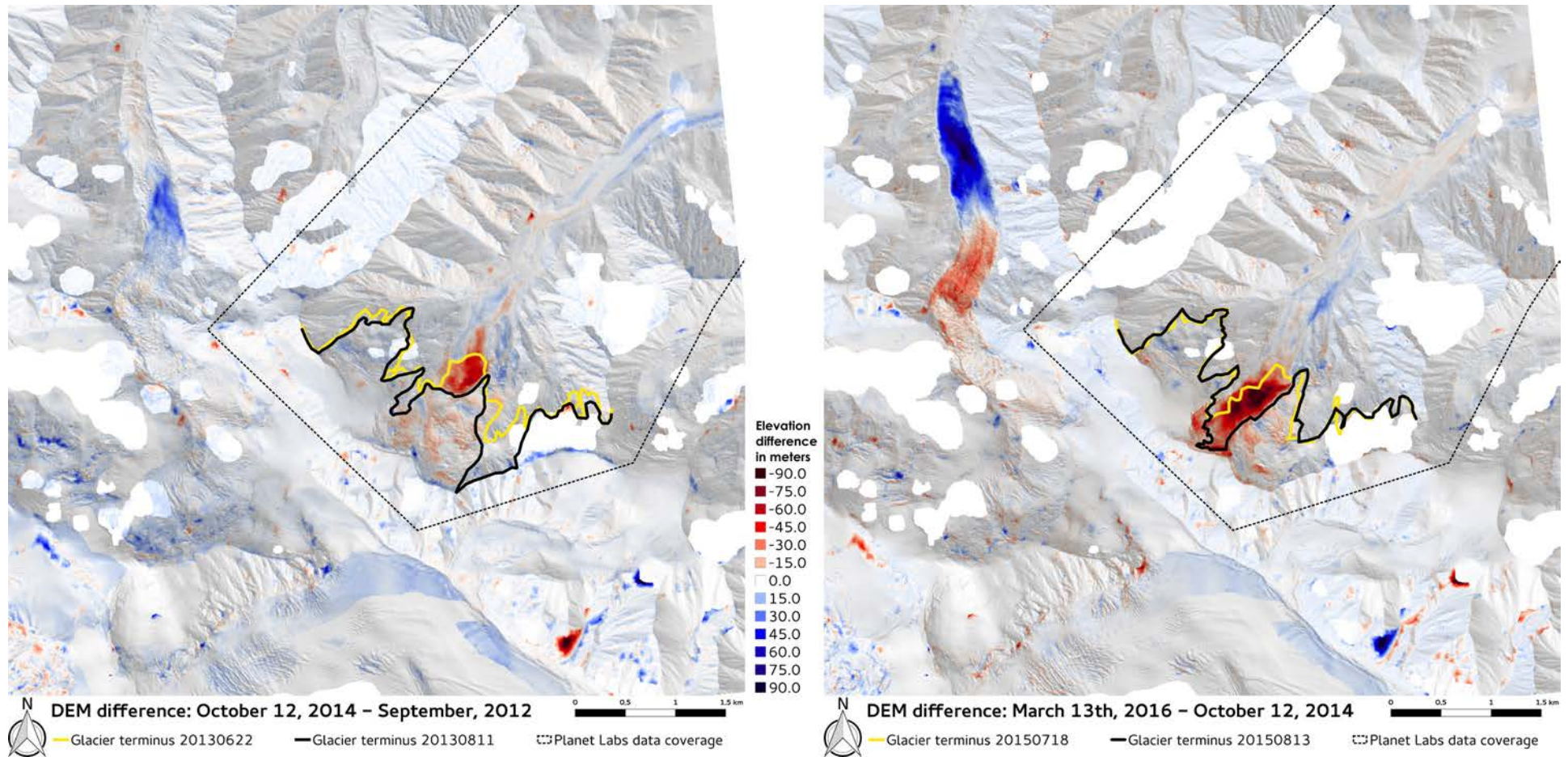
Though we didn’t witness them, it appears that the 2013 and 2015 events, based on what we can tell from their deposits, fit McPhee’s description reasonably well. Except that they also contained ice, according to Tom Vaden. The 2016 event captured on video, which carried mostly ice, hardly resembled McPhee’s description. We might call it a *slushalanche*, but that’s a term without precedent in the scientific literature. Even the earlier events appeared to have been quite wet and ice rich, which forced us to confront two central questions in our research: what is causing these flows and where is all the ice and water coming from?

As a starting point for answering those questions, we used satellite data to compare images and elevations from before and after the slides to identify

the changes that took place during each event. Frequent cloud cover in this part of the world makes it hard to track changes in satellite images, but Planet Lab’s army of small cube satellites passes over the area very often (Planet Team 2017). Their high-resolution data (pixel size=16.4 feet [5 m]) provided a valuable resource to track the changes as closely as possible. Vast areas of white spruce forest were overrun by the 2013 and 2015 events. In the lower part of the valley, the 2013 flow left a narrow deposit of debris 2.3 miles (3.7 km) long and 260-820 feet (80-250 m) wide. In some places, the deposit is more than 65 feet (20 m) thick. Two years later, once again during peak melt season in mid-summer, the second slide bulldozed down the valley. In 2013, the flow had deposited debris atop what we informally named West Hill (Figure 2), a riverside knob that stands

more than 300 feet (100 m) tall. The 2015 flood was even bigger, overflowing the entire hill leaving a wide path of destruction. It travelled over the top of the 2013 deposit, destroyed yet more spruce forest, and covered almost 3,700 acres (0.4 ha; or ~2,800 American football fields).

The most notable observation from those satellite images, however, is that large parts of the glacier that occupied the head of Flat Creek disappeared during the 2013 and 2015 events. An image from 11 August 2013 shows that the front third of the glacier tongue were missing and large pieces of ice flanked the river below. In 2015, the ice in the central trough of the glacier disappeared altogether (Figure 4). To better understand these apparently sudden ice losses, we used digital surface models (DSM or DEM for digital



elevation model) to quantify changes in glacier surface elevation. DSMs were available to us for the years 2012 (AK IfSAR DSM based on airborne synthetic aperture radar), 2014 and 2016 (ArcticDEM made from optical satellite images, available at no cost through the Polar Geospatial Center). These products are spaced just right to bracket the individual events in 2013 and 2015. Comparing these datasets revealed that about 244-395 million cubic feet (6.9-11.2 million m³ or roughly 4,000 Olympic swimming pools) and 614-965 million cubic feet (17.4-19.7 million m³ or ~7,200 Olympic pools) of

the upper Flat Creek basin washed downstream in the 2013 and 2015 events, respectively (Figure 5).

These volume losses were concentrated almost entirely in the glacier-covered areas of the watershed and, importantly, included not just the glacier terminus, but ice up to and including the highest portions of the accumulation zone. Because the 2013 and 2015 events transported large amounts of sediment, we know that the volume losses we calculated from DEMs are not solely due to ice loss; some of the volume removed from the upper watershed

Figure 5. A closer view of the debris-flow source areas showing topography (gray shading) and elevation changes (colored areas) computed by differencing DEMs. Gaps indicate missing data. Left panel: 2014 minus 2012 elevation differences show the effects of the 2013 event. Right panel: 2016 minus 2014 differences show the effects of the 2015 events. In each panel, elevation loss is shown in shades of red and elevation gain in shades of blue. Digitized before-event and after-event glacier terminus outlines are drawn in black and yellow. Note the initiation (left panel) and rapid progress (right panel) of a glacier surge in the drainage west of Flat Creek during this same time period. 2014 and 2016 DEMs created by the Polar Geospatial Center from DigitalGlobe, Inc. imagery.

had to have included subglacial bedrock or sediment. But the inescapable conclusion remains: those events (including the 2016 event, which obviously contained a large volume of glacier ice even though we have not been able to determine where it came from) involved the substantial, nearly instantaneous collapse of a large, full-thickness section of the Flat Creek Glacier.

While both satellite data and DEMs are useful for identifying large-scale changes at Flat Creek, they can only tell us so much about the process that drove these catastrophic events. In order to better understand them, and to evaluate the threat similar events might pose to visitors and infrastructure in the parks and elsewhere, we conducted the first on-site field investigation of Flat Creek during summer 2018.

Without question, our first and strongest impression from the site of the debris flows was how overwhelmingly big these events were (Figure 6). The runout distance of approximately 7 miles (11.26 km) is astounding, especially given that the maximum fall height from glacier crest to valley floor is only about 4,900 feet (1,500 m). Because of how well the glacier extent matches the failure outline, we argue that this is not a case of a glacier getting caught in a rock avalanche. Instead, we believe that the glacier detached from its bed, entraining rock and debris. We are only aware of three places in the world where catastrophes of similar magnitude and character (long, low-angle runouts associated with sudden upstream glacier collapse) have occurred: the 2002 detachment of Kolka Glacier in the Russian Caucasus (Evans et al. 2009), the 2016 failures of two glaciers in northern Tibet (Kääb et al. 2018), and several glacier detachments at Iliamna, a volcano in Cook Inlet, Alaska (Caplan-Auerbach and Huggel 2007).

Another conspicuous feature of the deposit is the absence of boulders. McPhee's "Chevrolet-sized



Figure 6. National Park Service geologist Michael Loso descends the grassy tundra towards Flat Creek where the 2013 and 2015 debris flows, barreling down the valley from the headwall on the left, stripped the streambed and banks of all vegetation. West Hill, 360 feet (109 meters) tall is visible on the far side of the creek just inside the large bend in the river. Photo courtesy of Mylène Jacquemart, CU Boulder

boulders" are almost completely missing from the runout zone. Hardly anything larger than a toy truck seems to have survived this slide. Part of the reason for that is likely the quality of rock that makes up the headwall, where the slide originated. It is composed of dark grey and reddish brown mudstone, mapped in this region as part of the early Permian Hasen Creek Formation. Importantly, the headwall also lines up with the late Quaternary Totschunda Fault, though we found no seismic triggers for the collapse. The primary strand of the fault itself is not obviously visible in Flat Creek, but the bedrock in the area

exhibits numerous faults, igneous intrusions, and possibly thermal alterations that collectively compromise these already weak sedimentary rocks.

The low quality of the rock is further illustrated by conical debris mounds, termed molards, that we found throughout the deposit. Several hypotheses have been formulated to explain molards, but in this instance, we favor some newer evidence suggesting that molards are often a product of landsliding in permafrost terrain. Boulder-sized clasts of weak bedrock cemented by ice get transported to lower



Figure 7. Geoscientists-in-the-parks guest scientist John Sykes in the runout zone of the Flat Creek debris flows studying one of the many molards scattered throughout the runout. Each conical mound was characteristically one of two distinct colors (as shown here). We interpret the molards as blocks of weak (but perhaps frozen) bedrock that were transported whole by the debris flow, but then disintegrated after deposition. The White River flows from left to right in the middle distance, beyond the trees.

Photo courtesy of Jasmine Hansen, CU Boulder



Figure 8. A stream-eroded exposure of the debris-flow deposit along the east bank of Flat Creek near West Hill. Many of these deposits, in particular upstream of West Hill, were still ice rich, bearing witness to the significant amount of glacier ice involved in these events. The light-colored, rounded clasts are composed of ice. Very little sediment is needed to shield ice from the warmth of the sun, so it is possible that some of this ice is left over from the earliest 2013 event.

Photo courtesy of Mylène Jacquemart, CU Boulder

elevation sites, where they thaw and fall apart to form conical mounds (Brideau et al. 2009, Milana 2016). Their generally homogenous physical properties (Figure 7) supports the interpretation of each molard as a transported instance of a single coherent rock type (rather than transport of a previously mixed material moved by glaciers and deposited by streams [*glaciofluvial*] or loose, unconsolidated [*colluvial*] sedimentary deposit).

This interpretation is supported by our observation that frozen ground (in mid-July) was present at a depth of 31.5 inches (80 cm) and that we measured a ground temperature of only 34.2°F (1.2°C) at a depth of 27.5 inches (70 cm). While a

single measurement is not conclusive, it suggests that the source area, at least where unglaciated, contains permafrost (permanently frozen ground). Our findings are also supported by the permafrost map created by Jorgenson and others (2008), which suggests that permafrost is present in more than 90% of Flat Creek basin. This may be relevant because several studies have tied warming permafrost to a potential increase in landslide activity (Huggel et al. 2012).

Along the drainage toward the headwall, we found numerous stream-eroded outcrops of ice-rich debris. The ice was, in most cases, present as individual clasts of massive, rather than interstitial,

ice and we interpreted it as glacier ice transported by the debris flows (Figure 8). The survival of ice clasts from events in 2016, 2015, or even 2013 is not surprising, given the fact that even just a few inches of debris are enough to insulate the subsurface and dramatically slow ice melt. We know from looking at satellite images, however, that much of the ice that was deposited at the surface of the deposit has since melted. It is very difficult, unfortunately, to estimate the relative proportions of ice and bedrock and sediment transported by each event.

The headwall of the valley is an impressive sight (Figure 9). It is surprising that the area where the ice failed appears to be among the least steep parts

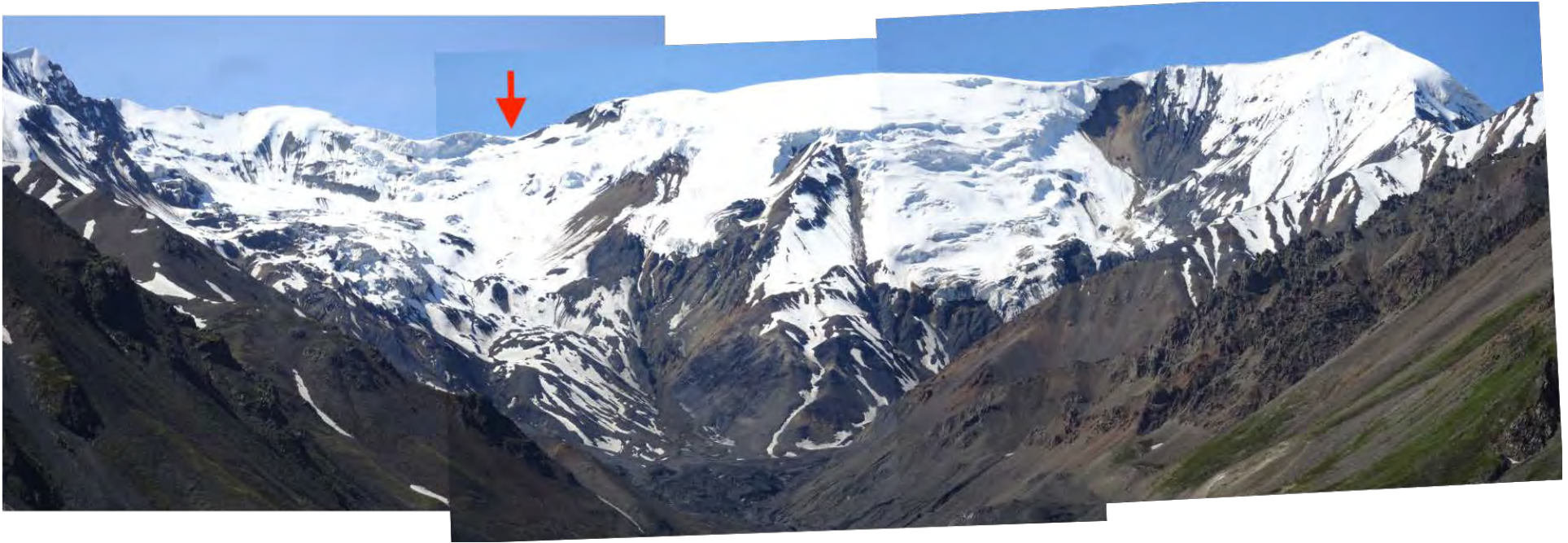


Figure 9. Composite panorama of the southern, upstream end of Flat Creek. The unnamed glaciers at the head of the creek adhere to steep, heavily faulted, weak mudstone cliffs. Both the 2013 and the 2015 failures originated in the central trough (red arrow).

Photo courtesy of Mylène Jacquemart, CU Boulder

of the glacier. The glacier topography does not appear to have been steep enough to generate an ice avalanche, at least in the sense of the term normally used for serac falls originating from steep ice cliffs. This is one of the persistent mysteries of this project: how to characterize and understand the sudden loss of glacier ice. The loss was too sudden to be called a glacier surge (a rapid advance of the glacier tongue, not usually catastrophic); too rapid and kinematic to be compared with more typical climate-driven glacier melt; and it involved too much low-angle ice to be considered an ice avalanche. In fact, parts of the glacier, bizarrely crevassed and folded, are still attached to much steeper cliffs surrounding the

portion of the glacier that failed. In contrast, the exposed, post-failure mountainside, presumably the failure plane, only has a slope of about 20 degrees. For safety reasons we did not access the headwall on foot, but instead flew a small, multi-rotor Unmanned Aerial Vehicle (UAV) towards the release zone to record more detail. We found the black mudstone to be heavily folded and fractured, with signs of crumbling rock and ice everywhere. In many areas, ice was mixed with sediment to the point where it was impossible to tell them apart. We found this typically in steep outcrops weeping black debris over lower-angle ice and snow below.

A definitive statement about what exactly happened at Flat Creek remains difficult. We can say with confidence that each event involved some variable mix of glacier ice and lithic material, that together formed a wet slurry that flowed downstream at high velocities as something that resembled a debris flow. But how and why did the ice fail? Did the ice collapse precipitate further collapse of adjacent or underlying bedrock? Or did the failures originate in bedrock and incorporate the overlying ice? Finally, where did all the water come from? Flat Creek is a very small stream and ice avalanches rarely (if ever) generate enough water by themselves to sustain a water-rich downstream flow. However, our preliminary analysis

of climate data does show that 2013 and 2015 were very warm years, with above-freezing temperatures likely generating significant amounts of meltwater, even at high elevations. Anticipating that another event may yet occur, we left time-lapse cameras in Flat Creek at the end of our 2018 field season.

In the meantime, we are conducting further analyses of meteorological and satellite data; completing lab work on rock, sediment, and tree core samples; and running numerical models of the flow itself. Ultimately, our goals in studying these events are not only to understand the nature of the flows themselves, but to identify the trigger (or triggers) that led to the collapse of Flat Creek Glacier. As mentioned earlier, the type of glacier detachment and runout that apparently occurred here has only a few known precedents worldwide, but those precedents are sobering. In the 2002 Caucasus glacier collapse, over 120 people were killed and an entire village was obliterated. In the 2016 event in Tibet, nine people and hundreds of herd animals were killed. In both cases, the precipitating glacier collapse was later characterized by researchers as extraordinary and outside the normal boundaries of expected glacier behavior. Of course, this is a reflection, at least in part, of our incomplete understanding of glacier and debris-flow dynamics. Does it also mean that the worldwide trend toward accelerated glacier mass loss is accompanied by new and potentially more dangerous forms of retreat? In a national park with over 3,000 individual glaciers and a collective glaciated area of over 11,000 square miles (>29,000 km²; Loso et al. 2014), that question is an urgent one.

REFERENCES

- Brideau, M., D. Stead, C. Hopkinson, M. Demuth, J. Barlow, S. Evans, and K. Delaney. 2008. Preliminary description and slope stability analyses of the 2008 Little Salmon Lake and 2007 Mt. Steele landslides, Yukon: The Little Salmon Lake landslide reactivation. *Yukon Explor. Geol.* November: 119-134.
- Caplan-Auerbach, J. and C. Huggel. 2007. Precursory seismicity associated with frequent, large ice avalanches on Iliamna volcano, Alaska, USA. *J. Glaciol.* 53(180):128-140.
- Costa, J. E. 1984. Physical Geomorphology of Debris Flows, in Developments and Applications of Geomorphology, Springer-Verlag Berlin Heidelberg, pp. 268-317.
- Evans, S. G., O. V. Tutubalina, V. N. Drobyshev, S. S. Chernomorets, S. McDougall, D. A. Petrakov, and O. Hungr. 2009. Catastrophic detachment and high-velocity long-runout flow of Kolka Glacier, Caucasus Mountains, Russia in 2002. *Geomorphology* 105(3-4): 314-321.
- Huggel, C., J. J. Clague, and O. Korup. 2012. Is climate change responsible for changing landslide activity in high mountains? *Earth Surf. Process. Landforms* 37(1): 77-91.
- T. Jorgenson, K. Yoshikawa, M. Kanevskiy, Y. Shur, V. Romanovsky, S. Marchenko, and G. Grosse. 2008. Permafrost Characteristics of Alaska. *Proc. Ninth Int. Conf. Permafr.* 29:121-122.
- Kääb, A., S. Leinss, A. Gilbert, Y. Bühler, S. Gascoïn, S. G. Evans, P. Bartelt, E. Berthier, F. Brun, W. A. Chao, D. Farinotti, F. Gimbert, W. Guo, C. Huggel, J. S. Kargel, G. J. Leonard, L. Tian, D. Treichler, and T. Yao. 2018. Massive collapse of two glaciers in western Tibet in 2016 after surge-like instability. *Nat. Geosci.* 11(2):114-120.
- Loso, M. G., A. Arendt, C. Larsen, J. Rich, and N. Murphy. 2014. Alaskan national park glaciers – status and trends: Final report. National Resource Technical Report NPS/AKRO/NRTR—2014/922. National Park Service, Fort Collins, Colorado.
- McPhee, J. 1988. Los Angeles against the Mountains. The New Yorker, September 26 issue. Available at: <https://www.newyorker.com/magazine/1988/09/26/los-angeles-against-the-mountains-i> (accessed 2019-05-04)
- J. P. Milana. 2016. Molards and their relation to landslides involving permafrost failure. *Permafr. Periglac. Process.* 27(3): 271–284.
- Planet Team. 2017. Planet Application Program Interface: In Space for Life on Earth. San Francisco, CA. Available at: <https://api.planet.com> (accessed 2018-09-02)

Aerial photograph of the Flat Creek runout zone after the 2015 debris flow. The large braided river in the upper third of the image is the White River. The Flat Creek debris flows came down the channel from the bottom left of the image.

Photo courtesy of Michael Loso, NPS





An Initial Assessment of Areas Where Landslides Could Enter the West Arm of Glacier Bay, Alaska and Implications for Tsunami Hazards

Jeffrey A. Coe, Robert G. Schmitt, and Erin K. Bessette-Kirton, U.S. Geological Survey

Tsunamis generated by landslides in Glacier Bay are uncommon, but have potential to be extraordinarily destructive when they occur. This article identifies areas that are susceptible to landslides that could generate tsunamis and discusses approaches to characterize hazard and risk from these events.

Citation:

Coe, J. A., R. G. Schmitt, and E. K. Bessette-Kirton. 2019. An initial assessment of areas where landslides could enter the West Arm of Glacier Bay, Alaska and implications for tsunami hazards. *Alaska Park Science* 18(1): 26-37.

The combination of recent deglaciation, relatively frequent earthquakes, steep rocky slopes, and narrow inlets suggests that many locations in Glacier Bay have the potential for generating large tsunami waves.

Landslides and Giant Waves
(National Park Service 2018a:1)

As implied by the quote above, Glacier Bay National Park and Preserve (GBNPP, Figure 1) is susceptible to tsunamis generated by landslides. Landslides capable of generating tsunamis include rockslides, rock avalanches, and soft-sediment slides that begin both above (*subaerial*) and below (*submarine*) water (e.g., Suleimani et al. 2015). Rock avalanches are landslides of fragmented rock that begin from rockslides and can be extremely hazardous because of their large size (>1 million (M) yard³ [>1 M m³]) and ability to move long distances (>0.6 mi [>1 km]) at extremely rapid speeds (up to 220 mi/hr [100 m/s], Pudasaini and Krautblatter 2014). GBNPP has a history of both earthquake- and climate-induced subaerial rockslides and rock avalanches (Miller 1960, Post 1967, Evans and Clague 1999, Geertsema 2012, Bessette-Kirton and Coe 2016, Coe et al. 2018, Bessette-Kirton et al. 2018). Throughout this article, we use the term *landslide* as a general term for all types of slope failures, including the three types listed above.

Although historical records of tsunamis generated by landslides in GBNPP are uncommon, there are records that document the extraordinary destructive power of at least three landslide-generated tsunamis in Lituya Bay on the west side of the park (Miller 1960). In 1958, when Lituya Bay was part of Glacier Bay National Monument (the area was established as a national park and preserve in 1980; National Park Service 2018b), the largest of these tsunamis was generated by a rockslide triggered by a M 7.8 earthquake (USGS 2018a) on the Fairweather Fault (Miller 1960; Figure 1). This rockslide was approximately 39 M yard³ (30 M m³) in volume and generated a tsunami that ran up the opposite shoreline to 1,719 feet (524 m) above sea level and killed two people in a small boat (Miller 1960, Fritz et al. 2009). Another rockslide at Tidal Inlet on the eastern side of the West Arm of Glacier Bay (Figures 1 and 2) appears to be active today. This slide has a volume of 6.5 to 14.5 M yard³ (5 to 11 M m³) and has been moving slowly (1-1.5 inch/yr [3-4 cm/yr] between 2002-2004) since at least 1892 (Wieczorek 2007). If catastrophic failure occurred, the landslide has the potential to generate a tsunami with waves >33 feet (>10 m) high in Glacier Bay proper near the mouth of the inlet (Geist et al. 2003; Wieczorek et al. 2007). The largest historical rock avalanche in GBNPP was the June 28, 2016 Lamplugh rock avalanche (Figure 1) with a volume of about 92 M yard³ (70 M m³; Bessette-Kirton et al. 2018). Luckily, this rock avalanche did not enter the water of the West Arm

A cruise ship in the Johns Hopkins Inlet with a June 28, 2016 rock-avalanche deposit on the Lamplugh Glacier.
Photo courtesy of Paul Swanstrom, Mountain Flying Service

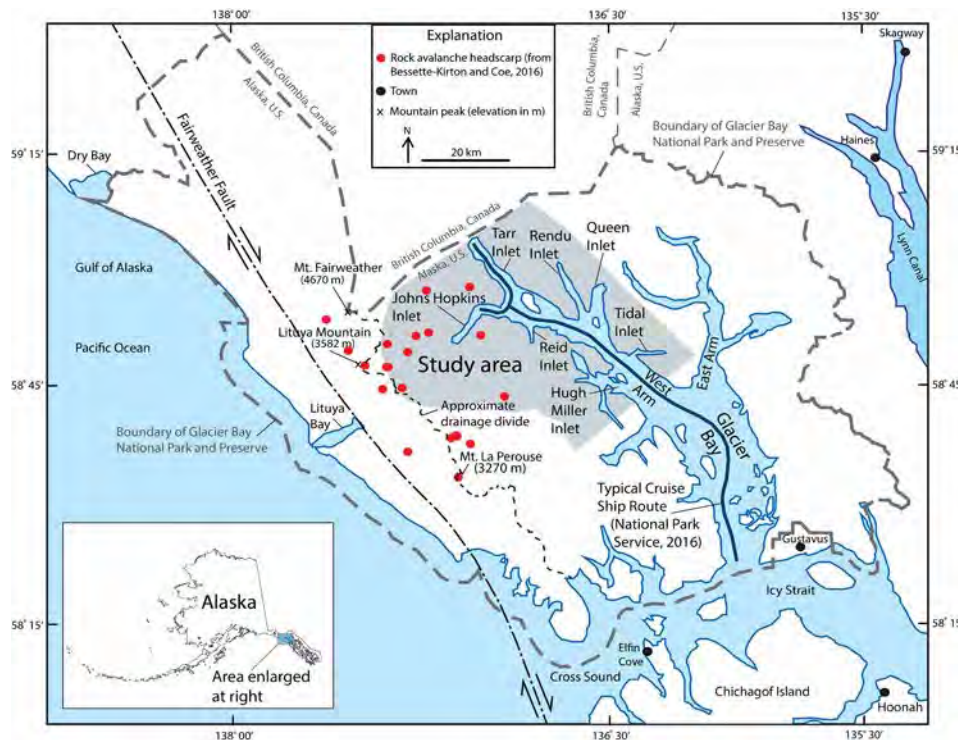


Figure 1. Map of Glacier Bay National Park and Preserve and the study area surrounding the West Arm. The drainage divide separates basins that drain to the west from those that drain to the east.



Figure 2. The Tidal Inlet landslide along the north shore of Tidal Inlet. Photo from Wiczorek et al. (2003). Relief from the highest point on the headscarp to the water is about 1,970 feet (600 m).

of Glacier Bay, but instead was deposited entirely on the Lamplugh Glacier. Another noteworthy rock avalanche occurred in October 2015 in Wrangell-St. Elias National Park and Preserve. This 99 M yard³ (76 M m³) rock avalanche traveled onto Tyndall Glacier and then into Taan Fiord where it generated a tsunami that ran about 623 feet (190 m) up the shoreline (Haeussler et al. 2018, Higman et al. 2018, [Higman et al. this volume](#)).

In 2017, about 540,000 people visited GBNPP on cruise ships and tour boats (National Park Service 2018b). Regulations that went into effect in January 2007 specify that a maximum of two cruise ships are allowed to enter Glacier Bay each day, year-round (Janiskee 2011). The typical cruise ship route traverses the entire length of Glacier Bay with two northern terminus points in the Johns Hopkins and Tarr Inlets to view glacier calving at the Johns Hopkins and the Grand Pacific glaciers, respectively (National Park Service 2016; Figure 1). The peak June-August cruise ship visitor season is also the season when climatically induced, subaerial-rockslides and rock avalanches are most likely to occur (Bessette-Kirton and Coe 2016, Coe et al. 2018). This temporal correspondence between high numbers of visitors and landslide hazard begs multiple questions, including:

1. What areas of Glacier Bay are susceptible to rockslides or rock avalanches that could enter the water and potentially generate tsunamis?
2. What is the likelihood that these slides and tsunamis could occur and how large will they be?
3. If they occur, what is the risk to park visitors?
4. If a substantial risk to visitors exists, what should be done about it?

None of these questions have easy answers, but in this article, we begin to address the first question and provide suggestions for approaches that could be used to better understand and quantify landslide and tsunami hazards and risk in GBNPP. We focus our initial effort on the West Arm of Glacier Bay where the cruise ship terminus points are located (Figure 1) and produce several maps that can be used to prioritize areas of the West Arm where additional work is needed. We concentrate this initial effort on landslides that initiate on land and then enter the water, because we currently know very little about landslides that initiate underwater in Glacier Bay.

Geologic Setting

Glacier Bay National Park and Preserve is located along the approximately 745-mile-long (1,200-km) transform boundary where the Pacific and North American tectonic plates slide past each other. The plate boundary is marked by two interconnected strike-slip faults, the Fairweather Fault in the north (e.g., Plafker et al. 1978), and the Queen Charlotte Fault in the south (e.g., Brothers et al. 2018). The Fairweather Fault, which is onshore in GBNPP (Figure 1), accommodates a large portion of the relative motion between the plates through dextral (right lateral) slip of about 1.5 inches/year (43 mm/yr; Elliott et al. 2010).

Much of GBNPP is currently covered by ice, but the area has undergone extensive deglaciation during the last 250 years (Larsen et al. 2005, Connor et al. 2009). For example, in 1860, the entire West Arm of Glacier Bay (a fjord) was filled with ice. Viscoelastic rebound from deglaciation causes GBNPP to have one of the highest rates of uplift on Earth (up to about an inch/year or 30 mm/yr; Larsen et al. 2005, see Husson et al. 2018 for global rates). Elevations in the area range from sea level up to 15,325 feet (4,671 m) at Mount Fairweather at the U.S.-Canada

border (Figure 1). The combination of glacial scour, followed by deglaciation and extremely rapid uplift, has resulted in long, narrow inlets with steep, rocky walls that define Glacier Bay. These steep walls are periodically interrupted by tidewater glaciers that calve icebergs into the bay. At least nine tidewater glaciers terminate in inlets of the West Arm (Figure 1).

Bedrock in GPNPP is exposed at mountain peaks, flanks, and ridgelines, and in coastal zones. The bedrock geology is complex and consists of Paleozoic and Mesozoic accretionary terranes containing Tertiary sedimentary, intrusive, and volcanic rocks (Brew et al. 1978, Wilson et al. 2015). Bedrock units that surround the West Arm are: Tertiary, Oligocene, and Eocene granitic rocks; the Cretaceous Chugach accretionary complex consisting of flysch, graywacke, and basalts; Cretaceous and Jurassic quartz monzodiorite; Cretaceous foliated granitic rocks; and Devonian to Ordovician shale, chert, and argillite (Wilson et al. 2015). Gruber (2012a and 2012b) indicates a high likelihood that mountain permafrost is present in rock in high-elevation areas of GBNPP (see Gruber 2012b for map data and Coe et al. 2018 for historical landslides with respect to permafrost areas).

Processes Influencing Landslide and Tsunami Hazards

Landslides in rock are commonly triggered by shaking from earthquakes or by increases in pore-water pressures within rock fractures. The position of GBNPP along a tectonic plate boundary ensures that earthquakes capable of generating rock-slope failures have occurred and will continue to occur in the future. Since the 1958 M 7.8 earthquake that triggered the Lituya Bay rockslide and tsunami, there have been at least 90 earthquakes >M 4 within 62 miles (100 km) of the study area (the largest

were two M 6.1 earthquakes, one in January 2000 and the other in July 2014; USGS 2019). However, we currently have no evidence that any of these earthquakes triggered rock-slope failures in the study area. Instead, all recent rockslides and rock avalanches in GBNPP have been associated with climatic triggers (Coe et al. 2018). Between 1984 and 2016, there were at least 24 climatically induced rock avalanches in GBNPP (Besette-Kirton and Coe 2016) and available evidence indicates that these avalanches have increased in size and travel distance (mobility) with time (Coe et al. 2018).

There are at least four possible factors that could influence climatically induced landslides in GBNPP, these include: (1) degradation of mountain permafrost, (2) debutressing of rock slopes from thinning of glaciers, (3) increased precipitation, and (4) weakened rocks due to changes in regional crustal strain. The first three factors are related to ongoing climate change (e.g., Stevens et al. 2018). Geertsema and others (2013) summarized the impacts of the first two factors on national parks in Alaska, and Coe and others (2018) hypothesized that the first factor, the degradation of mountain permafrost, was the primary driver responsible for the observed increase in rock-avalanche size and travel distance in GBNPP. Mountain permafrost (ice within fractures in rocks) acts to strengthen rocks on steep slopes. However, well-documented increases in both long-term (e.g., Walsh et al. 2014) and short-term air temperatures (e.g., Walsh et al. 2017) degrade (weaken or thaw) permafrost, thus increasing the likelihood of large, hazardous rockslides and rock avalanches. Regarding the third factor, all climate projections show increasing long-term precipitation in Alaska through the end of the 21st century (van Oldenborgh et al. 2013, Walsh et al. 2014). This forecast, combined with increasing temperatures, can increase long-term pore-water

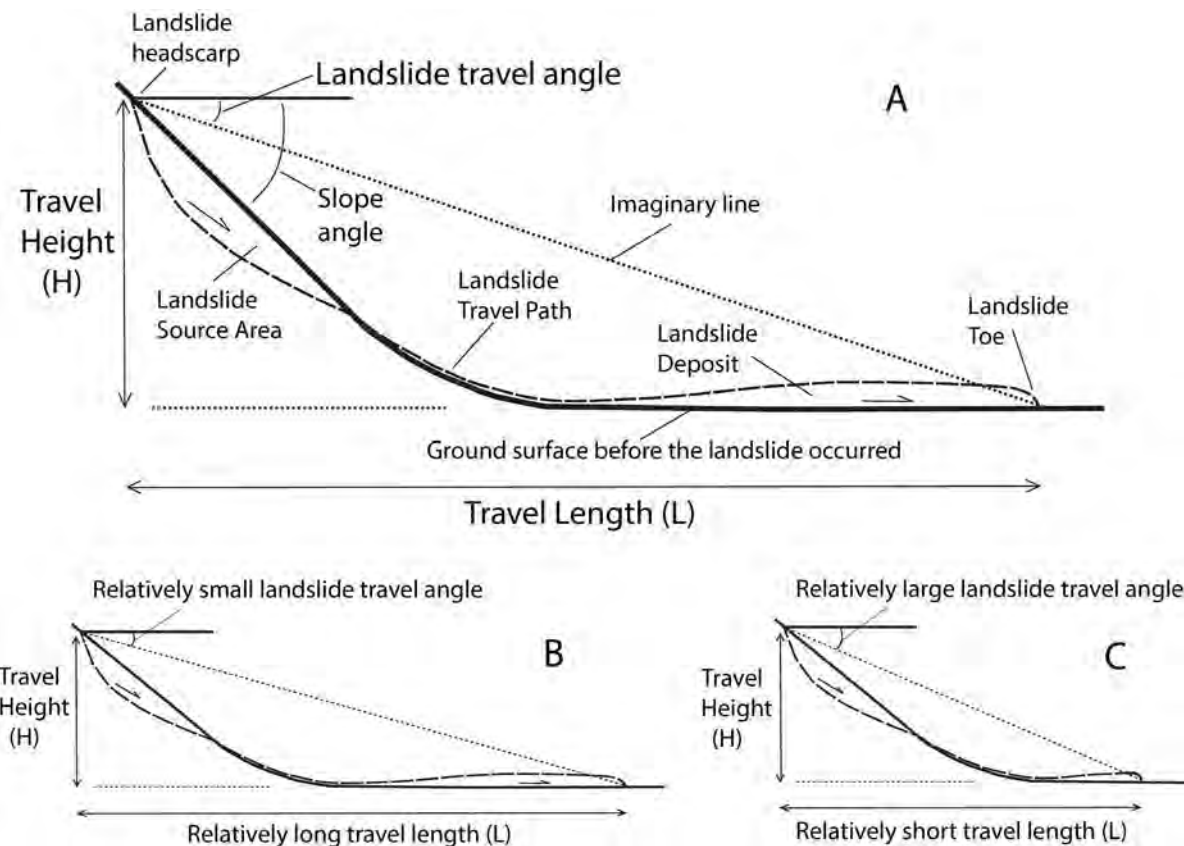


Figure 3. Diagram showing: (A) landslide travel height, travel length, and travel angle with respect to source area and deposit. (B) The relation between a relatively small travel angle and long travel distance. (C) The relation between a relatively large travel angle and short travel distance. See Corominas (1996) for additional details.

pressures within rock fractures, thereby increasing the likelihood of landslides. The last factor is due to the location of GBNPP along an active tectonic plate boundary. In the interim between large earthquakes along this boundary, strain (deformation) in the crust accumulates and can structurally weaken rock masses, thereby leading to increased susceptibility to the first three factors that contribute to landslides.

The long and narrow geometry of inlets in Glacier Bay lend themselves to destructive tsunamis. Narrow inlets and fjords can cause amplification of waves and unpredictable wave oscillations from tsunamigenic landslides (e.g., Geist et al. 2003, Harbitz et al. 2014). Large variations in wave characteristics, inundation height, and current velocity can result from variations in local bathymetry and the irregular geometry of the coastline, and wave activity can last for hours after an initial wave (Harbitz et al. 1993, Geist et al. 2003, Harbitz et al. 2014).

Determining Where Landslides Could Cause Tsunamis

As previously stated, our primary goal in this article is to determine areas in the West Arm of Glacier Bay

where subaerial landslides could enter the water and potentially initiate tsunamis. To meet this goal, we (1) determined subaerial areas that are susceptible to landslides, and (2) forecasted areas where these landslides could travel, including whether they could reach the water. Previous work has shown that the characteristics of tsunamis generated from subaerial landslides entering water are determined by both the landslide characteristics at impact with the water and by the dynamics of landslides once they are in the water (e.g., Mohammed and Fritz 2012, Yavari-Ramshe and Ataie-Ashtiani 2016).

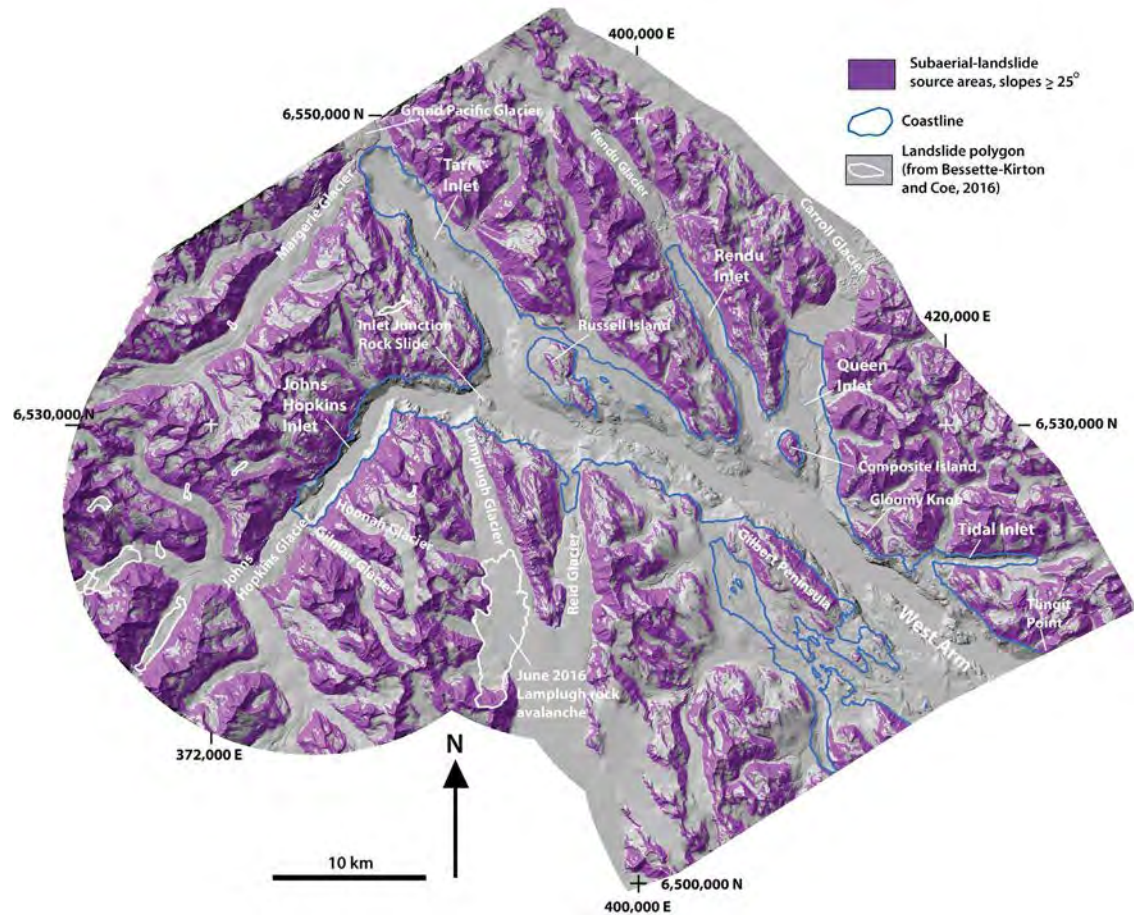
We currently lack detailed knowledge of geologic units, structures, and past failures along the coastline of Glacier Bay that could be used to define varying levels of subaerial landslide susceptibility. So, for our work, we assume that mountainsides that have adequate steepness to produce landslides, have equal potential to produce them. To delineate areas capable of generating landslides in GBNPP, we used data from Bessette-Kirton and Coe (2016). Specifically, we used headscarp locations for 24 rock avalanches in the Bessette-Kirton and Coe (2016) database and extracted slope values from a 10 m digital elevation model (DEM) for each location. These slope values showed that the rock avalanches initiated from slopes $>26^\circ$. For our work in this article, we were slightly conservative and defined areas susceptible to landslides (source areas) as areas that had slope values $>25^\circ$.

To estimate potential travel distances for landslides that initiate from source areas, we used landslide-travel angles (Figure 3) defined by landslide-travel height (H) and travel length (L) values contained in Bessette-Kirton and Coe (2016). A travel angle is the angle determined by an imaginary line connecting the landslide headscarp to the landslide toe, and, as such, should not be confused with slope angle, which is the inclination of the ground surface at any

given location (Figure 3A). Landslides with low-travel angles have long travel distances compared to landslides with higher-travel angles (Figures 3B and C). Data from Bessette-Kirton and Coe (2016) showed that travel angles for the 24 historical rock avalanches ranged from 9 to 31°, with a mean value of 19°.

We used the gravitational flow routing model Flow-R (Horton et al. 2013) to estimate potential-landslide travel distances. Flow-R has been used by the Geological Survey of Norway to model rockslides and rock avalanches in fjords, a very similar setting to Glacier Bay (Oppikofer et al. 2016). We used Flow-R to estimate landslide distances both on land and in the water. One limitation is that Flow-R does not distinguish differences in the physics controlling landslide movement and dynamics in these two environments. In other words, we used Flow-R to simulate a landslide-travel path across a continuous merged elevation surface of both subaerial and submarine topography. A similar subaerial and submarine landslide routing approach was used by Mazzanti and Bozzano (2011) to investigate the Scilla landslide and tsunami in southern Italy.

Input data for Flow-R consisted of a 30 m DEM of combined subaerial and submarine topography; our pre-defined landslide-source areas, which correspond to thousands of 30 m x 30 m DEM cells; and three travel angles, 9°, 19°, and 31°, which established thresholds for progressively higher levels of relative probability for landslide-travel distances. Subaerial DEM data were from the USGS National Elevation Dataset (USGS 2018b) and submarine data (i.e., bathymetric data) were from the National Oceanic and Atmospheric Administration (NOAA 2018). Within Flow-R, we used the modified Holmgren (1994) algorithm with a direction memory inertial algorithm (Horton 2018) to model the travel distance of landslides that could initiate from



source areas. We used the three landslide-travel angles to define high, medium, and low levels of relative probability for landslide-travel distances. These different relative-travel probabilities can be interpreted as the relative probability of areas being impacted by landslides, with areas encompassed by high-travel angles having a higher probability of being impacted than areas defined by low-travel angles (see Figure 3B and C). This relative probability ranking is intuitive in that it indicates that areas closest to landslide-source areas will have a higher chance of being impacted than areas that are farther away from source areas.

Figure 4. Map showing potential subaerial-landslide source areas in the West Arm study area. Coordinates shown are UTM zone 8.

Results and Implications

Subaerial locations that are susceptible to landslides surrounding the West Arm are shown in Figure 4. Figure 5 shows the relative probability of areas being impacted by landslides that initiate from subaerial source areas surrounding the West Arm. Figure 6 is a simplified version of Figure 5 in that it shows the relative probability for landslide impact

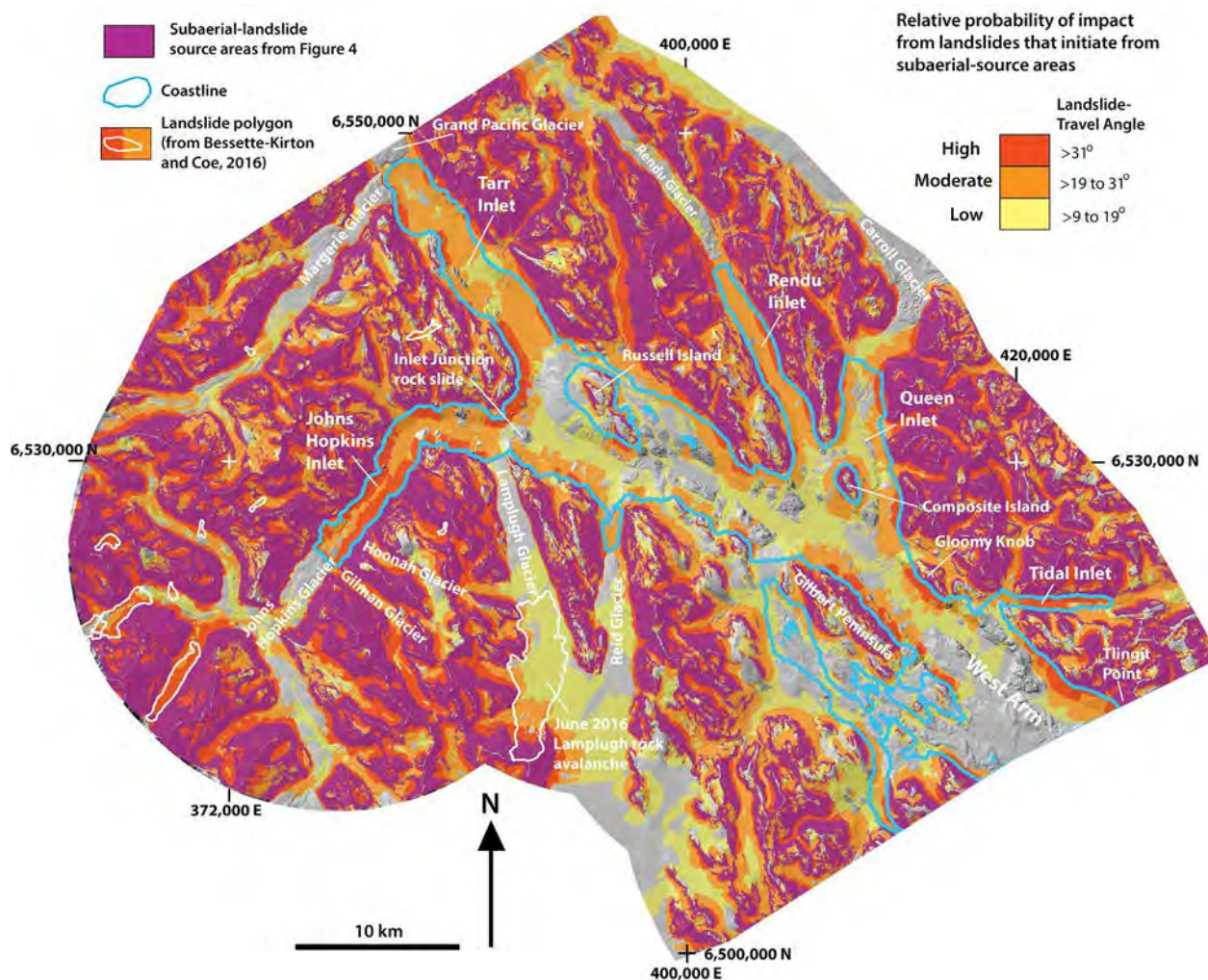


Figure 5. Map showing modeled relative probability of impact from landslides that initiate from subaerial source areas shown in purple. The landslides were routed both above, and below water using Flow-R software, with the boundary of each impact zone determined using travel angles from historical subaerial landslides. The coastline is shown with blue lines. The map does not portray impact zones for landslides that initiate from areas that are underwater (i.e., submarine landslides). Coordinates shown are UTM zone 8.

at the coastline of the West Arm. Said another way, Figure 6 shows the relative probability of landslides entering the water along the coastline of the West Arm. Figures 5 and 6 indicate that there are large areas of moderate- to high-relative probability for landslide impacts in the Johns Hopkins, Tarr, Rendu, and Tidal Inlets. Other locations with extensive moderate to high probability of impact are the eastern and western shores of Queen Inlet, the eastern side of Gilbert Peninsula, the western side of Gloomy Knob, the eastern shore of the West Arm between Tidal Inlet and Tlingit Point. Figures 5 and 6 can be used to prioritize areas in and around the West Arm where further, more detailed subaerial landslide and landslide-generated tsunami investigations are needed.

Results shown in Figures 4, 5, and 6 do not account for landslides that initiate underwater. However, we examined the morphology of submarine features revealed by bathymetric data in our preparation of this article. Our examination led us to discover a large rockslide (Figure 7) near the junction of Johns Hopkins and Tarr Inlets (Figures 1, 4, 5, and 6), which we herein call the Inlet Junction rockslide (IJRS). We know the IJRS occurred sometime after 1892, because that is when the toe of the Johns Hopkins glacier covered the location where the landslide is located (e.g., Seramur et al. 1997). The deposit of the IJRS is almost entirely underwater, but the headscarp is above water and is clearly identifiable by its characteristic arcuate shape and higher elevation compared to the upper most, subaerial part of the deposit (Figure 7). Based on the dimensions and cross section through the IJRS, we estimate that its minimum volume is about 105 M yard³ (80 M m³), which makes it the largest known landslide within GBNPP. The headscarp of the IJRS is delineated as a source area in Figure 4 and the deposit is in the moderate and low landslide-

impact probability zones (Figure 5). The relatively low-travel angle indicates that the rockslide had a relatively long-travel distance (L; about 7,315 feet or 2,230 m) with respect to a relatively small change in elevation between the headscarp and the toe (H; about 1,410 feet or 430 m). This example highlights our knowledge gap regarding submarine landslides in Glacier Bay. For example, the relatively low-travel angle may be because the rockslide moved over and “loaded” water-saturated soft sediments. Loading of saturated sediments can rapidly elevate pore-water pressures within the sediments, which could work to enhance landslide travel distance. Another issue that is uncertain is whether or not this mostly submarine landslide would have caused a tsunami. Tsunami generation from landslides is based on the volume, dimensions, velocity, and internal deformation of the moving mass, as well as the depth of water (e.g., Ward 2001, Yavari-Ramshe and Ataie-Ashtiani 2016). Tsunami modeling at this location using a range of landslide volumes and dynamics would help to improve our understanding of tsunami hazards from submarine landslides in GBNPP.

To more accurately understand the subaerial landslide and landslide-generated tsunami hazards in the moderate- to high-probability landslide-impact areas (Figures 5 and 6), as well as other areas of Glacier Bay, several approaches could be taken. First, the moderate- to high-probability areas should be visited in the field to better characterize the geology at a scale appropriate for hazard assessments (1:20,000 or larger). This field work would serve to better differentiate landslide susceptibility. For example, it is possible that some areas of the bay that have been identified as having moderate-to-high landslide-impact probability, could have source areas with low susceptibility to failure, that is, they may be stable. Other areas, such as the Tidal Inlet landslide described by Wieczorek et al. (2007), would have a

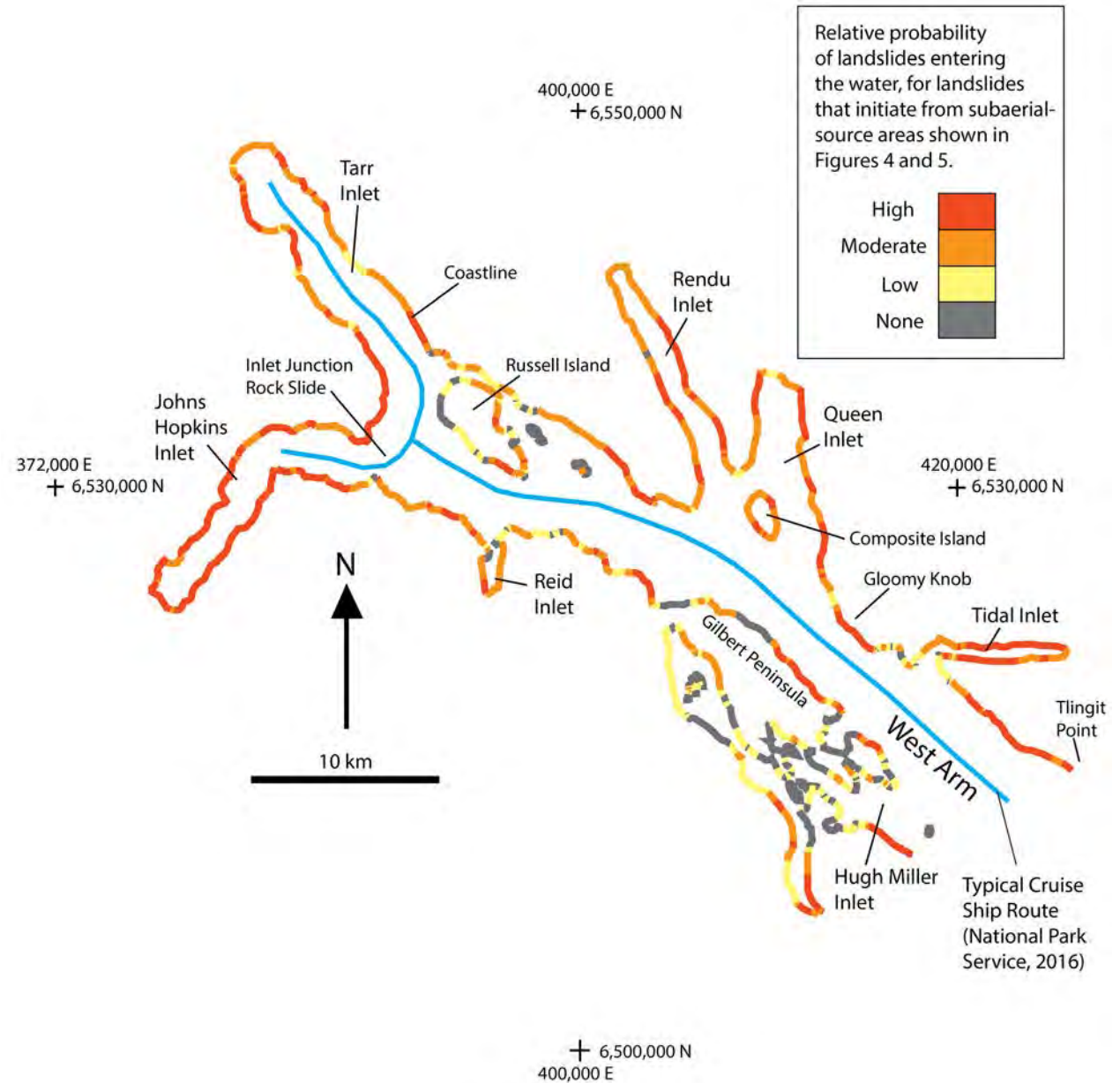


Figure 6. Map showing the relative probability of landslides entering the water along the coastline of the West Arm. Map is derived from landslide-impact zones shown in Figure 5. Coordinates shown are UTM zone 8.

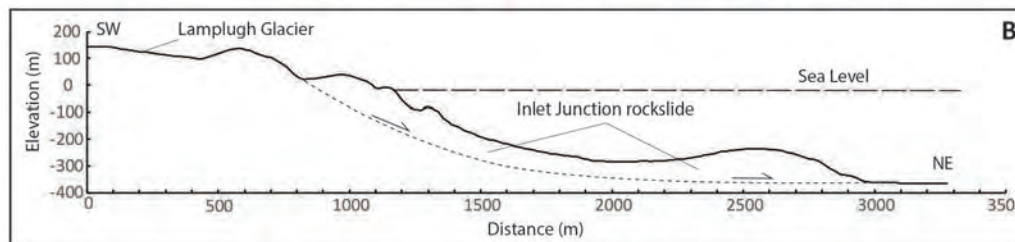
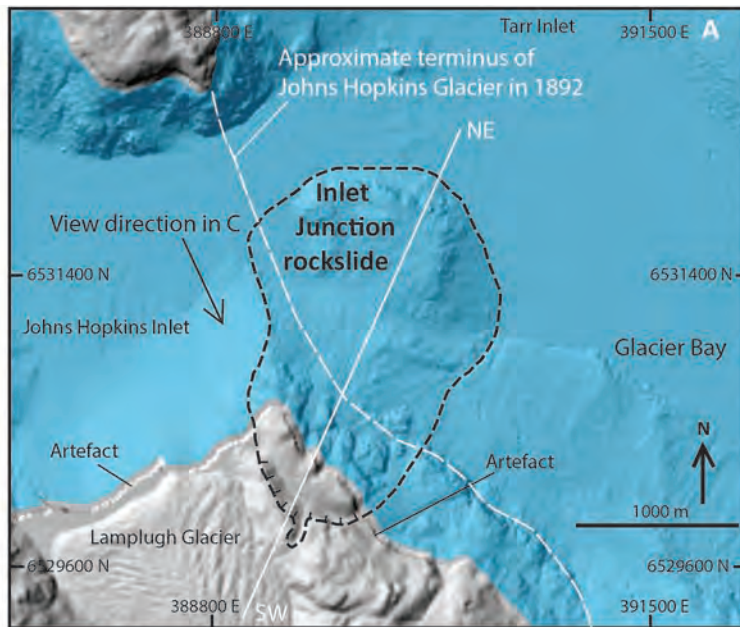
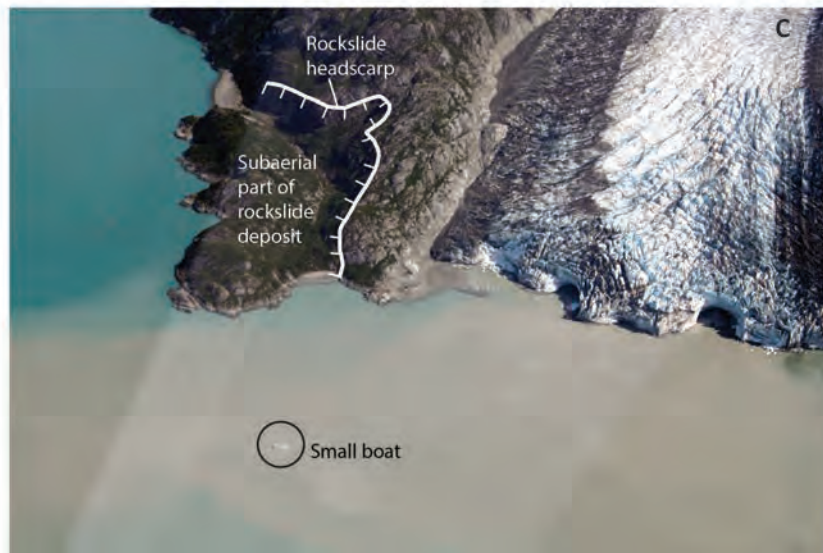


Figure 7. (A) Diagram showing approximate outline of the Inlet Junction rockslide. See Figures 4-6 for location. Blue color shows areas that are under water. (B) Cross section through the Inlet Junction rockslide. (C) Photograph of the subaerial portion of the rockslide near the terminus of the Lamplugh Glacier taken July 13, 2009 by Mike and Susan Molloy. Width of the Lamplugh Glacier visible in this photo is about 2,625 feet (800 m). View is to the southeast. See <https://molloy2009ak.blogspot.com/2009/07/glacier-bay-flight-seeing-july-13.html> for additional details.



high-susceptibility ranking because of their history of movement. Second, for areas that are deemed to be highly susceptible to failure from field investigations, estimating landslide volumes and modeling landslide runout would enable an assessment of the size, character, and velocity of landslides that could enter the water. The acquisition of new, high-resolution topographic data (i.e., lidar data) for GBNPP would greatly aid this effort. Additionally, systematic monitoring of steep slopes along the coastline using remote sensing techniques such as interferometric synthetic-aperture radar (InSAR) or multitemporal photogrammetry could potentially be used to detect slow movement or deformation prior to catastrophic failure (e.g., Higman et al. 2018, Roberti et al. 2018). Lastly, as with submarine landslides, tsunami modeling to assess the size, velocity, and duration of waves generated from subaerial landslides entering the water would help to determine the size of a boat or ship that could be threatened by landslide-generated waves.

Acknowledgements

We thank Matthew Thomas, Eric Bilderback, Lisa Etherington, Chad Hults, Nina Chambers, Janet Slate, Leigh Welling, and Jim Lawler for their constructive reviews of this article. Thierry Oppikofer provided helpful advice regarding the use of Flow-R. Any use of trade, firm, or product names is for descriptive purposes only and does not imply endorsement by the U.S. Government.

REFERENCES

- Bessette-Kirton, E. K. and J. A. Coe. 2016.**
Inventory of rock avalanches in western Glacier Bay National Park and Preserve, Alaska, 1984-2016. A baseline data set for evaluating the impact of climate change on avalanche magnitude, mobility, and frequency. U.S. Geological Survey data release, doi: 10.5066/F7C827F8
- Bessette-Kirton, E. K., J. A. Coe, and W. Zhou. 2018.**
Using stereo satellite imagery to account for ablation, entrainment, and compaction in volume calculations for rock avalanches on glaciers: Application to the 2016 Lamplugh rock avalanche in Glacier Bay National Park, Alaska. *Journal of Geophysical Research - Earth Surface* 123(4): 622-641. doi: 10.1002/2017JF004512
- Brew, D. A., B. R. Johnson, D. Grybeck, A. Griscom, D. F. Barnes, A. L. Kimball, J. C. Still, and J.L. Rataj. 1978.**
Mineral resources of the Glacier Bay National Wilderness study area, Alaska. U.S. Geological Survey Open-File Report 78-494, U.S. Geological Survey, Reston, Virginia, 670 p., 6 sheets, scale 1:125,000. <https://pubs.er.usgs.gov/publication/ofr78494>
- Brothers, D. S., B. D. Andrews, M. A. L., Walton, H. G. Greene, J. V. Barrie, N. C. Miller, U. Ten Brink, East, A. E., P. J. Haeussler, J. W. Kluesner, and J. E. Conrad. 2018.**
Slope failure and mass transport processes along the Queen Charlotte Fault, southeastern Alaska. Geological Society, London, Special Publications, 477. <https://doi.org/10.1144/SP477.30>
- Coe, J. A., E. K. Bessette-Kirton, and M. Geertsema. 2018.**
Increasing rock-avalanche size and mobility in Glacier Bay National Park and Preserve, Alaska detected from 1984–2016 Landsat imagery. *Landslides* 15(3): 393–407. <https://doi.org/10.1007/s10346-017-0879-7>
- Connor, C., G. Streveler, A. Post, D. Monteith, and W. Howell. 2009.**
The Neoglacial landscape and human history of Glacier Bay, Glacier Bay National Park and Preserve, southeast Alaska, USA. *Holocene* 19:381-393. doi: 10.1177/0959683608101389
- Corominas, J. 1996.**
The angle of reach as a mobility index for small and large landslides. *Canadian Geotechnical Journal* 33:260–271. doi: 10.1139/t96-005
- Elliott, J. L., C. F. Larsen, J. T. Freymueller, and R. J. Motyka. 2010.**
Tectonic block motion and glacial isostatic adjustment in southeast Alaska and adjacent Canada constrained by GPS measurements. *Journal of Geophysical Research* 115, B09407, doi:10.1029/2009JB007139
- Evans, S.G., and J. J. Clague. 1999.**
Rock avalanches on glaciers in the Coast and St. Elias Mountains, British Columbia. In: Slope stability and landslides. Proceedings of the 13th Annual Geotechnical Society Symposium, Vancouver, B.C., 115-123. https://www.researchgate.net/publication/283476315_Rock_avalanches_on_glaciers_in_the_Coast_and_St_Elias_Mountains_British_Columbia
- Fritz, H. M., F. Mohammed, and J. Yoo. 2009.**
Lituya Bay landslide impact generated mega-tsunami. 50th anniversary: *Pure and Applied Geophysics* 166:153-175, doi:10.1007/s00024-008-0435-4
- Geist E. L., M. Jakob, G. F. Wiczorek, and P. Dartnell. 2003.**
Preliminary hydrodynamic analysis of landslide-generated waves in Tidal Inlet, Glacier Bay National Park, Alaska. U.S. Geological Survey Open-File Report 03-411, 20 p. <https://pubs.usgs.gov/of/2003/0411/>
- Geertsema, M. 2012.**
Initial observations of the 11 June 2012 rock/ice avalanche, Lituya Mountain, Alaska. The First Meeting of Cold Region Landslides Network, Harbin, China, 5 p. 10.13140/2.1.2473.5682
- Geertsema, M., J. J. Clague, and A. Hasler. 2013.**
Influence of climate change on geohazards in Alaskan Parks. *Alaska Park Science* 12:81-85. http://www.nps.gov/akso/nature/science/ak_park_science/PDF/Vol12-2/APS_Vol12-Issue2_complete.pdf
- Gruber, S. 2012a.**
Derivation and analysis of a high resolution estimate of global permafrost zonation. *The Cryosphere* 6:221-233. doi:10.5194/tc-6-221-2012
- Gruber, S. 2012b.**
Global Permafrost Zonation Index Map. Available at: http://www.geo.uzh.ch/microsite/cryodata/pf_global/ (accessed July, 2017)
- Haeussler, P. J., S. P. S. Gulick, N. McCall, M. Walton, R. Reece, C. Larsen, D. H. Shugar, M. Geertsema, J. G. Venditti, and K. Labay. 2018.**
Submarine deposition of a subaerial landslide in Taan Fiord, Alaska. *Journal of Geophysical Research - Earth Surface* 123(10):2443-2463. <https://doi.org/10.1029/2018JF004608>
- Harbitz, C. B., S. Glimsdal, F. Løvholt, V. Kveldevisk, G. K. Pedersen, and A. Jensen. 2014.**
Rockslide tsunamis in complex fjords: From an unstable rock slope at Åkerneset to tsunami risk in western Norway. *Coastal Engineering* 88: 101-122.
- Harbitz, C. V., G. Pedersen, and B. Gjevik. 1993.**
Numerical simulations of large water waves due to landslides. *Journal of Hydraulic Engineering* 119(12): 1325-1342.
- Higman, B., D. H. Shugar, C. P. Stark, G. Ekström, M. N. Koppes, P. Lynett, A. Dufresne, P. J. Haeussler, M. Geertsema, S. Gulick, A. Mattox, J. G. Venditti, M. A. L. Walton, N. McCall, E. Mckittrick, B. MacInnes, E. L. Bilderback, H. Tang, M. J. Willis, B. Richmond, R. S. Reece, C. Larsen, B. Olson, J. Capra, A. Ayca, C. Bloom, H. Williams, D. Bonno, R. Weiss, A. Keen, V. Skanavis, and M. Loso. 2018.**
The 2015 landslide and tsunami in Taan Fiord, Alaska. *Scientific Reports* 8:12993. doi: 10.1038/s41598-018-30475-w
- Holmgren, P. 1994.**
Multiple flow direction algorithms for runoff modelling in grid based elevation models: An empirical evaluation. *Hydrologic Processes* 8: 327–334, doi:10.1002/hyp.3360080405.

Horton, P., M. Jaboyedoff, B. Rudaz, and M. Zimmermann. 2013.

Flow-R, a model for susceptibility mapping of debris flows and other gravitational hazards at a regional scale. *Natural Hazards Earth System Science* 13:869-885, doi:10.5194/nhess-13-869-2013.

Horton, P. M. 2018.

Flow-R software web site. Available at: <http://www.flow-r.org/> (accessed September 2, 2018)

Husson, L., T. Bodin, G. Spada, G. Choblet, and C. Kreemer. 2018.

Bayesian surface reconstruction of geodetic uplift rates: Mapping the global fingerprint of glacial isostatic adjustment. *Journal of Geodynamics* 122: 25-40. <https://doi.org/10.1016/j.jog.2018.10.002>

Janiskee, B. 2011.

By the numbers: Glacier Bay National Park and Preserve: National Parks Traveler. Available at: <https://www.nationalparkstraveler.org/2011/06/numbers-glacier-bay-national-park-and-preserve8248> (accessed on February 17, 2019)

Larsen, C. F., R. J. Motyka, J. T. Freymueller, K. A. Echelmeyer, and E. R. Ivins. 2005.

Rapid viscoelastic uplift in southeast Alaska caused by post-Little Ice Age glacial retreat. *Earth and Planetary Science Letters* 237: 548-560. doi: 10.1016/j.epsl.2005.06.032

Mazzanti, P. and F. Bozzano. 2011.

Revisiting the February 6th 1783 Scilla (Calabria, Italy) landslide and tsunami by numerical simulation. *Marine Geophysical Research* 32:273-286. doi: 10.1007/s11001-011-9117-1.

Miller, D. J. 1960.

Giant waves in Lituya Bay Alaska. U.S. Geological Survey Professional Paper 354-C, pp. 51-86, one 1:50,000 scale sheet. <https://pubs.usgs.gov/pp/0354c/report.pdf>

Mohammed, F. and H.M. Fritz. 2012.

Physical modeling of tsunamis generated by three-dimensional deformable granular landslides.

Journal of Geophysical Research 117:C11015. doi:10.1029/2011JC007850

National Park Service. 2016.

Typical cruise ship route in Glacier Bay. Available at: <https://www.nps.gov/glba/planyourvisit/typical-cruise-ship-route-in-glacier-bay.htm> (accessed on August 16, 2018)

National Park Service. 2018a.

Landslides and Giant Waves. Available at: <https://www.nps.gov/glba/planyourvisit/landslides-and-giant-waves.htm> (accessed on August 19, 2018)

National Park Service. 2018b.

Glacier Bay: 2018 Fact Sheet. Available at: <https://www.nps.gov/glba/learn/management/glacier-bay-fact-sheet.htm> (accessed July 10, 2018)

NOAA. 2018.

Bathymetry data. Available at: <https://maps.ngdc.noaa.gov/viewers/bathymetry/> (accessed August 2018)

Oppikofer, T., R. L. Hermanns, G. Sandøy, M. Böhme, M. Jaboyedoff, P. Horton, N. J. Roberts, and H. Fuchs. 2016.

Quantification of casualties from potential rock-slope failures in Norway. In: Aversa, S., Cascini, L., Picarelli, L., and Scavia, C., Landslides and Engineered Slopes, Experience, Theory, and Practice. CRC Press, pp. 1537-1544.

Pflaker, G., T. Hudson, T. Bruns, and M. Rubin. 1978.

Late Quaternary offsets along the Fairweather fault and crustal plate interactions in southern Alaska. *Canadian Journal of Earth Sciences* 15:805-816. doi: 10.1139/e78-085

Post, A. 1967.

Effects of the March 1964 Alaska earthquake on glaciers. U.S. Geological Survey Professional Paper 544-D, 42 p. <https://pubs.usgs.gov/pp/0544d/>

Pudasaini, S. P. and M. Krautblatter. 2014.

A two-phase mechanical model for rock-ice avalanches. *Journal of Geophysical Research* 119(10): 2272-2290. <https://doi.org/10.1002/2014JF003183>

Roberti, G., B. Ward, B. van Wyk de Vries, P. Friele, L. Perotti, J.J. Clague, and M. Giardino. 2018.

Precursory slope distress prior to the 2010 Mount Meager landslide, British Columbia. *Landslides* 15:637-647. doi: 10.1007/s10346-017-0901-0

Seramur, K., R. Powell, and P. Carlson. 1997.

Evaluation of conditions along the grounding line of temperate marine glaciers: an example from Muir Inlet, Glacier Bay, Alaska. *Marine Geology* 140:307-327.

Stevens, D., G. Wolken, T. Hubbard, and K. Hendricks. 2018.

Landslides in Alaska: Alaska Division of Geological & Geophysical Surveys Circular 65, 2 p. <http://doi.org/10.14509/29849>

Suleimani, E., D. Nicolisky, and R. Koehler. 2015.

Tsunami inundation maps of Elfin Cove, Gustavus, and Hoonah, Alaska: Alaska Division of Geological & Geophysical Surveys, Report of Investigations 2015-1, 79 p., 3 map sheets. <http://dggs.alaska.gov/pubs/id/29404>

USGS. 2018a.

Earthquake Hazards earthquake catalog. <https://earthquake.usgs.gov/earthquakes/eventpage/iscgem884702#executive>

USGS. 2018b.

National Elevation Dataset (NED) web site. Available at: <http://nationalmap.gov/elevation.html> (accessed August 2018)

USGS. 2019.

Earthquake Hazards earthquake catalog. Available at: <https://earthquake.usgs.gov/earthquakes/search/> (accessed February 2019)

van Oldenborgh, G. J., M. Collins, J. Arblaster, J. H. Christensen, J. Marotzke, S. B. Power, M. Rummukainen, and T. Zhou. 2013.

Annex I: Atlas of global and regional climate projections. In: Stocker, T. F., Qin, D., Plattner, G. -K., Tignor, M., Allen, S. K., Boschung, J., Nauels, A., Xia, Y., Bex, V., Midgley, P. M., (eds.), *Climate Change 2013: The Physical Science Basis. Contribution of*

Working Group I to the Fifth Assessment Report of the Intergovernmental Panel on Climate Change. Cambridge University Press, Cambridge and New York, NY, pp. 1311-1393. https://www.ipcc.ch/pdf/assessment-report/ar5/wg1/WG1AR5_AnnexI_FINAL.pdf

Walsh, J., D. Wuebbles, K. Hayhoe, K. Kossin, K. Kunkel, G. Stephens, P. Thorne, R. Vose, M. Wehner, J. Willis, D. Anderson, S. Doney, R. Feely, P. Hennon, V. Kharin, T. Knutson, F. Landerer, T. Lenton, J. Kennedy, and R. Somerville. 2014.

Chapter 2: Our changing climate. In: Melillo, J. M., Richmond, T. C., Yohe G. W., (eds.), Climate change impacts in the United States: The third national climate assessment, U.S. Global Change Research Program. pp. 19-67. <http://nca2014.globalchange.gov/report>

Walsh J. E., P. A. Bieniek, B. Brettschneider, E. S. Euskirchen, R. Lader, and R. L. Thoman. 2017.

The exceptionally warm winter of 2015/16 in Alaska. *Journal of Climate* 30:2069–2088. <https://doi.org/10.1175/JCLI-D-16-0473.1>

Ward, S. N. 2001.

Landslide tsunami. *Journal of Geophysical Research* 106(6):11,201-11,215.

Wieczorek, G. F., M. Jakob, R. J. Motyka, S. L. Zirnheld, and P. Craw. 2003.

Preliminary assessment of landslide-induced wave hazards: Tidal Inlet, Glacier Bay National Park, Alaska: U.S. Geological Survey Open File Report 03-100. <https://pubs.usgs.gov/of/2003/ofr-03-100/ofr-03-100.html>

Wieczorek, G. F., E. L. Geist, R. J. Motyka, and M. Jakob. 2007.

Hazard assessment of the Tidal Inlet landslide and potential subsequent tsunami, Glacier Bay National Park, Alaska. *Landslides* 4:205-215. doi: 10.1007/s10346-007-0084-1

Wilson, F. H., C. P. Hulst, C. G. Mull, S. M. Karl. 2015.

Geologic map of Alaska: U.S. Geological Survey Scientific Investigations Map 3340, 197 p., 2 sheets, scale 1:584,000, doi: 10.3133/sim3340.

Yavari-Ramshe, S. and B. Ataie-Ashtiani. 2016.

Numerical modeling of subaerial and submarine landslide-generated tsunami waves—recent advances and future challenges. *Landslides* 13:1325-1368. doi:10.1007/s10346-016-0734-2



Risk and Recreation in a Glacial Environment: Understanding Glacial Lake Outburst Floods at Bear Glacier in Kenai Fjords National Park

Deb Kurtz, Kenai Fjords National Park

Gabriel Wolken, Alaska Division of Geological and Geophysical Surveys

Glaciers and the landscapes they create are beautiful, dynamic places to experience as a distant observer, skilled adventurer, or inquisitive scientist. They can also be dangerous; ice falls, calvings, collapses, and outburst floods can and do occur without warning. We study and monitor Bear Glacier to better understand hydrological processes leading to glacial lake outburst floods so we can mitigate their impacts.

Citation:

Kurtz, D. and G. Wolken. 2019. Risk and recreation in a glacial environment: Understanding glacial lake outburst floods at Bear Glacier in Kenai Fjords National Park. *Alaska Park Science* 18(1): 38-43.

The dynamic forces at work in coastal south-central Alaska where glaciers, mountains, and oceans meet provide rich habitats, scenic vistas, and outstanding recreational opportunities. These extreme environments can also result in geohazards such as landslides, floods, and other glacier-related risks. Here we present our efforts to understand a reoccurring glacial lake outburst flood affecting a popular recreational area in Kenai Fjords National Park and preliminary results from a glacial lake outburst flood that occurred in August 2018.

Kenai Fjords National Park is located on the southeastern edge of the Kenai Peninsula in southcentral Alaska. It is characterized by rugged mountains, a jagged coastline, and large dynamic glaciers that cover nearly half of the park. Most of these glaciers descend from the Harding Icefield, a mass of ice covering nearly 700 square miles (1,800 km²). Visitors come from around the world to see, explore, and experience the glaciers. Of particular interest is Bear Glacier, the longest glacier in the park, situated between the tidewater glaciers that occupy the fjords in the south and land-locked Exit Glacier in the north. Bear Glacier is one of four lake-terminating glaciers in the park and is the closest one to the city of Seward, making it the most accessible to visitors. The unnamed proglacial lake where Bear Glacier terminates is a surreal landscape where calm turquoise waters full of glacial silt invite visitors to kayak and stand-up paddleboard (SUP) among towering icebergs, surrounded by steep mountain

slopes and the terminus of Bear Glacier itself (Figure 1). Local commercial outfitters have capitalized on the remarkable recreational opportunities provided by this striking environment by providing day or overnight kayaking trips and SUP adventures, accessing the lake by helicopter, jet boat, or landing craft.

In recent years, marketing of these activities near Bear Glacier has increased and become more widespread via print periodicals (Shivley 2013, Parsons 2016), often with fabulous cover photos highlighting recreational activities at Bear Glacier as the cover story (Dickerson 2016, Parsons 2016), and through online social media (both commercial and personal) resulting in increased interest in this area. One local kayak guiding company reported that people have walked into their office with a magazine photo of a person on a SUP in front of a glacier and stated: "I want to do this!" The same glacial environment that attracts people also poses risks. Sudden, dynamic events such as iceberg calving, calving-induced seiches (waves), and glacial lake outburst floods (GLOFs) are natural occurrences in these environments. Bear Glacier, in particular, is becoming well known among Seward's summer residents for its GLOFs.

GLOFs occur when water stored on, under, adjacent to, or within a glacier is suddenly released, causing water levels in the rivers and lakes downstream of the glacier to increase rapidly. These

Figure 1. The proglacial lake at Bear Glacier is a popular site for watersports. Photo courtesy of NPS/D. Kurtz, September 2015.

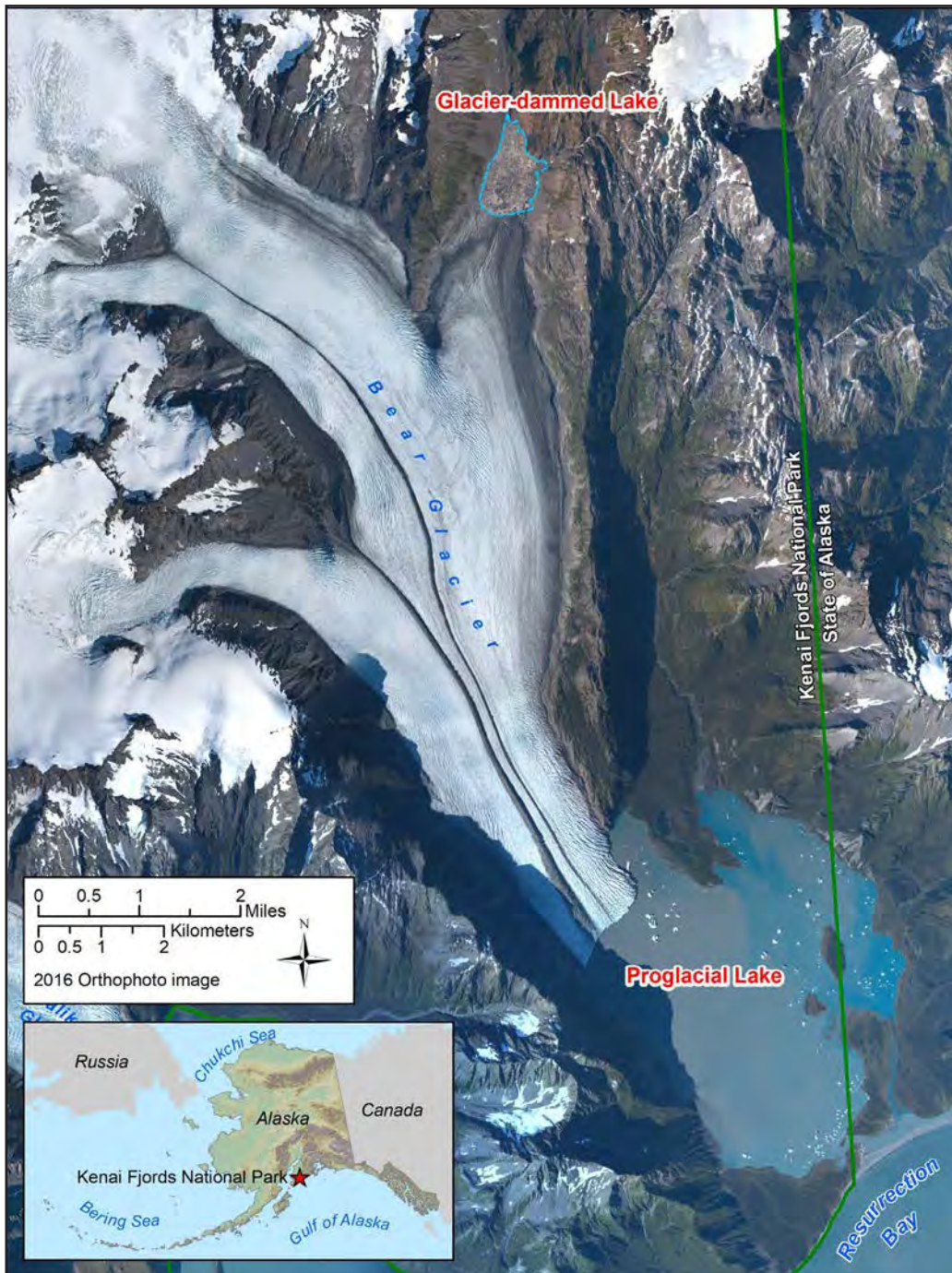


Figure 2. Map of Bear Glacier showing the glacier-dammed lake and proglacial lake.

releases often result in floods that are one or two orders of magnitude greater than precipitation-driven events. GLOFs occur at various locations on the Kenai Peninsula including Skilak, Snow, and Bear glaciers as well as many other locations around Alaska (Post and Mayo 1971).

Seven miles (12 km) above the terminus of Bear Glacier an unnamed lake occupies an ice-free tributary valley (Figure 2). Bear Glacier blocks the natural drainage path of this valley and creates a lake. Every few years the lake empties, sending enormous volumes of water under Bear Glacier and down to its terminus, where it floods the proglacial lake. According to anecdotal reports from backcountry outfitters guiding in the proglacial lake at Bear Glacier, the resultant high water levels can persist for a period of several days to several weeks before subsiding to normal levels. Although known to occur, we do not understand the timing or the causes that trigger the drainage events that cause these floods.

Knowledge of this present-day glacier-dammed lake on Bear Glacier pre-dates establishment of Kenai Fjords National Park. Marcus identified this lake in an inventory of glacier-dammed lakes in the Chugach and Kenai Mountains in a 1968 report, but there was no discussion of GLOFs associated with this lake at that time (Marcus 1968). This may have been due to little human-presence and/or use in front of the glacier, likely because the terminus of Bear Glacier extended farther out, filling most of the present-day proglacial lake.

Up until 2008, GLOFs and their potential risks at Bear Glacier were of limited concern to park managers, due to low visitation and low park staff presence in the proglacial lake. As local tour companies began to guide visitors into the proglacial lake more frequently, they started to observe a pattern of floods occurring every 2-3 years. Icebergs

often choked the mouth of the outflow river between the lake and the bay, preventing access by jet boat or landing craft. Occasionally, water bypassed the river and ran over the moraine that separates the lake and the bay. With increased visitor use came increased awareness of the phenomenon, as well as increased risk to people and property.

In August 2014, a GLOF occurred at Bear Glacier that raised water levels until they eroded the moraine separating the lake and outlet from the ocean. This resulted in a full breach of the moraine and allowed silt-laden, freshwater from the lake to pour directly into the bay. This breach was immediately followed by a dramatic drop in the water levels in the proglacial lake. Although no one was injured during this outburst event, there were reports that kayaks and a canoe were washed out into the bay. Fortunately, this flood occurred near the end of the visitor season, a time of reduced recreational use in the proglacial lake. Although the presence of people allowed detection of the event, it also created risk.

While our awareness of this glacier-dammed lake and the GLOFs it creates has increased, many questions related to the mechanisms, timing, and frequency of this drainage remain. In 2012, Kenai Fjords park staff and researchers at the University of Montana attempted to (1) identify historical changes in the water level of the glacier-dammed lake and (2) measure the timing and frequency of a real-time drainage event to better quantify potential hazards associated with the GLOF (Wilcox et al. 2014). This work resulted in a history of changes to the glacier-dammed lake area and an inventory of evidence of drainage events from the last decade. The researchers' recommendations included continued study of the glacier-dammed lake through remotely sensed and on-site data collection and analysis.

In 2017, Kenai Fjords National Park and State of Alaska Division of Geological and Geophysical Surveys researchers installed a satellite-telemetered camera at the glacier-dammed lake. This timelapse camera takes a daily photo and, within a couple hours, emails it to us via satellite (Figure 3). This method and equipment allow us to monitor the filling and drainage of the lake without risk of losing the equipment during a drainage and provide us with near-real time information of the status of the lake. These observations can be used with elevation data to help us to calculate water levels and volume.

Although we would like to measure water depth directly from the glacier-dammed lake itself, there are numerous challenges to installing any equipment in the lake. Two previous attempts to do so resulted in loss of equipment, likely due to ice scouring or strong currents that formed during the drainage. Also, installation requires traversing steep, loose scree slopes to access the edge of the lake. Finally, it is difficult to calculate the difference in lake levels at the time of installation and the time of removal. That information is critical to prevent the equipment from sitting on the bottom of the lake where it could get buried in sediment, damaged by ice, or become inaccessible due to high water levels.

A second timelapse camera was installed next to the proglacial lake near the glacier terminus. Photos from this basic SLR camera (requiring manual downloading) document flooding and calving activity that could occur in the event of a GLOF. A pressure transducer was installed near this timelapse camera site to measure water depth throughout the summer. This data will help us understand how long it took for the water to reach the proglacial lake after it started draining from the glacier-dammed lake and other seasonal water level dynamics in the proglacial lake.

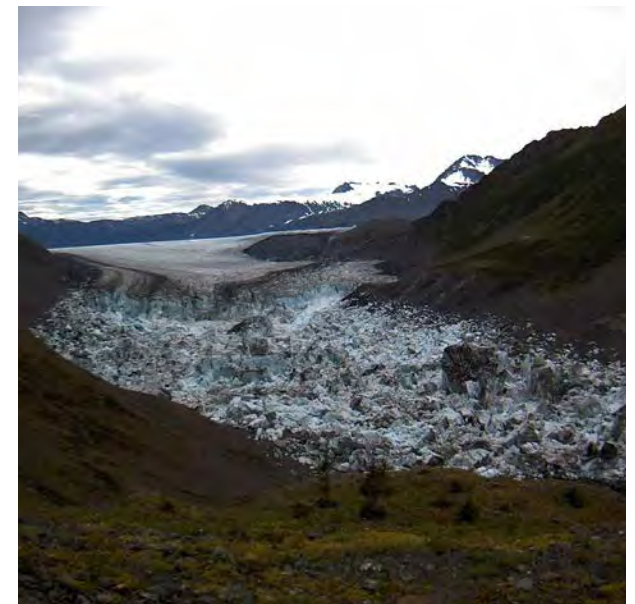


Figure 3. The glacier-dammed lake at maximum water level on August 7, 2018 (top). The glacier-dammed lake at its minimum level on August 14 following complete drainage, resulting in a GLOF below (bottom).

At the time of the first camera installation, the glacier-dammed lake had little water in it and grounded blocks of ice were distributed well above the water line. The last time the lake was observed by park staff prior to the camera installation was about a year earlier, on July 16, 2016. At that time, the water levels in the lake were higher than in June 2017 and all of the calved chunks of ice were floating, allowing us to infer that there was an undetected drainage event at some time during the previous year. Over the course of the first summer, the daily photos allowed us to observe and document the filling of the basin and formation of the glacier-dammed lake.

From the satellite-delivered photos, we observed the glacier-dammed lake fill throughout the 2017 summer, freeze in the winter, and continue to fill for most of summer 2018. On August 8, 2018 we observed a slight decrease in water levels in the glacier-dammed lake. On August 9, an additional decrease in water levels alerted us to the beginning of a GLOF. Based on analysis of the timelapse photos,

water levels in the glacier-dammed lake decreased by 50-65 feet (15-20 m) per day during the first days of the drainage, releasing at least 2,600 Olympic-sized swimming pools of water per day into the proglacial lake below.

Water levels in the proglacial lake rose nearly 1.5 feet (0.5 m) per day for a total of 6.5 feet (2 m) in 96 hours, with the fastest rate of rise occurring between August 9-11 (Figure 4).

On August 11, a pilot observed that water in the proglacial lake had breached the moraine that separates the freshwater lake and outlet from the marine waters of Resurrection Bay. This allowed water to bypass a large section of the normal outflow channel (which subsequently dried up and remained unnavigable the remainder of the season) and flow over the moraine and directly into the bay. The erosion of the moraine was so deep that water taxis, small skiffs, and jet boats were able to enter the lake by boating over the moraine at the location of the

breach during a higher tide. This was the only boat access into the proglacial lake; the normal outlet was completely dry or too shallow for navigation. Data from the pressure transducer indicated that the water level began to drop during the morning of August 11, two days after the glacier-dammed lake started to drain, likely due to this more direct route into the ocean. On August 13, water levels dropped below the level of the pressure transducer, preventing us from knowing the subsequent rate of lake lowering and the actual minimum water level. When we retrieved the equipment on August 25, the water level was approximately one meter below the pressure transducer. Based on this observation, it is likely that the water levels dropped approximately 11 feet (3.4 m).

By monitoring the daily timelapse photos, we were able to detect a decrease in the glacier-dammed lake levels early in the drainage event. This allowed us to notify the National Weather Service's Alaska-Pacific River Forecast Center who put out a timely flood

Bear Glacier Proglacial Lake
Meters of Water Column Above Transducer

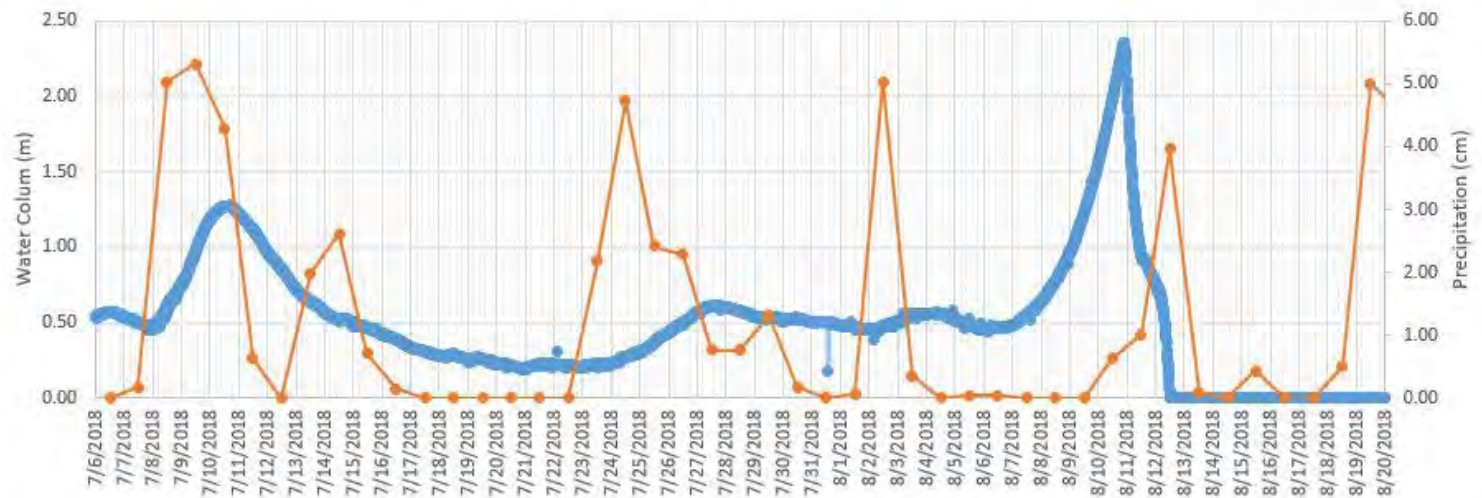


Figure 4. Water levels in the proglacial lake are charted in blue. Daily precipitation is charted in orange. Precipitation is from the Pedersen Lagoon RAWS, 9.8 km west of the site of the pressure transducer installation.

alert for this area. This early observation provided sufficient time for commercial guides to plan for the event and prevented one group from certain loss of an equipment cache.

Within a week of the GLOF, an NPS flight was able to collect aerial photography that will allow us to create highly detailed topographic maps of the drained lake basin. The pre- and post-drainage topographic data will allow us to accurately calculate water storage volume in the glacier-dammed lake. In combination with photographic and lake-level data from the proglacial lake, this will allow us to refine our volume estimate of the GLOF and improve our ability to predict flood magnitudes and rates during subsequent GLOFs.

Glaciers and the landscapes they create are beautiful, dynamic places to behold and experience as a distant observer, skilled adventurer, or inquisitive scientist. Ice falls, calvings, collapses, and outburst floods can and do occur without warning. People should always use caution when playing, working or traveling around glaciers.

Kenai Fjords and State of Alaska researchers will continue to study and monitor the Bear Glacier glacier-dammed lake to better understand hydrological processes leading to GLOFs, and increase awareness about glacier-related hazards in and around the park.

REFERENCES

- Dickerson, S. 2016.**
Cold World. *Transworld Surf: The Alaskan Issue*, May 2016.
- Marcus, M. 1968.**
Effects of glacier-dammed lakes in the Chugach and Kenai Mountains. In, *The Great Alaska Earthquake of 1964 Hydrology* (publication 1603), National Academy of Sciences, Washington D.C., pp. 326-347.
- Taylor, W. 2012.**
Exploring the Frozen Frontier. *SUP Magazine*, Winter 2012. Available at:
<https://www.supthemag.com/videos/from-the-mag-exploring-the-frozen-frontier/> (accessed 12/11/2018)
- Parsons, R. 2016.**
Liquid Adventures: Glacial SUP tours in Alaska. *SUP Magazine* Available at:
<https://www.supthemag.com/gear/shop-talk/liquid-adventures-glacial-sup-tours-in-alaska/> (accessed 12/11/2018)
- Post, A. and L. R. Mayo, L.R. 1971.**
Glacier Dammed Lakes and Outburst Floods in Alaska. Hydrologic Investigations Atlas HA-455. Anchorage, Alaska. U.S. Geological Survey, Denver CO.
- Shivley, D. 2013.**
Paddling with icebergs in Seward, Alaska. *Easy Reader News* Available at:
<https://easyreadernews.com/paddling-with-ice-bergs-in-seward-alaska/> (accessed 12/11/2018)
- Wilcox, A., A. Wade, and E. Evans. 2014.**
Drainage events from a glacier-dammed lake, Bear Glacier, Alaska: Remote sensing and field observations. *Geomorphology* 220: 41-49.



Geohazard Risk Reduction along the Denali National Park Road

Denny Capps and Molly McKinley, Denali National Park and Preserve

Douglas A. Anderson, Federal Highways Administration

The dramatic landscapes of Denali National Park are largely a result of geologic forces. The park road, the main access to the park for visitors and staff, is especially susceptible to landslides that have blocked access for days. We monitor geohazards in the park and actively reduce risk.

Citation:

Capps, D., D. A. Anderson, and M. McKinley. 2019. Geohazard risk reduction along the Denali National Park Road. *Alaska Park Science* 18(1): 44-51.

Geohazards are geologic processes that may pose a risk to humans and infrastructure. Geohazards are: (1) generally forecastable events through scientific evaluation; (2) amenable to risk analysis based on probabilities; (3) subject to linkages between different geohazards and the physical environment (e.g., earthquakes and heavy rains can cause landslides); (4) causing increased impacts because of expansion of infrastructure; and (5) manageable through minimization of their consequences (Keller and Blodgett 2006). While managing geohazards is challenging, new programmatic tools are making it easier for park managers to improve safety and resiliency. This article provides an overview of Denali National Park and Preserve's (hereafter "Denali") geohazard risk reduction program.

Denali's Geohazards

Denali is a prime location for the study of geohazards, with over 20,000 feet (6,000 m) of topographic relief, 1,400 square miles (3,700 km²) of glaciers (Loso et al. 2014), active tectonics, and widespread permafrost. A focus on geohazards is most relevant for the 92-mile (148-km) road that visitors and staff use to access the park. In 2017, Denali had approximately 600,000 visitors, resulting in \$632 million in visitor spending, 8,150 jobs, and \$924 million in general economic output (Denali National Park and Preserve 2018). As a result, Denali and the road represent a major economic engine for the region.

In Denali, geohazards include earthquakes, landslides, rockfall, debris (mud) flows, glacier outburst floods, ice and snow avalanches, river erosion/deposition, and others (Capps et al. 2017). While ice and snow avalanches have killed at least 49 mountaineers since 1976 and injured many others (Wright and Chenoweth 2012), landslides, rockfalls, and debris flows are the source of greatest concern because they have repeatedly blocked and damaged the Denali Park Road (hereafter "road," Figure 1) and threatened the safety of visitors and staff. For example, the Igloo landslide has blocked the road numerous times, once for four days (Figure 2). Thankfully, these events have occurred in September and October, after Denali's busy summer season. However, the 2016 Eagle's Nest landslide occurred in July during the park's busy season. This landslide blocked the road completely for four days and limited traffic for six more (Figure 3).

Risk management associated with geohazards varies depending on location. In the backcountry, particularly for mountaineers, individuals and teams generally must mitigate their own risks. Much of the allure of mountaineering is to combat and survive the often harsh and challenging environment. By contrast, in developed areas, there is an expectation that parks maintain a safe environment for visitors and staff. This is accomplished by managing visitor access and through education.

Denali staff collecting GPS data at the Pretty Rocks landslide near mile 45 of the Park Road on March 22, 2019. The survey rod she is holding is 6.5 feet (2.0 m) tall, is placed near centerline of the road and shows the amount of displacement since September 14, 2018. Photo courtesy of Denny Capps, NPS.

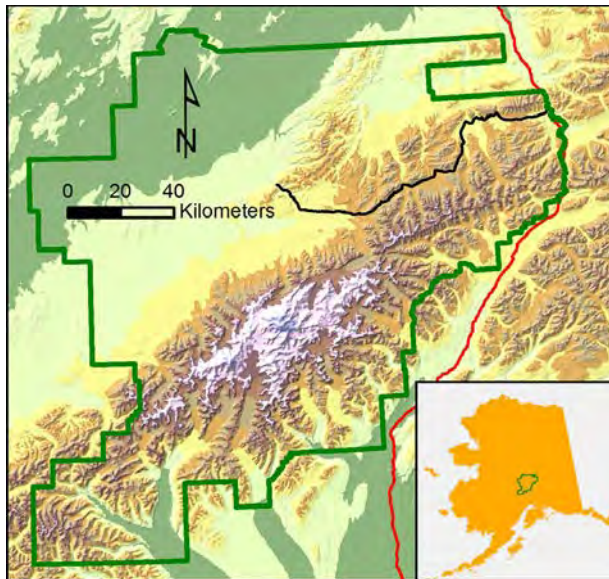


Figure 1. Shaded-relief map of Denali National Park and Preserve outlined in green, black line Denali Park Road, red line George Parks Highway. Inset map shows location of park (green boundary) in Alaska.

The Denali road is a front-country environment. The Alaska Road Commission (ARC) constructed the road between 1922 and 1938 to provide access for park visitors and staff and as a haul road for mining activities. Because of this dual purpose, the ARC had to adapt their methods from creating a series of tangents to the aesthetic design standards of the National Park Service (NPS). NPS standards required blending the road into the natural landscape so that the act of driving would be more interesting (Mathews et al. 2019). The State of Alaska and the NPS have nominated the current road alignment for listing in the National Register of Historic Places. Traffic on the road is restricted, with most visitors traveling in buses driven by highly trained staff. All other drivers are required to watch a Denali-specific training video that provides information about how to travel the road safely.

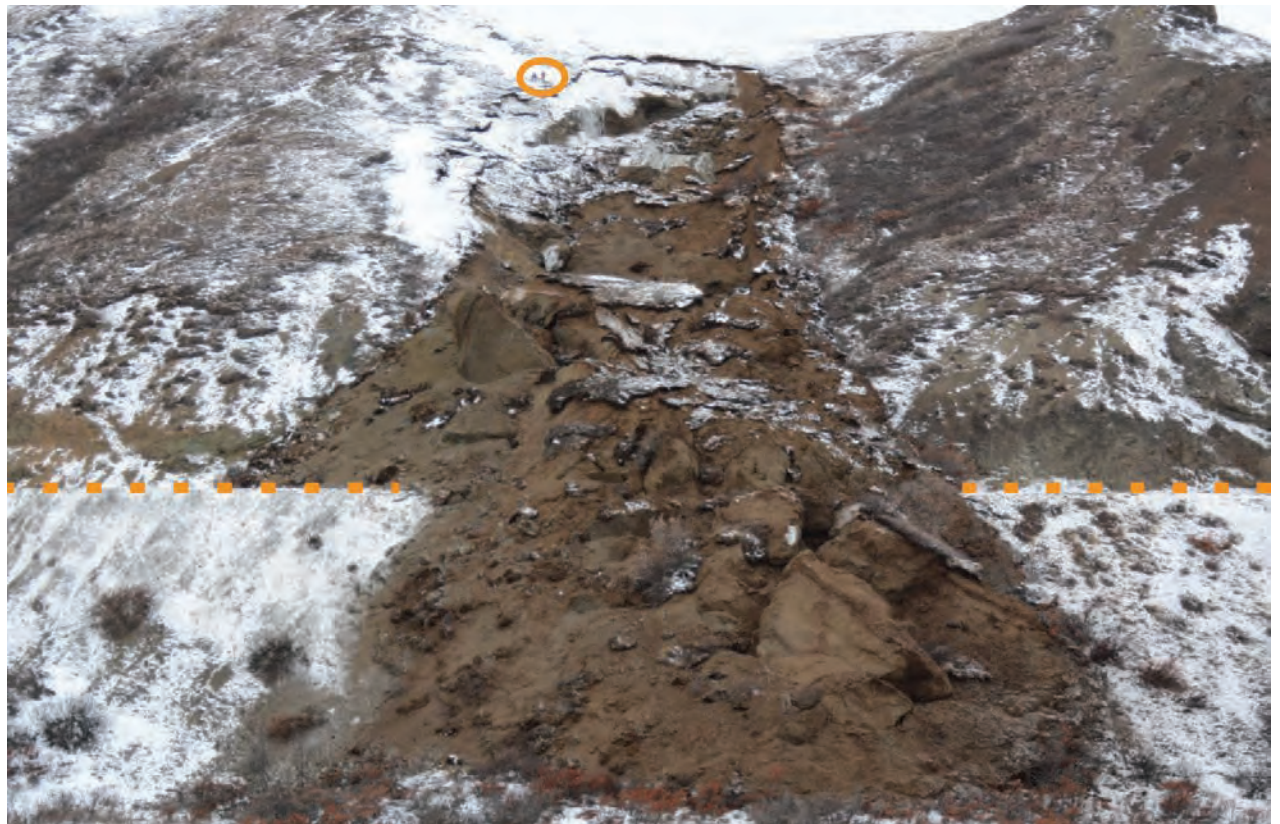


Figure 2. Photograph of the 2013 Igloo landslide. Two people circled for scale. Road grade bench indicated by dashed orange line.

Influential Processes

Tectonics and climate greatly influence Denali's geohazards. Plate tectonics motion creates the high topographic relief of the Central Alaska Range. High relief, in turn, creates slopes conducive to landslides, debris flows, and rockfall. Earthquakes occur daily in Denali, but most are too small for people to notice. Several are felt each year, particularly in the Kantishna area. More rarely, a large event occurs. For example, a M 7.9 earthquake struck 19 miles (30 km) east of the park on November 2, 2002 (Alaska Earthquake Center 2016). This earthquake released more energy than all earthquakes in the lower-48

states over the previous 30 years combined (M. West, personal communication, June 15, 2015). The Alaska Earthquake Center, the U. S. Geological Survey (USGS), and various academic institutions lead research efforts on earthquakes and an extensive body of information is available on this topic. Earthquakes are particularly important because they can trigger landslides, debris flows, rockfall, and other associated hazards.

While they present challenges, these processes create many of the landscapes that we enshrine in national parks. For example, without earthquakes, there would be no mountains. Without mountains,

there would be no Dall's sheep (important for Denali's foundation) or world-class scenery. Without sheep and scenery there would be no Denali. As Robert Sterling Yard (who cofounded the National Parks Conservation Association with Stephen Mather) stated, "*Geology is the anatomy of scenery.*" Denali's geologic backbone draws many people to seek solace and test their outdoor skills in a rugged landscape.

Climate also substantially influences Denali's geohazards. Recent climate records indicate that the mean annual temperatures are considerably warmer than the 1981-2010 30-year normal (+1.0°C in 2014 and 1.3°C in 2015; Sousanes 2016). Climate forecasts through the end of the century indicate that Denali is likely to experience increasing warming (~4.0°C) and heightened variability in seasonal precipitation (Gonzalez et al. 2018, Rupp and Loya 2009).

This anticipated warming will cause permafrost thaw, which can destabilize slopes. Subsurface temperature measurements indicate significant warming in Alaska since the 1980s. Greater permafrost warming has occurred on the North Slope (<4.0°C) with less (<1.0°C) occurring in the Denali region. Latent heat effects partially explain the lesser change in Denali as temperatures near 0°C (Osterkamp 2007, Romanovsky et al. 2010). Models indicate that approximately 75% of Denali was underlain by shallow permafrost during the 1950s and was reduced 50% during the 2000s. According to the model's projections, shallow permafrost will only cover 6% of the park by the 2050s and 1% by the end of the century (Panda et al. 2014). Permafrost thaw and degradation is already influencing landslide activity in the park and modeling predicts even more activity. Rapid permafrost thaw increases landslide susceptibility by altering physical and hydrologic properties of hillslope materials, including reduced cohesion of the soils and increased hydraulic



Figure 3. Photograph of the 2016 Eagle's Nest landslide. Yellow dotted line delineates the landslide margins. The slide originated beyond the bottom right of image. Note two front loaders with seven-cubic-yard (five-cubic-meter) buckets on road near top center.

connectivity (Patton et al. 2019). These properties contribute to the occurrence of landslides on slopes as shallow as a few degrees.

Impacts

Geohazards physically threaten the safety of our visitors, staff, and resources. Therefore, our first and

foremost goal is to use research to improve safety. The 1916 NPS Organic Act declares that we shall "conserve the scenery and the natural and historic objects and the wild life therein and to provide for the enjoyment of the same in such manner and by such means as will leave them unimpaired for the enjoyment of future generations." The mandate

to provide access as well as protect park resources implies a responsibility for visitor safety. Because Denali is very large (over six million acres) and remote, we focus attention on locations where visitors spend the most time. Here, the concept of *exposure* (i.e., whether or not people and assets are in areas prone to slope failures) is critical. To frame the idea, a geohazard affecting an occasionally used trail will have a lower exposure level than if it was threatening a busy road or housing area (Stock and Collins 2014). We must also be vigilant with the safety of our own staff, whose relative numbers may be low, but who often work for long periods in high-risk areas. Maintenance staff often work for hours, days, or sometimes even weeks at sites with known geohazards. These staff feel a sense of pride in keeping park infrastructure functioning, yet may not be fully cognizant of the risks they face in areas prone to geohazards.

Geohazards may also subject the government to tort claims, a civil process of seeking compensation for damages or harm. In common law jurisdictions such as a national park, individuals who suffer loss or harm may expect the government or government employees to hold legal liability for their safety. The information gathered from geohazards research also helps protect the government from successful tort claims by developing knowledge of the risk and expanding funding where there will be a maximum benefit-to-cost ratio, such as rehabilitating deteriorating infrastructure in high-risk areas. Both federal (Merando v. United States 2008) and state (Helm v. State of Washington 2015) legal precedents demonstrate the effectiveness of this approach. In both cases, courts found that the U. S. Government and State of Washington, respectively, were not liable for damages incurred because they demonstrated appropriate use of a proactive, strategic approach to managing their hazards.

Improving Safety and Resiliency

Another goal of our geohazard research is to improve the resiliency of park infrastructure. Resilient infrastructure will enable minimal disturbances to the current traffic and use patterns for both park staff and associated businesses. With visitation numbers in Denali and other Alaska national parks increasing, we appear to have entered into a new normal of increased geohazards and risk threat. This is caused by a combination of increased load-carrying capacity needs (resulting in greater human exposure), changes in climate, and associated geotechnical asset deterioration (road cuts, embankment slopes, etc.).

Denali has worked to improve resiliency since the earliest days of the park. For example, in 1927 Alaska Road Commission President James G. Steese wrote:

Opening up frozen ground and completing a standard road in one season is impossible . . . It is cheaper and better in the long run to extend operations over several seasons. The final surfacing should not be applied until sub-grade has thoroughly thawed out, become drained, and stabilized (Steese 1927).

The 2013 Igloo landslide (Figure 2) kick-started Denali managers into a more proactive stance on geohazards. This event occurred concurrently with the development of the Unstable Slope Management Program for Federal Land Management Agencies, or USMP (Federal Highway Administration–Federal Lands Highway Division 2019). Denali joined development of the USMP in the early stages and remains active in its implementation.

Through the USMP system, Denali and the Federal Highways Administration (FHWA) have quantified and are tracking over 140 unstable slopes along the road (Figure 4). We've also conducted a Quantitative Risk Assessment (QRA) of the top-ten

highest-ranking USMP sites to help inform future risk reduction (Capps et al. 2017). We are now developing conceptual designs for all high-ranking USMP entries. Conceptual designs and estimated costs provide a range of risk reduction techniques for park management to choose what they deem as most appropriate. These designs will range from relatively simple education and outreach efforts (e.g., appropriate signage) to complex engineering projects. Program managers will then proactively seek funding for sites where benefits outweigh costs, thus completing the first USMP cycle. As new events or new activities at preexisting sites develop, we will (re)evaluate them, re-sort all USMP scores, and work through the prioritization process using the benefit/cost analyses, as previously described.

A landslide inventory database (Capps et al. 2017) records the spatial and temporal distribution, relative activity, and geomorphic attributes of all known landslides within the road corridor. The USMP, in contrast, only records unstable slopes that have previously affected the road or trails. Adjacent landslides provide useful contextual information about conditions along the road. Using this inventory, we created a susceptibility model to estimate landslide probability along the road corridor (Capps et al. 2017).

Denali and the USGS are working together on two projects. One began in 2017 to produce a digital map and database of the surficial geology and associated processes along the road corridor. To properly understand and reduce the risk of geohazards, park managers must know the substrate and understand its associated processes. We expect to complete this five-year project in 2021. The second project planned to begin in 2019 will determine our vulnerability to geologic hazards. Reducing and managing risks requires an understanding of not only the hazards, but also how facilities, infrastructure, staff, and visitors



Figure 4. Annotated screen capture of the [Geotechnical Asset Management Program story map](#) from mile 44 to 46 of the Denali Park Road. On the webpage managers can click on icons for more detailed information about each entry. [Ratings are based on the frequency and severity of rockfall and landslide events.]

are vulnerable. Understanding the vulnerability of people and facilities to geohazards involves characterizing their exposure, sensitivity (i.e., pre-existing infrastructure conditions and demographics of at-risk individuals), and adaptive capacity (i.e., the ability to avoid hazards before negative impacts occur either due to effective evacuations of individuals or the movement of infrastructure out of high-risk areas; N. J. Wood, personal communication, March 19, 2018).

FHWA planned and supervised numerous geotechnical borings and surveys for unstable slopes along the road. FHWA has instrumented some of

these borings to monitor water level, temperature (for seasonal frost and permafrost), and land displacement. A team of government and university researchers is using this data to fine tune thermal, deformation, and rockfall models. The models will, in turn, inform appropriate conceptual designs, benefit/cost assessments, and eventual risk reduction. The U.S. Army Corps of Engineers Cold Regions Research and Engineering Lab also deployed a suite of complementary geophysical techniques to determine the presence of permafrost and depth to bedrock along approximately 10 miles (16 km) of road that has experienced past geotechnical challenges (Bjella et al. 2017).

Summary

Geohazards always have been, and always will be, part of Denali. To maximize safety, resiliency, and the wisest use of our resources, we should continue to manage geohazards proactively. This requires a substantial and sustained effort and a range of new programmatic tools are now making this easier.

In the future we hope to: (1) support additional permafrost studies in areas where permafrost thaw may be a contributing factor to instability; (2) instrument and monitor additional sites of concern; (3) refine the landslide susceptibility modeling; (4) maintain the USMP; (5) improve funding structures; (6) continue implementation of risk reduction; (7) maintain and expand our network of partners; and (8) increase geohazard awareness. While these efforts will reduce the risk from geohazards along the road, we never can fully eliminate this risk in such a dynamic environment. For up-to-date information, see the park webpage (<https://www.nps.gov/denali/learn/nature/landslides.htm>).

Acknowledgements

A large number of individuals and organizations made this research possible. We would like to thank participating staff and students from: all divisions of Denali National Park and Preserve; the Federal Highway Administration-Western Federal Lands Highway Division; NPS Alaska Regional Office; NPS Geological Resources Division; the USGS Geosciences and Environmental Change Science Center, and Western Geographic Science Center; Montana State University and Western Transportation Institute; Colorado State University, University of Alaska Fairbanks, University of Alaska Anchorage; Landslide Technology; Alaska Department of Transportation and Public Facilities, the Army Corps of Engineers, and many others.

REFERENCES

Alaska Earthquake Center. 2016.

Earthquake Monitoring in Denali. Available at <http://www.nps.gov/articles/denali-earthquake-monitoring.htm> (accessed October 10, 2018)

Bjella, K., S. Saari, A. Balsler, and A. Staples. 2017.

Denali National Park Road - Geophysical Investigations: Subsurface Features for the Park Entrance, Dog Kennels Loop, Igloo Forest, Polychrome Pass, and Stony Point Areas: Cold Regions Research and Engineering Laboratory, U.S. Army Engineer Research and Development Center, Western Federal Lands Highway Division Geotechnical Report No. 03-17.

Capps, D. M., R. Rosenberg, A. Collins, D. A. Anderson, S. Hooper, H. Rogers, B. Collins, and E. Bilderback. 2017.

Geohazards Risk Assessment of the Denali National Park Road, in Proceedings North American Symposium on Landslides, Roanoke, VA. Association of Environmental & Engineering Geologists.

Denali National Park and Preserve. 2018.

Park Statistics. Available at: <https://www.nps.gov/denali/learn/management/statistics.htm> (accessed December 18, 2018)

Federal Highway Administration, Federal Lands Highway Division. 2019.

Unstable Slope Management Program for Federal Land Management Agencies, Publication No. FHWA-FLH-19-002.

Gonzalez, P., F. Wang, M. Notaro, D. J. Vimont, and J. W. Williams. 2018.

Disproportionate magnitude of climate change in United States national parks. *Environmental Research Letters* 13: 12.

Helm v. State of Washington. 2015.

Tracy Helm and Christopher Helm, husband and wife, Michael Brady Helm, a minor, and Hailey Nicole Helm, a minor v. State of Washington, Department of Transportation, a division of Washington State government, and Paula J. Hammond, Secretary of Transportation, Court of Appeals of the State of Washington, p. 1.

Keller, E. A. and R. H. Blodgett. 2006.

Natural hazards: Earth's processes as hazards, disasters, and catastrophes, Upper Saddle River, NJ, Pearson Education, Inc., 395 p.

Loso, M., A. Arendt, C. Larsen, J. Rich, and N. Murphy. 2014.

Alaskan national park glaciers - status and trends: final report: National Park Service, Natural Resource Technical Report NPS/AKR/NRTR—2014/922.

Mathews, L., R. Z. Melnick, R. Edmonds, E. San Filippo, and M. Murthy. 2019.

Cultural Landscape Report for Mount McKinley National Park Road Historic District: Denali National Park and Preserve, Alaska.

Merando v. United States. 2008.

Anton Merando, as General Administrator and Administrator AD Prosequendum of the Estates of Kathleen Merando and Kaylyn Merando, Appellant v. United States of America; County of Sussex; Township of Walpack; Public Service Electric and Gas; John Does 1-10 (Said Names Being Fictitious); XYZ Corps. 1-10 (Said Names Being Fictitious); Jersey Central Power and Light. Court of Appeals for the Third Circuit.

Patton, A. I., S. L. Rathburn, and D. M. Capps. 2019.

Landslide response to climate change in permafrost regions: *Geomorphology* 340(1): 13.

Rupp, S. and W. Loya. 2009.

Projected climate change scenarios for Denali National Park & Preserve: University of Alaska Fairbanks, Climate change summary reports of National Parks, Preserves and Monuments.

Sousanes, P. 2016.

Denali Climate and Weather Monitoring. Available at <https://www.nps.gov/articles/denali-crp-climate-weather-monitoring.htm> (accessed December 18, 2018)

Steese, J. 1927.

Letter from James Steese to Arno Cammerer, Assistant Director of the National Park Service, Denali National Park archives.

Stock, G. and B. Collins. 2014.

Reducing rockfall risks in Yosemite National Park. *Eos* 95(29): 2.

Wright, K. and T. Chenoweth. 2012.

Historical analysis of avalanche fatalities in Denali National Park, in Proceedings 2012 International Snow Science Workshop, Anchorage, AK, International Snow Science Workshop, p. 8.





Volcanic Hazards in Alaska's National Parks

Katherine Mulliken, Kristi Wallace, Cheryl Cameron, and Chris Waythomas, Alaska Volcano Observatory

There are over 100 volcanoes in Alaska, 54 of which are considered historically active, and 14 are found in Alaska national parks, preserves, and monuments. The Alaska Volcano Observatory monitors and conducts research on volcanoes in Alaska in order to better understand volcanic processes and determine the likelihood of future volcanic hazards, with a primary goal of informing the public about volcanic hazards and impending volcanic activity.

Citation:
Mulliken, K., K. Wallace, C. Cameron, and C. Waythomas. 2019. Volcanic hazards in Alaska's national parks. *Alaska Park Science* 18(1):52-61.

There are over 100 volcanoes in Alaska, 54 of which are considered historically active. A historically active volcano is one that fits one of the following criteria: (1) a documented or strongly suspected eruption since the year 1700, (2) persistent fumaroles near boiling point, (3) significant deformation with a volcanic cause, or (4) an earthquake swarm with a volcanic cause (Cameron and Schaefer 2016). Alaska's national parks, preserves, and monuments contain a total of 14 historically active volcanoes (Figure 1). In addition, there are numerous other volcanoes within Alaska's parks that are not considered historically active, but which could erupt at some point in the future.

In the past 100 years, there have been seven confirmed eruptions from historically active volcanoes within Alaska's parks. The Alaska Volcano Observatory (AVO) monitors and conducts research on volcanoes in Alaska in order to better understand volcanic processes and determine the likelihood of future volcanic hazards, with a primary goal of informing the public and local, state, and federal entities about volcanic hazards and impending volcanic activity. Volcanic hazards in Alaska's parks include both proximal hazards (within 19 miles [30 km] of the vent) and distal hazards that are capable of impacting areas at the regional, national, or international scale.

Historically Active Volcanoes in National Park Service Lands in Alaska

Aniakchak National Monument and Preserve

Aniakchak Crater

Katmai National Park and Preserve

Mount Douglas, Fourpeaked Mountain, Kukak Volcano, Snowy Mountain, Mount Griggs, Mount Mageik, Mount Martin, Trident Volcano, Novarupta, and Mount Katmai

Lake Clark National Park and Preserve

Iliamna Volcano and Redoubt Volcano (both are National Natural Landmarks)

Wrangell-St. Elias National Park and Preserve

Mount Wrangell

National Natural Landmarks in Alaska

Iliamna, Redoubt, and Shishaldin volcanoes; Mount Veniaminof, Aniakchak Crater, and Bogoslof Island

Aerial view of Shishaldin Volcano with Isanotski Peaks in the background, taken from a helicopter overflight during geology field work on Unimak Island in the Aleutians. Photo courtesy of Matt Loewen, USGS/AVO, on August 15, 2018. [AVO image ID 118571](#)

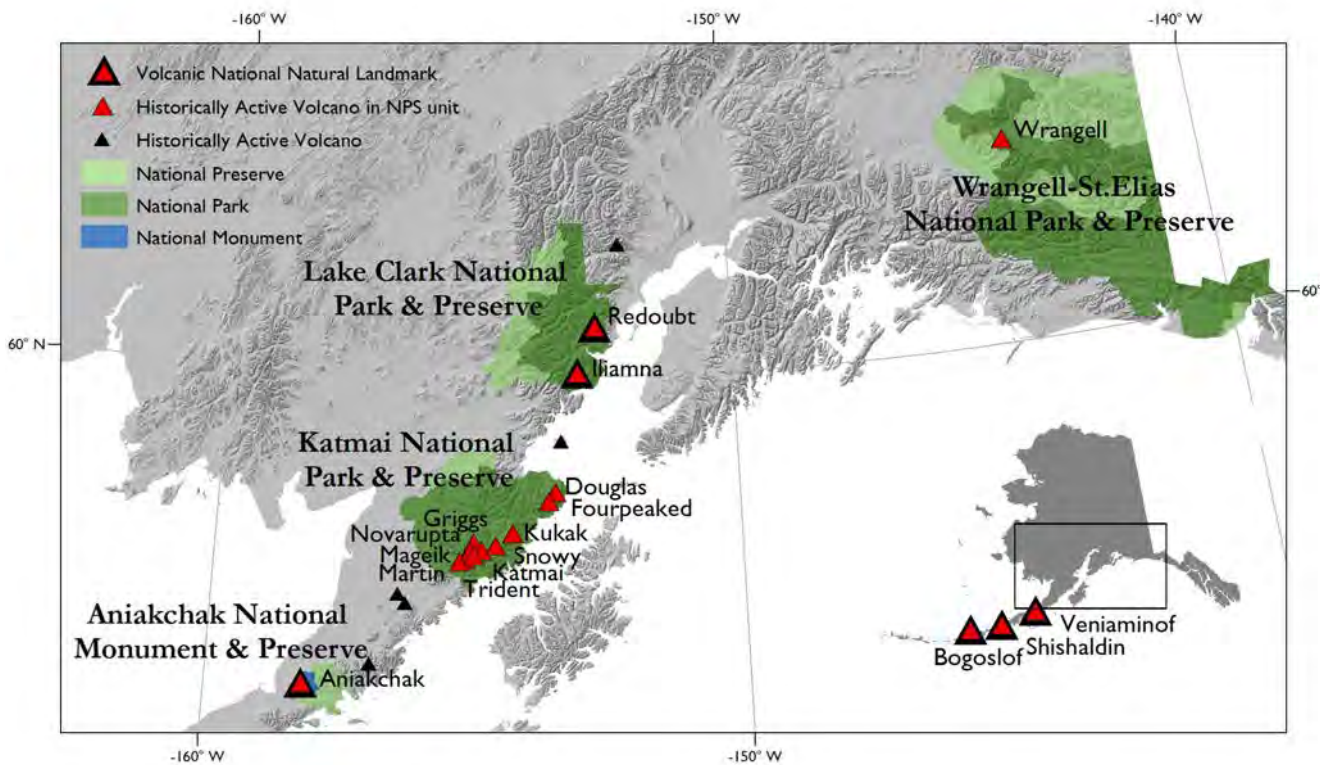


Figure 1. Map showing the historically active volcanoes and national parks, preserves, or monuments in Alaska. Historically active volcanoes within park boundaries and Alaska volcanoes that are [National Natural Landmarks](#) are highlighted in red.

The Alaska Volcano Observatory: Assessing Volcanic Hazards in Alaska

AVO conducts geologic studies to better characterize past volcanic activity and inform on the likely effects and hazards of future eruptions. As products of this work, AVO publishes research articles, reports, geologic maps, and hazard assessments. Much of this material is available to the public on the AVO website, which provides information on past and current activity at volcanoes in Alaska.

AVO monitors volcanoes in Alaska via a network of instruments including seismometers, global positioning system (GPS) stations, web cameras, and infrasound sensors that telemeter real-time data to observatory staff (Figures 2 and 3). Daily review of satellite imagery and annual or opportunistic overflights to measure gas emissions complement the real-time monitoring data and new technologies and tools, such as lightning detection, which can indicate the presence of volcanic plumes, are continually being developed and used to better detect volcanic activity. Occasionally, there are false reports of volcanic activity, especially regarding Mount Wrangell and Iliamna Volcano, which AVO can authoritatively confirm as “non-eruptions” by checking for changes in these real-time monitoring data.



Figure 2. Cyrus Read, AVO/USGS, installing the new, zoom-capable web camera at the AVO research hut north of Redoubt Volcano.

[AVO image ID 18139](#)

In the United States, a standardized volcano alert system is used to assign monitored volcanoes an Alert Level and Aviation Color Code, both of which convey a volcano’s level of activity and presence of potentially hazardous conditions on the ground or in the air (Figure 4; Gardner and Guffanti 2006). Changes observed in the monitoring data of a volcano, such as an earthquake swarm, may merit a change in its Alert Level and Aviation Color Code and such a change is communicated to the public via the AVO website, social media and news outlets, and the Volcanic Activity Notification Service.

During an eruption, AVO responds as appropriate by increasing the number of field instruments, the frequency of review of monitoring data streams, and communication of hazards information to other government agencies, affected industries, and the general public (Neal et al. 2010). AVO’s responsibility is to detect signs of volcanic unrest and report that information along with potential volcanic hazards; however, other state and federal agencies, including the Federal Aviation Administration (FAA), the National Weather Service (NWS), and the Alaska

Department of Homeland Security and Emergency Management, also have reporting responsibilities related to volcanic activity. The Alaska Interagency Operating Plan for Volcanic Ash Episodes (AVO et al. 2017) enables rapid and efficient communication of volcanic hazards by outlining the specific roles and responsibilities of each agency during a volcanic crisis.

Volcanic Hazards in Alaska

Due to the remote location of many of the volcanoes in Alaska, the volcanic hazards that are of the greatest concern typically are those with the potential to affect distal areas. These hazards are often aviation-oriented and primarily include drifting ash clouds and ashfall. Volcanic hazards within Alaska's parks also include proximal hazards that could be of concern to employees and visitors.

Distal Volcanic Hazards

Because volcanic ash is so readily transported, parks in Alaska may be affected by ash clouds or ashfall from volcanic eruptions that occur both within and outside of their boundaries. Ash clouds are formed when an explosive eruption energetically fragments magma, rapidly injecting small particles (ash) into the atmosphere, sometimes to heights of greater than 32,000–65,600 feet (10–20 km) above the volcano within less than an hour (Figure 5). Ash is highly abrasive and the particles can severely damage aircraft, eroding and adhering to engine and electrical parts and abrading windows, wings, and landing gear. Electrical disturbances and gases within an ash cloud may impair the aircraft's ability to transmit messages and cause respiratory problems for those on board. Many visitors to Alaska's parks arrive via small aircraft that typically travel at altitudes where volcanic ash is most likely to be present (10,000–20,000 feet [3–6 km] above sea level). Thus, sustained ash emissions during

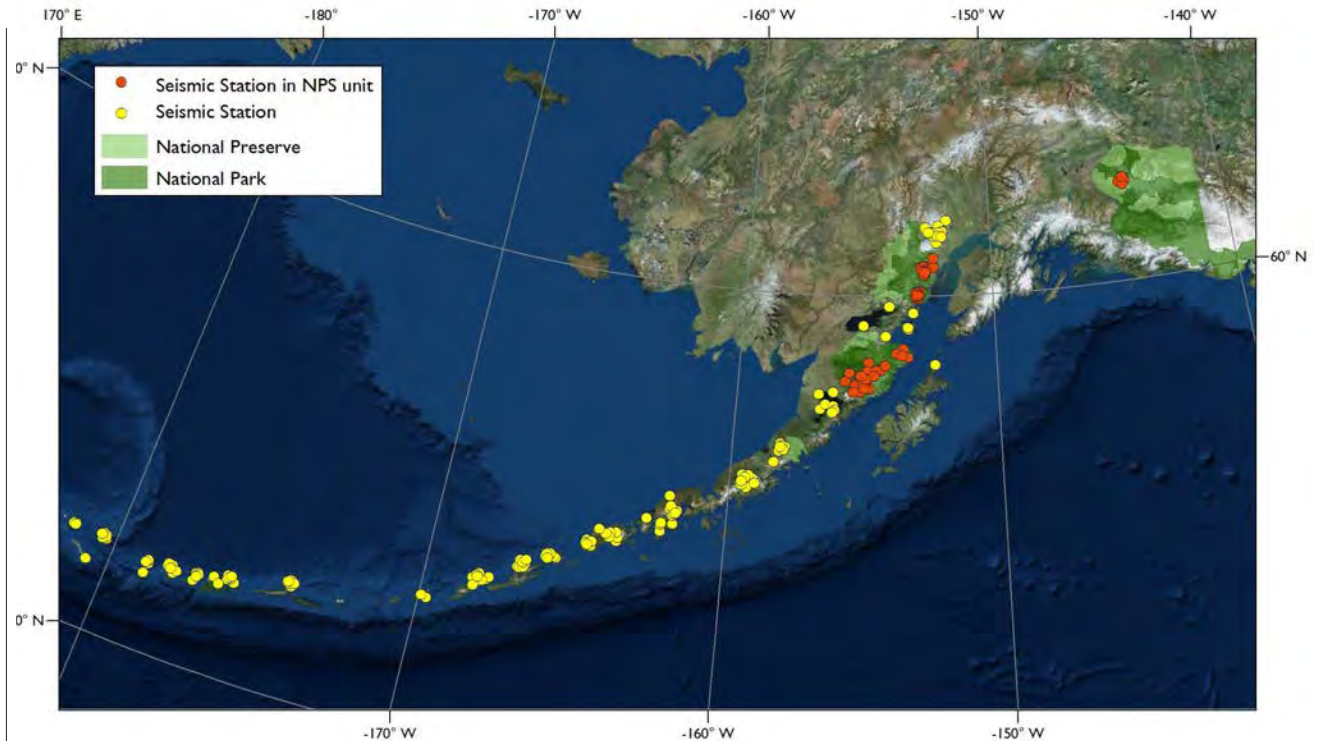


Figure 3. AVO maintains 212 seismic stations (34 networks) covering over 1,700 miles (2,736 km).

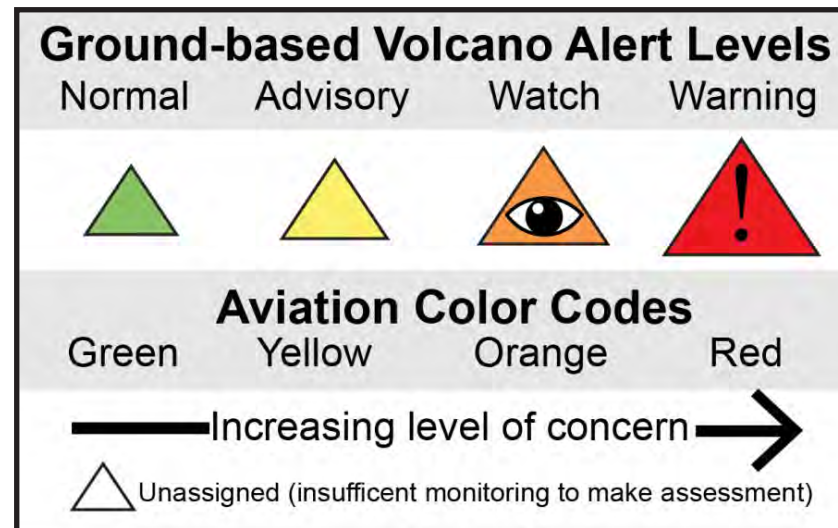


Figure 4. The volcano alert system in the United States assigns a ground-based Alert Level and Aviation Color code to convey the level of activity at a volcano. For more information, see: <https://volcanoes.usgs.gov/vhp/about/alerts.html>.

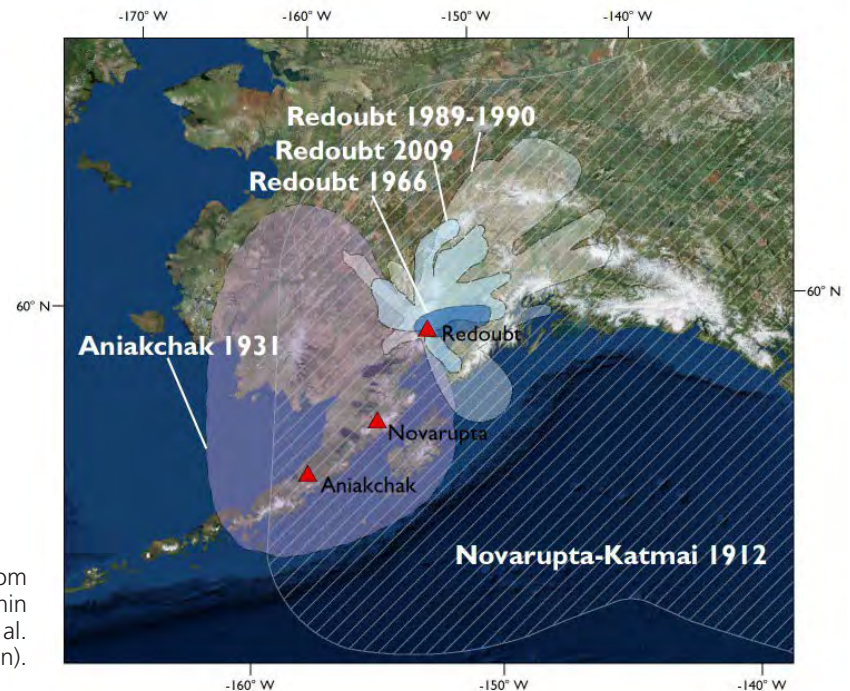


Figure 5. March 26, 2009 ash cloud from Redoubt, approaching Homer, Alaska, looking south-southwest. Photo courtesy of Dennis Anderson, [AVO image ID 17091](#)

summer, by volcanoes erupting within or outside of parks, could significantly curtail or inhibit access to parklands. Flight cancellations and delays could significantly impact passengers and cargo.

Ash fallout can occur in both proximal and distal locations relative to the volcanic vent that

Figure 6. Distribution of ashfall from historical eruptions of volcanoes within National Park Service areas (Mulliken et al. 2018 and references therein).



is erupting. Typically, larger particles (which are heavier) are deposited closer to the vent, whereas smaller particles are suspended in the air for longer and thus may be transported farther from the vent prior to being deposited. Trace ashfall (<1/32 of an inch [0.08 cm]) is common in distal areas and typically causes low-level impacts such as eye and respiratory irritation. However, greater amounts of ashfall accumulation may adversely impact plants and animals and cause problems for infrastructure. Wet ash is significantly denser than dry ash and if significant amounts accumulate on buildings, structural failure may result. Thick accumulations of volcanic ash can make roads impassable, degrade surface and drinking water supplies, and interfere with communication systems.

Multiple historical eruptions of volcanoes located within Alaska's parks have produced ash clouds and resulted in ashfall that affected and sometimes continue to affect large areas beyond

their boundaries (Figure 6). Ash from the 1912 eruption of Novarupta-Katmai, which was the most voluminous of the twentieth century (Hildreth and Fierstein 2012), poses an ongoing seasonal hazard due to resuspension during very high winds and dry conditions (see Wallace and Schwaiger, this volume). The 1931 eruption of Aniakchak volcano resulted in millimeters of ashfall as far as Kodiak Island (Bacon et al. 2014). During the 1989-1990 eruption of Redoubt Volcano, multiple jetliners encountered the ash cloud, in one case as far away as Texas (Casadevall 1994). A 747-400 jet aircraft inadvertently flew through the 1989-1990 Redoubt ash cloud near Anchorage and temporarily lost power in all four engines. Although the plane landed safely, it incurred \$80 million in damages. This event led to the expansion of AVO and remains an important example of the need for vigorous volcano monitoring and hazard communication (Guffanti et al. 2010).

Proximal Volcanic Hazards

Proximal hazards include ballistics, lahars, pyroclastic flows, lava flows and domes, rockfalls, landslides, debris avalanches, and volcanic gases.

Ballistics

Ballistics are volcanic bombs of pebble- to boulder-sized clasts that are ejected explosively from the volcano during an eruption and typically deposited within a few kilometers of the vent. Ballistic fallout can cause damage and injury to people and structures in the fallout zone.

Lahars

Lahar is an Indonesian word for a flowing mixture of water, rock debris, and mud on a volcano. Lahars can be hot or cold and can consist of material ranging in size from boulders to fine sediment. Typically, lahars have the consistency of wet concrete and can flow along valley floors many tens of kilometers from their volcanic sources. Lahars at volcanoes in Alaska typically occur during volcanic eruptions due to the interaction of hot volcanic debris with ice and snow. The AVO hazard assessments for many of the volcanoes within Alaska's parks show the extent of lahar inundation in river valleys likely to be affected by lahars. Lahars may also be generated during non-eruptive times due to heavy rainfalls that saturate unconsolidated deposits on steep slopes.

During the 2009 eruption of Redoubt Volcano, lahars traveled more than 25 miles (40 km) down the Drift River valley and inundated parts of the Drift River Oil Terminal, resulting in emergency evacuation of personnel and eventually cessation of terminal operations (Schaefer 2012; Figure 7). The Drift River Oil Terminal area also experienced lahars during the 1989-1990 and 1966-1968 eruptions of Redoubt.



Figure 7. Aerial view of the lower Drift River and the Drift River Oil Terminal after 2009 eruptive activity on Redoubt Volcano. April 4th lahar deposits (lighter color on right) overlie older darker lahar deposits from earlier event(s) in March. Image taken by Max Kaufman on June 8, 2009 and courtesy of the AVO/UAF-GI, [AVO image ID 19402](#)

Pyroclastic Flows and Surges

Pyroclastic flows are hot, turbulent mixtures of gas and rock debris that travel downslope during explosive volcanic eruptions. Pyroclastic flows may form when a lava dome or eruption column collapses and may travel more than 19 miles (30 km) from the source vent. Pyroclastic surges are similar to flows, but contain more gas. Pyroclastic flows and surges are generally confined by existing streams and drainages, but also may travel over topographic features. Eruptions of Redoubt in 1989-1990 and 2009 produced pyroclastic flows that

moved down the Drift glacier gorge and eroded and melted glacier ice that contributed large amounts of water to the valley floor that resulted in lahar generation (Figure 8). Pyroclastic flows produced during the 1912 eruption of Katmai-Novarupta, the largest eruption in the world during the 20th Century, include approximately 2.6 cubic miles (11 km³) of pyroclastic material that filled nearby valleys (Fierstein and Hildreth 1992). This deposit, one of the most spectacular examples of such deposits on Earth, is known today as the Valley of Ten Thousand Smokes.



Figure 8. Aerial view of the north flank of Redoubt Volcano following the early morning eruption on April 4, 2009. Pyroclastic debris that advanced down the Drift glacier gorge overtopped the west shoulder (right side in this image) and flowed onto the crevassed glacier ice. Steam rises from where the hot debris is sifting down into crevasses.

Image taken by K.F. Bull and courtesy of AVO/USGS, [AVO image ID 47211](#)

Lava Flows and Domes

Due to their composition, lava flows in Alaska typically travel slowly and therefore are an avoidable hazard. Some lava flows in Alaska are associated with sustained lava fountaining whereby fountain-fed lava flows develop and may extend several kilometers down the flank of the volcano. When lava flows interact with water or ice, additional hazards may include explosions and ballistic production. Lava domes are viscous, plug-like masses of lava that form at the top of a volcanic conduit (Figure 9). Lava domes may become unstable and susceptible to collapse, resulting in the formation of a type of pyroclastic flow called a block and ash flow that can travel several kilometers and be quite hazardous.

Volcanic eruptions in Alaska parks have produced lava flows and domes at several locations. Typically, a

lava flow poses no hazard to people as it is possible to walk away from an advancing lava flow without harm. In the unlikely event that a person was near an actively growing lava dome, this could pose a more substantial hazard because of the possibility for gravitational collapse and the formation of block and ash flows. Additionally, lava flows advancing over snowfields can cause unstable ground conditions due to surface and subsurface melting. These processes can happen quickly and typically there would not be sufficient time for a person to move to a safer location.

Eruptions of Redoubt Volcano, Mount Veniaminof, and several volcanoes within the Katmai cluster have generated lava flows during historical eruptions. Some of these lava flows interacted with glacier ice, such as during the 2013 eruption of Mount Veniaminof, where lava flowed over glacier ice and snow within the ice-filled caldera, producing voluminous steam and melting a small ice cauldron in the glacier (Figure 10; Dixon et al. 2015).

Mass Movement: Rockfalls, Landslides, and Debris Avalanches

Because volcanoes are constructed of fragmental volcanic material that is poorly consolidated and often very altered, they are somewhat unstable and may be susceptible to mass movement. Whereas a rockfall is a localized event that may not impact a large area, landslides involve mobilization of loose material over a larger range of surface areas, and debris avalanches involve massive collapses of parts of a volcanic edifice.

Rockfall and landslide hazards are an ongoing concern to park visitors in all locations with steep volcanic terrain and high relief. Large landslides can be triggered by tectonic earthquakes especially in landslide-prone areas where they have happened previously. Large flank-collapse debris avalanches

are generally uncommon, although most volcanoes experience one or two large flank failures in their life history, typically associated with other types of volcanic unrest or eruptive activity. At Iliamna Volcano, small volume rockfalls and landslides are occasionally observed and are typically associated with an area of persistent fumarolic activity on the upper southeast flank of the volcano (Figure 11). Small rock-ice-snow avalanches are also common on the upper edifice of Redoubt Volcano, but are usually confined to the summit crater area.

Volcanic Gases

The magma that fuels volcanic eruptions contains dissolved gases. Volcanic gases are released from the magma during eruptions, but can also be passively released when the volcano is not erupting. Typical volcanic gases include water vapor, carbon dioxide, sulfur dioxide, hydrogen sulfide, hydrogen, and fluorine (Myers et al. 2008). When a volcano degases passively, it does so via fumaroles and cracks in the volcanic edifice. Volcanic gases may irritate respiratory systems and eyes for those that are close to the vent area; gases may combine with water in the atmosphere, forming acid rain that damages plants and can impact animals and infrastructure. Because carbon dioxide is heavier than air, it may collect in low-lying areas thereby displacing oxygen making normal respiration difficult or impossible. Volcanic gases released into bodies of water create an acidic environment that is toxic to plant and animal life.

Volcanic gases emitted by active volcanoes within Alaska parks are typically not hazardous because many of the vents lack suitable topography that facilitates trapping of gases. Also, the frequent windy conditions at most volcanoes disperse volcanic gas and inhibits build up to toxic levels. Nevertheless, actively degassing areas within craters have the potential to collect gas and fumarolic areas on the flanks. This may lead to unstable ground conditions



Figure 9. Novarupta dome, June 2006. Image taken by Pavel Izbekov, courtesy of AVO/UAF-GI. [AVO image ID 14207](#)

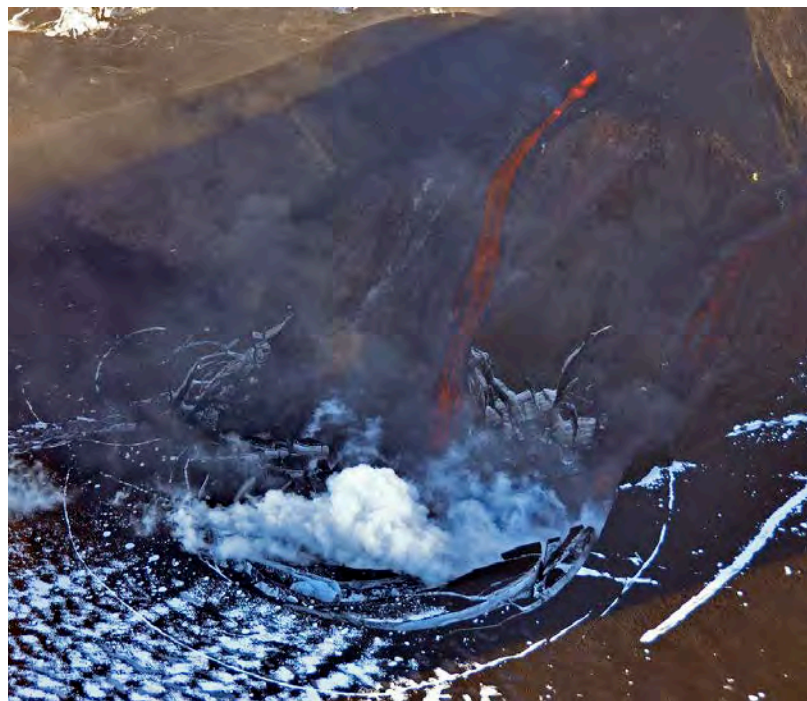


Figure 10. A steady stream of molten lava flows down the east flank of the intracaldera cone at Mount Veniaminof, advancing into an ice cauldron to produce a roiling steam plume. Photo taken on August 19, 2013 by Game McGimsey, AVO/USGS during an overflight co-sponsored by the National Geographic Society. [AVO image ID 54781](#)



Figure 11. AVO web-camera image of a small landslide on the eastern flank of Iliamna Volcano, April 13, 2017. [AVO image ID 54781](#)



Figure 12. Fumarole on northwest side of Fourpeaked Mountain. Yellow staining on snow is the result of sulfur emission from the vent. Image taken on February 22, 2007 by Cyrus Read, courtesy of AVO/USGS. [AVO image ID 13141.](#)

and such areas should be avoided. Occasionally, volcanic gas emissions can develop suddenly at unexpected locations on volcanoes. For example, Fourpeaked Mountain was not considered an historically active volcano until 2006, when steam explosions (also called phreatic explosions), sulfur compounds, and particulate emissions heralded the onset of fumarolic activity near the glacier-clad summit (Figure 12; Neal et al. 2009). In the western part of Wrangell-St. Elias National Park and Preserve near Glennallen, there are two areas bounding faults where carbon dioxide-charged warm saline water is issuing through ancient lake sediments at the surface creating mud volcanoes informally called the Tolsona and Klawasi group. Park visitors in areas of the mud volcanoes also risk exposure to volcanic gases.

Conclusion

AVO is responsible for monitoring, conducting research, and evaluating the hazards of volcanoes in Alaska, which includes the 14 historically active volcanoes within national parks, preserves, and monuments. As such, AVO relies on National Park Service support in enabling field operations, which encompasses monitoring station maintenance, geologic investigations, and eruption response. AVO maintains inter-agency relationships to allow for rapid communication of information regarding volcanic events, with the goal of protecting the public, including park personnel and visitors, from harm. Multiple volcanic hazards exist within park boundaries, including ash clouds, tephra fall, volcanic gases, pyroclastic flows and surges, lava flows, and mass movements such as rockfalls and landslides. As park personnel and visitors are made aware of the types of volcanic hazards, they can better know how to avoid them. One step toward increasing awareness of volcanic hazards within Alaska's national parks, preserves, and monuments is to encourage park personnel and visitors to familiarize themselves

with the volcano alert system and to subscribe to the Volcanic Activity Notification service. In addition, park personnel and visitors should always be aware of the Alert Level and Aviation Color Code for those volcanoes in their vicinity.

Get Alaska Volcano Information!



Alaska Volcano Observatory website: <https://avo.alaska.edu/>

Subscribe to the Volcanic Activity Notification (VAN) system:

<https://volcanoes.usgs.gov/vns2/>

Alaska Volcano Observatory on Social Media



on Twitter @alaska_avo



on Facebook @alaska.avo

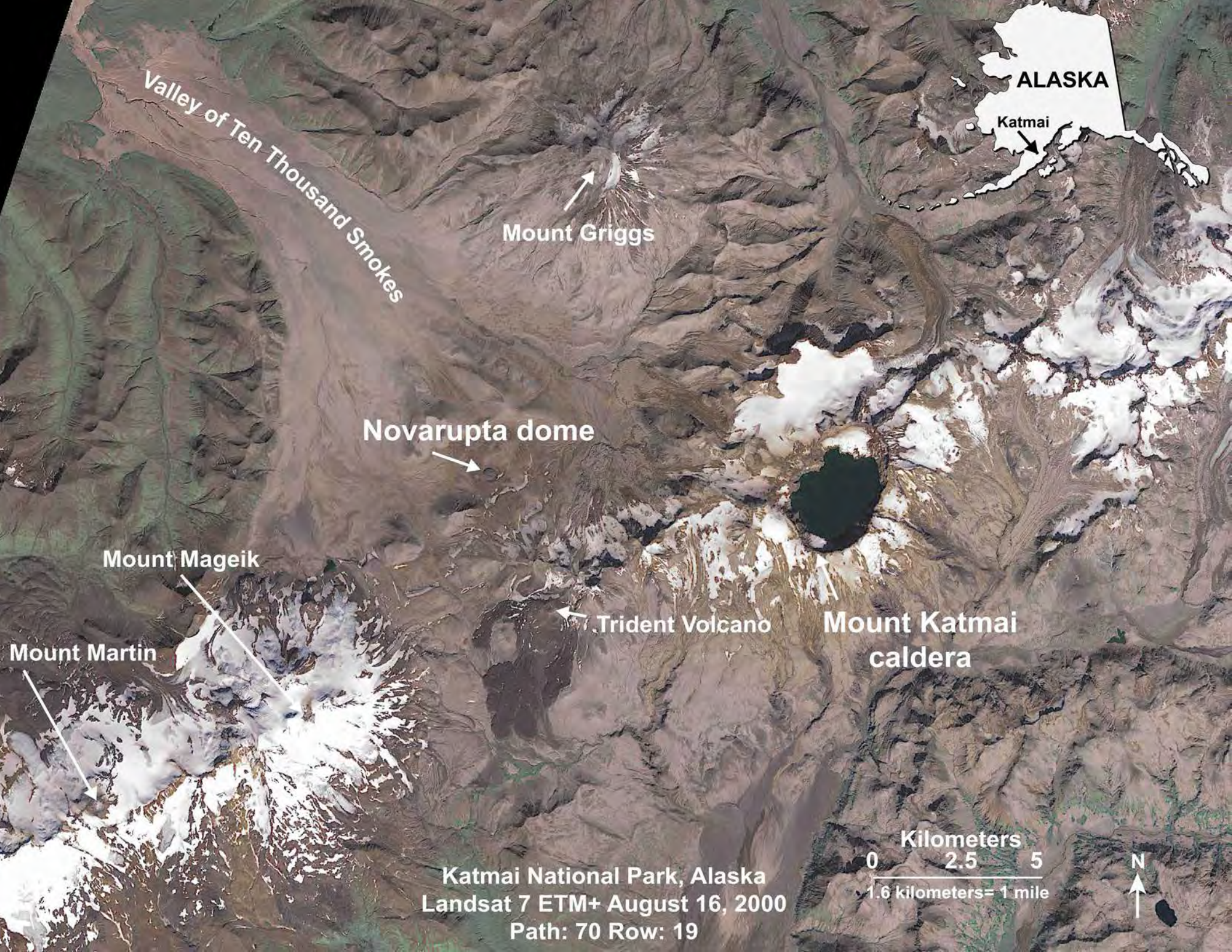
Hazard Assessments for Volcanoes in National Park Service Lands in Alaska

Hazard assessments for volcanoes in Alaska are all available at <https://avo.alaska.edu/downloads/classresults.php?pregen=haz>

USGS Volcano Hazards Program website: <https://volcanoes.usgs.gov/index.html>

REFERENCES

- Alaska Volcano Observatory, National Weather Service, Federal Aviation Administration, Department of Defense, United States Coast Guard, Division of Homeland Security and Emergency Management, Alaska Department of Environmental Conservation, and Alaska Department of Health and Social Services (participating agencies). 2017.
Alaska interagency operating plan for volcanic ash episodes, 49 p.
- Bacon, C. R., C. A. Neal, T. P. Miller, R. G. McGimsey, and C. J. Nye. 2014.
Postglacial eruptive history, geochemistry, and recent seismicity of Aniakchak volcano, Alaska Peninsula. U.S. Geological Survey Professional Paper 1810, 74 p., <http://dx.doi.org/10.3133/pp1810>
- Cameron, C. E. and J. R. Schaefer. 2016.
Historically active volcanoes of Alaska. Alaska Division of Geological & Geophysical Surveys Miscellaneous Publication 133(2): 1 sheet, <http://doi.org/10.14509/20181>
- Casadevall, T. J. 1994.
The 1989-1990 eruption of Redoubt Volcano, Alaska: impacts on aircraft operations. In Miller, T. P. and B. A. Chouet, (eds.), The 1989-1990 eruptions of Redoubt Volcano, Alaska. *Journal of Volcanology and Geothermal Research* 62(1):301-316.
- Dixon, J. P., C. Cameron, R. G. McGimsey, C. A. Neal, and C. Waythomas. 2015.
2013 Volcanic activity in Alaska - Summary of events and response of the Alaska Volcano Observatory. U.S. Geological Survey Scientific Investigations Report 2015-5110, 92 p., <http://dx.doi.org/10.3133/sir20155110>
- Fierstein, J. and W. Hildreth. 1992.
The plinian eruptions of 1912 at Novarupta, Katmai National Park, Alaska. *Bulletin of Volcanology* 54(8):646-684.
- Gardner, C. A., and M. C. Guffanti. 2006.
U.S. Geological Survey's alert notification system for volcanic activity. U.S. Geological Survey Fact Sheet 2006-3139, 4 p.
- Guffanti, M. C., T. J. Casadevall, and K. Budding. 2010.
Encounters of aircraft with volcanic ash clouds: A compilation of known incidents, 1953-2009. U.S. Geological Data Series 545, ver. 1.0, 12 p., plus 4 appendixes including the compilation database, available only at <http://pubs.usgs.gov/ds/545>
- Hildreth, W. and J. Fierstein. 2012.
The Novarupta-Katmai eruption of 1912: Largest eruption of the twentieth century: Centennial perspectives. U.S. Geological Survey Professional Paper 1791, 259 p., available at: <http://pubs.usgs.gov/pp/1791/>
- Mulliken, K. M., J. R. Schaefer, and C. E. Cameron. 2018.
Geospatial distribution of tephra fall in Alaska: a geodatabase compilation of published tephra fall occurrences from the Pleistocene to the present. Alaska Division of Geological & Geophysical Surveys Miscellaneous Publication 164, 46 p. <http://doi.org/10.14509/29847>
- Myers, B., S. R. Brantley, P. Stauffer, and J. W. Hendley, II. 2008.
What are Volcano Hazards? U.S. Geological Survey Fact Sheet 002-97.
- Neal, C. A., R. G. McGimsey, J. P. Dixon, A. Manevich, and A. Rybin. 2009.
2006 Volcanic activity in Alaska, Kamchatka, and the Kurile Islands: Summary of events and response of the Alaska Volcano Observatory. U.S. Geological Survey Scientific Investigations Report 2008-5214, 102 p.
- Neal, C. A., T. L. Murray, J. A. Power, J. N. Adleman, P. M. Whitmore, and J. M. Osiensky. 2010.
Hazard information management, interagency coordination, and impacts of the 2005-2006 eruption of Augustine Volcano. Chapter 28 of Power, J. A., Coombs, M. L., and J. T. Freymueller (eds.), The 2006 eruption of Augustine Volcano, Alaska. U.S. Geological Survey Professional Paper 1769, p. 645-667.
- Schaefer, J. R. (ed.). 2012.
The 2009 eruption of Redoubt Volcano, Alaska, with contributions by Bull, Katharine, Cameron, Cheryl, Coombs, Michelle, Diefenbach, Angie, Lopez, Taryn, McNutt, Steve, Neal, Christina, Payne, Allison, Power, John, Schneider, Dave, Scott, William, Snedigar, Seth, Thompson, Glenn, Wallace, Kristi, Waythomas, Chris, Webley, Peter, and Werner, Cynthia. Alaska Division of Geological & Geophysical Surveys Report of Investigation 2011-5, 45 p.



Valley of Ten Thousand Smokes



Mount Griggs

Novarupta dome

Mount Mageik

Trident Volcano

Mount Katmai caldera

Mount Martin

Kilometers
0 2.5 5
1.6 kilometers = 1 mile



Katmai National Park, Alaska
Landsat 7 ETM+ August 16, 2000
Path: 70 Row: 19

Volcanic Ash Resuspension from the Katmai Region

Kristi L. Wallace and Hans F. Schwaiger, Alaska Volcano Observatory, U. S. Geological Survey

Volcanic ash is not only a hazard during an eruptive event; in strong winds, previously deposited volcanic ash can be reincorporated into dust clouds. Resuspension and transport of fine-grained volcanic ash from Katmai National Park and Preserve has been observed and documented many times over the past several decades and has likely been occurring since the 1912 Novarupta-Katmai eruption, the largest 20th century eruption in the world.

Citation:

Wallace, K. L. and H. F. Schwaiger. 2019. Volcanic ash resuspension from the Kamai region. *Alaska Park Science* 18(1): 62-69.

Volcanic ash is not only a hazard during an eruptive event; in strong winds, previously deposited loose volcanic ash can be picked up and reworked into dust clouds. Resuspension and transport of fine-grained volcanic ash from Katmai National Park and Preserve, Alaska has been observed and documented many times over the past several decades and has likely been occurring throughout the time interval since the 1912 Novarupta-Katmai eruption (Hadley et al. 2004). This eruption, the largest in the world during the 20th Century, produced approximately 4 cubic miles (17 km³) of ash deposits and 2.6 cubic miles (11 km³) of pyroclastic material that filled nearby valleys, creating what is today known as the Valley of Ten Thousand Smokes (VTTS; Fierstein and Hildreth 1992). Ash in this valley is up to 660 feet (200 m) thick and the valley remains almost entirely free of vegetation (Figure 1).

Volcanic ash describes fragments of volcanic material less than 0.08 inches (2 mm) in diameter. In the VTTS, ash and other fine-grained material can be picked up (reworked) into dust clouds during the spring and fall, or whenever strong northwesterly winds blow over the snow-free landscape. The ash is especially susceptible to reworking when the ground is very dry. These dust clouds have been observed visually by individuals downwind, in images acquired by remote web cameras, and also in satellite imagery (Figures 2, 3, and 4).

Figure 1. True color composite satellite image of the Valley of Ten Thousand Smokes and surrounding volcanoes. Image produced by Steve J. Smith. Modified from [AVO image ID 2152](#)

Novarupta: The Greatest Volcanic Eruption of the Twentieth Century

June 6, 1912 dawned clear and calm. People were busy getting ready for the upcoming fishing season, but for at least a week they had felt earthquakes. Earthquakes are common in Alaska, a region long known for geologic instability, but people living and working in what would later become Katmai National Park and Preserve noticed that these earthquakes were unusually frequent and getting stronger. This prompted families at Katmai Village to evacuate their homes and they never returned.

Around 1 PM on June 6, the skies darkened over Katmai and the world's largest eruption of the 20th century began. For the next 60 hours, the sun disappeared. In total, ash and magma exploded out of the earth at Novarupta, 30 times more than the 1980 eruption of Mount St. Helens.

Kodiak Island, 100 miles (160 km) downwind of the ash cloud, was plunged into a darkness so complete that a lantern held at arm's length could scarcely be seen. The darkness lasted three full days. The terrified townspeople, some temporarily blinded by the sulfurous gas, crowded onto the U.S. Revenue Cutter Manning docked in Kodiak harbor, while one foot of ash (30 cm) smothered their town with three closely spaced periods of ash fall. The weight of the ash collapsed roofs in Kodiak; buildings were wrecked by ash avalanches that rushed down from nearby hill slopes; other structures burned after being struck by lightning from the ash cloud; and water became undrinkable. The ash cloud eventually encircled the Earth.

The summit of Mount Katmai, some 6 miles (10 km) distant from Novarupta collapsed as magma drained from underneath and vented through Novarupta. The former summit of Mount Katmai is now a caldera 1.9 miles (3 km) wide and 2,000 feet (600 m) deep. The eruption also brought worldwide attention to a little-known and obscure region of the Alaska Territory. Scientific expeditions funded by the National Geographic Society in the 1910s led to the creation of Katmai National Monument in 1918.

[Witness: First Hand Accounts of the Largest Volcanic Eruption of the Twentieth Century](#)

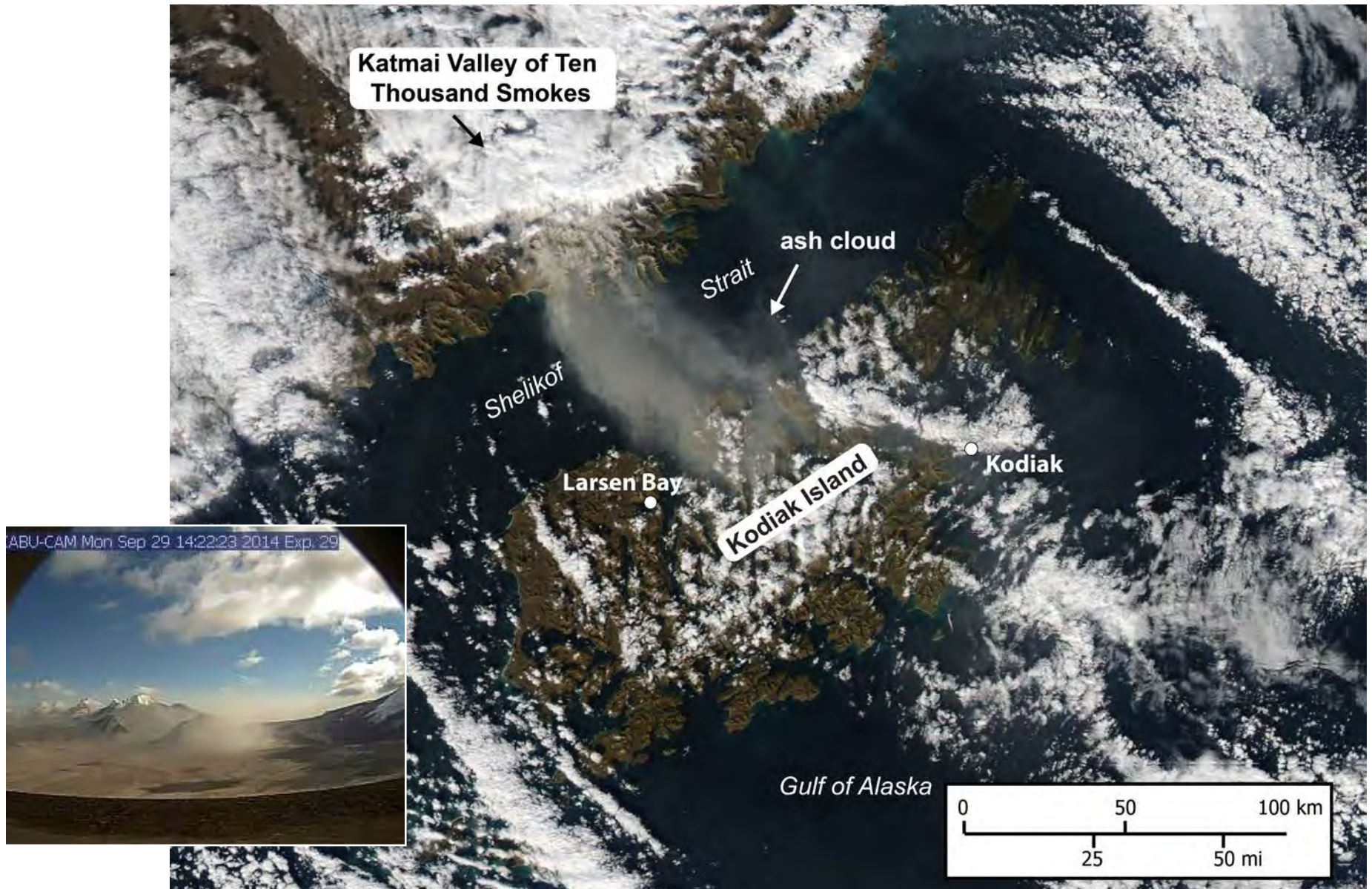


Figure 2. This MODIS Aqua 1-km-resolution true color satellite image shows a resuspended ash cloud generated from high winds scouring the dry, unvegetated deposits in the Valley of Ten Thousand Smokes. The cloud stretches across Shelikof Strait to western Kodiak Island. Image obtained October 5, 2014, courtesy of the National Aeronautics and Space Administration (NASA). [AVO Image ID 133541](#).

Figure 3 (inset). Image taken from a web camera in the Valley of Ten Thousand Smokes shows an example of resuspended ash from this region on September 29, 2014. [AVO image ID 80721](#)

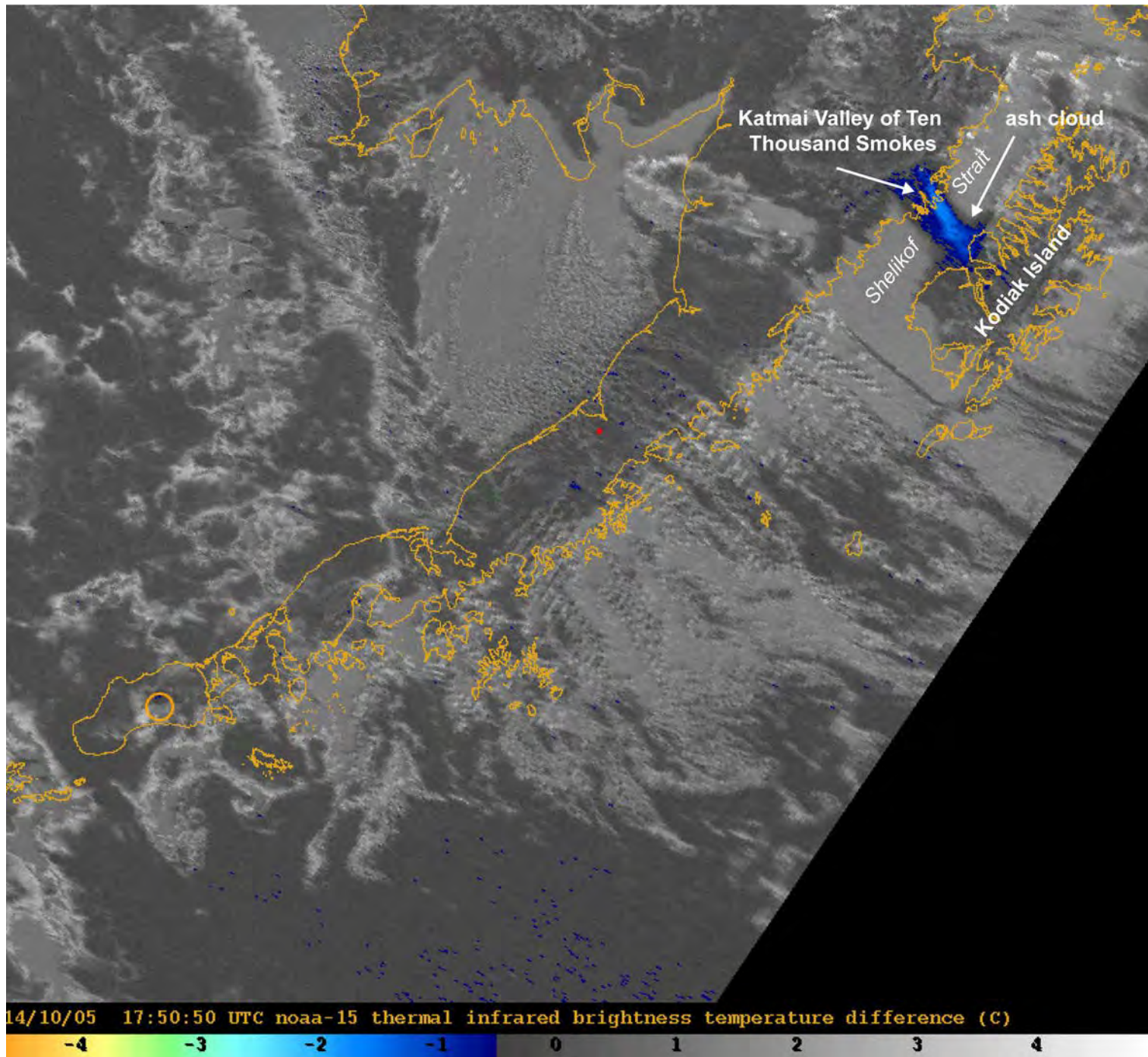


Figure 4. NOAA satellite image from October 5, 2014, showing the differences in brightness temperatures between two infrared channels, indicating the presence of airborne volcanic ash (blue area in the upper right). This plume of resuspended ash from the 1912 Novarupta-Katmai eruption deposit reached an altitude estimated at 4,000–6,000 feet (1.2–1.8 km) above sea level as it drifted southeast towards Kodiak Island. This satellite image is from the same resuspension event shown in Figure 3. [AVO image ID 80451.](#)

Ash resuspension events originating in the Katmai VTTS have been observed and recorded about 30 times since 2003 (Figure 5) when the Alaska Volcano Observatory began actively recording them. The dust clouds produced by these events are typically concentrated between 4,000 and 11,000 feet (1–3.4 km) above sea level and have traveled as far as 155 miles (250 km), usually drifting southeast over Shelikof Strait, Kodiak Island and the Gulf of Alaska. Trace amounts of ash (typically less than 1/32 inch or 1 mm) have fallen on communities on Kodiak Island.

Characteristics of Resuspension Events

- Occur in late spring and fall during snow free and dry conditions
- Occur with wind speeds of more than 20 knots
- Plumes of resuspended material reach 4,000–11,000 feet (1–3.4 km) above sea level
- Duration of hours to days
- Enhanced by local terrain effects (mountains, valleys, etc.)
- Extend up to about 155 miles (250 km) in the Gulf of Alaska
- Often trigger ash alerts notifying Alaska Volcano Observatory and National Weather Service staff to issue products

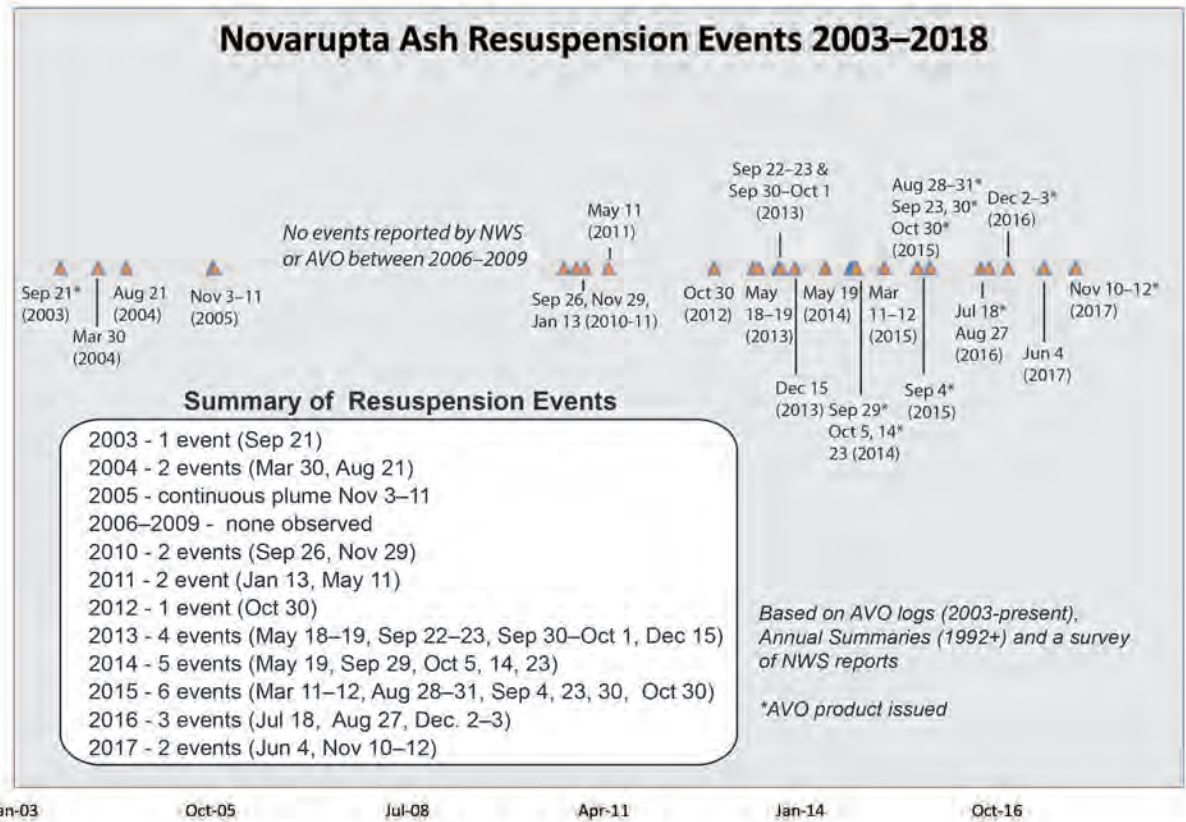


Figure 5. Summary of Katmai-area resuspension events known to AVO from 2003-2018.

Hazards and Impacts Associated with Resuspended Ash

During dry conditions, strong winds in the Katmai region can pick up and transport fine ash. This resuspended ash is composed primarily of volcanic glass shards (Figure 6) and is physically identical to ash produced in volcanic eruptions. Thus, the resulting plume looks like that produced during an explosive volcanic eruption (Figure 6).

Likewise, these ash clouds, even when relatively dilute, can pose hazards to human health and aircraft operation (Hadley et al. 2004). Ash clouds produced

during eruptions can abrade aircraft surfaces, such as cabin and cockpit windows, damage sensitive electronics, and erode and adhere to engine parts (Neal and Guffanti 2010). Resuspended volcanic ash plumes have not been well studied and much remains to be learned about the sizes and concentration of the ash particles and volumes mobilized. Moreover, impacts from the fallout of resuspended ash are not well known. The largest resuspension events observed so far only deposited trace amounts of ash (thicknesses less than 1/32 inch or 1 mm) on Kodiak Island communities. It is not known if this amount presents an air quality issue and thus a public health hazard.

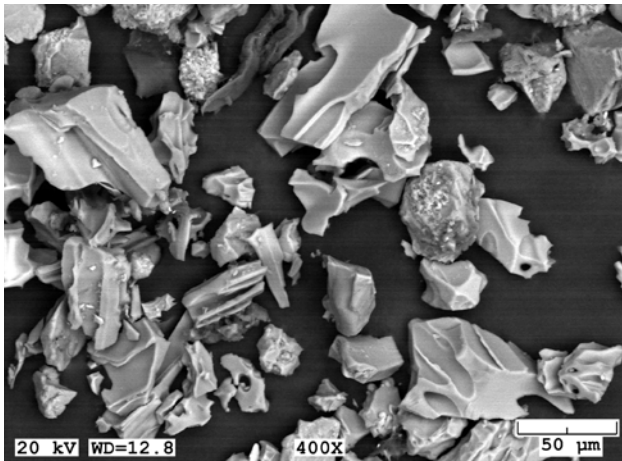


Figure 6. Backscatter electron image of resuspended volcanic ash from the 1912 Novarupta-Katmai deposits in the Katmai VTTS region, picked up during high winds on November 1, 2015 and carried to Larsen Bay on Kodiak Island, AK. Sample collected by Sherry Harmes of Larsen Bay. [AVO Image ID 94841](#).

Regardless, dust storms composed of resuspended ash within the Katmai region are likely to be hazardous to park visitors and staff owing to the high concentration of ash in dust clouds nearer to the source area (VTTS). Avoiding exposure, especially by people already at risk, such as children, the elderly, and those with existing respiratory or cardiovascular disease, is the best way to mitigate the hazard. If exposed to a dust storm in the VTTS, use of an industry-approved disposable N95 dust respirator mask is advised until the event ends. Because it is abrasive, resuspended ash may also irritate eyes and skin; this can be minimized by using eye goggles and protective clothing such as pants and long-sleeved shirts.

Ash Resuspension Monitoring

Ash Cloud Surveillance

The Alaska Volcano Observatory (AVO) and the National Weather Service (NWS) both monitor ash clouds using near-real-time satellite data. AVO

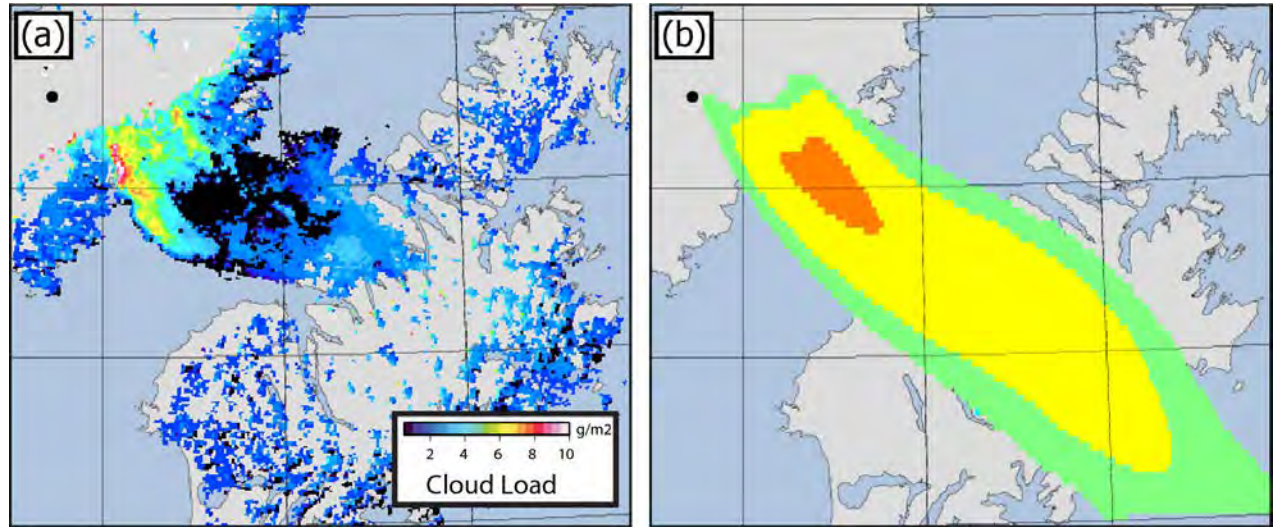


Figure 7. (a) The satellite-derived cloud load for a resuspension event on October 5, 2015. The Ash3d simulated cloud load for this event is shown in (b).

reviews available satellite data once per day and has automated alarms that alert staff of possible ash clouds. The NWS monitors for ash clouds continuously, also relying on automated systems to alert staff of ash clouds. Both agencies work closely and coordinate when such events are recognized. During times when the NWS forecasts high winds in the Katmai region, both agencies pay special attention to satellite data for signs of resuspension.

Resuspension Modelling

Since resuspended ash clouds pose the same hazards as those produced during an explosive eruption, AVO strives to anticipate when conditions are suitable for resuspension events to occur. Volcanic ash within the VTTS will begin to remobilize once the stresses from surface winds exceed a threshold. At that point, ash can be entrained in the air along the ground surface in the valley. If the lower levels of the atmosphere are stable, then this remobilized ash layer may remain close to the ground surface (Figure 3). However, if

the meteorological conditions are suitable for vertical mixing, the ash may be lofted several thousand feet, where it may then drift with the wind, predominantly southeast over Shelikof Strait and Kodiak Island.

AVO has modified their volcanic ash dispersion and deposition model (Ash3d; Schwaiger et al. 2012) to include the resuspension of ash deposits. Analysis of the meteorological and surface conditions (strength of the wind, atmospheric stability, precipitation, and snow cover) present during past occurrences of resuspended ash allows identification of the conditions conducive for generation of resuspension events. Thus, using numerical weather prediction forecast models, Ash3d can anticipate when resuspension events are most likely to occur.

For some events with particularly good satellite observations, it has been possible to estimate both the amount of ash in the atmosphere (Figure 7) and the height of the ash cloud, parameters crucial for determining the downwind aviation hazard.

Moreover, these satellite observations have helped to constrain the Ash3d model for predicting the onset and cessation of events. Ash3d is currently run automatically at AVO, sending text and email alerts to AVO staff when resuspension events are expected. These alerts provide situational awareness to AVO staff, who then coordinate with the NWS.

Air Quality Monitoring and Characterization of Deposits

Although aviation hazards are the more urgent concern with volcanic ash clouds, it is possible that dilute ash clouds can reduce the surface air quality sufficiently to pose a hazard to human health. To address these concerns, AVO, in partnership with the Alaska Department of Environmental Conservation-Air Quality Division (AK-DEC), deployed particulate instruments (PM-10, particulate matter of ≤ 10 microns in diameter) to Kodiak Island during the fall and spring months in 2015-2016 to monitor air quality impacts during ash resuspension events (Figure 8). These instruments were placed in two communities on Kodiak Island that historically have been impacted by resuspended volcanic ash: Larsen Bay and the city of Kodiak. During this time, only moderate resuspension events occurred, and recorded degradation of air quality associated with a few of these events with PM-10 values up to $60 \mu\text{g}/\text{m}^3$. These episodes did not exceed the Environmental Protection Agency (EPA) 24-hour PM-10 standard of $150 \mu\text{g}/\text{m}^3$; however, AVO continues to assess the forecast ground concentrations as well as air borne cloud load. The long-term impacts of resuspension and fallout of volcanic ash after large eruptions is becoming better documented (e.g., Gordian et al. 1996, Horwell and Baxter 2006, Thorsteinsson et al. 2012), but remains unknown from this region.

Samples of fallout from resuspended clouds collected during this short study, and others sent to AVO by citizens in Kodiak from past events, confirm that these ash clouds are composed predominantly of shards of volcanic glass. Even after more than 100 years of being deposited in the Katmai valley, these particles appear pristine and very similar to those deposited during an eruption.

How the Public is Notified of Resuspension Events

The Alaska Volcano Observatory works closely with the National Weather Service, which has the responsibility to issue forecasts and statements of resuspended volcanic ash. These include forecasts of airborne ash hazards to aircraft, volcanic ash

advisories, and forecasts of ashfall to communities and mariners. AVO also coordinates with the Alaska Department of Environmental Conservation, Division of Air Quality during ash resuspension, who has the responsibility to issue guidance on air quality hazards. In addition to these official warning products, AVO issues Information Statements during resuspension events from the Katmai region that clearly state they are not the result of an active volcanic eruption. Accordingly, since there is no eruption, AVO does not issue formal Volcanic Activity Notices (VANs) during resuspension events. The Information Statements are intended to corroborate products issued by the NWS and provide background on these events.



Figure 8. AVO staff working with Larsen Bay Mayor David Harmes on how to operate the particulate monitor used to monitor air quality on Kodiak Island.

[AVO Image ID 80871.](#)

Public Notification Products

Official warnings of ash resuspension events are issued by the National Weather Service

- Forecasts of airborne ash hazard to aircraft:
<http://aawu.arh.noaa.gov>
- Volcanic Ash Advisories (aviation product):
<http://vaac.arh.noaa.gov/>
- Forecasts of ashfall:
<http://pafc.arh.noaa.gov/>

Air quality hazards and guidance: Alaska Department of Environmental Conservation, Division of Air Quality

- Information on volcanic ash impacts and mitigation:
<http://volcanoes.usgs.gov/ash/>
- Information on health impacts and mitigation of volcanic ash:
<https://www.ivhhn.org/home>
- Protection from breathing volcanic ash: <https://www.ivhhn.org/ash-protection>

REFERENCES

- Fierstein, J. and Hildreth, W. 1992.**
The plinian eruptions of 1912 at Novarupta, Katmai National Park, Alaska. *Bulletin of Volcanology* 54(8): 646–684.
- Gordian, M. E., H. Ozkaynak, J. Xue, J., S. S. Morris, and J. D. Spengler. 1996.**
Particulate air pollution and respiratory disease in Anchorage, Alaska. *Environmental Health Perspectives* 104(3): 290.
- Hadley, D., G. L. Hufford, and J. J. Simpson. 2004.**
Resuspension of relic volcanic ash and dust from Katmai: Still an aviation hazard. *Weather and Forecasting* 19(5): 829-840.
- Horwell, C. J. and P. J. Baxter. 2006.**
The respiratory health hazards of volcanic ash: A review for volcanic risk mitigation. *Bulletin of Volcanology* 69(1): 1-24.
- Neal, C. A. and M. Guffanti. 2010.**
Airborne volcanic ash—a global threat to aviation. *U.S. Geological Survey Fact Sheet* 2010–3116, 6 p.
- Schwaiger, H. F., R. P. Denlinger, and L. G. Mastin. 2012.**
Ash3d: A finite-volume, conservative numerical model for ash transport and tephra deposition. *Journal of Geophysical Research* 117(B4).
- Thorsteinsson, T., T. Jóhannsson, A. Stohl, and N. I. Kristiansen. 2012.**
High levels of particulate matter in Iceland due to direct ash emissions by the Eyjafjallajökull eruption and resuspension of deposited ash. *Journal of Geophysical Research* 117(B9).



Spring Breakup on the Yukon: What Happens When the Ice Stops

Scott Lindsey, National Weather Service,
River Forecast Center

Spring breakup can create flooding and ice-scouring hazards for communities along major rivers in Alaska. This article gives examples of recent flood events along the Yukon River and describes the conditions that created them.

Citation:
Lindsey, S. 2019. Spring breakup on the Yukon: What happens when the ice stops. *Alaska Park Science* 18(1):70-75.

May 4, 2009 - I landed in Eagle, Alaska with Claude Denver from the State of Alaska Division of Homeland Security and Emergency Management and we discovered that the Yukon River ice downstream of town had jammed and Eagle was flooding. One local resident said it was the worst flood since 1937. That same day, upstream at Dawson, a run of ice and water passed town and caused water levels there to rise 8 feet (2.5 m). What was already a significant flood in Eagle became a full-fledged disaster that night as water levels rose an additional 10 feet (3 m) and ice chunks the size of bulldozers started to move ashore and crush people's homes.

The mighty Yukon River enters the United States just upstream of Eagle, Alaska and proceeds to wind to the northwest through the Yukon-Charley Rivers National Preserve (Figure 1). It passes the villages of Circle and Fort Yukon before turning southwest and heading for the Bering Sea. A traveler would cover about 1,200 miles (1,930 km) of Alaskan wilderness following the river from the border to the mouth. During the summer, residents and visitors use the river as a highway connecting villages and allowing access to subsistence resources and to remote parts of the state by boat. The winter months bring a solid ice cover often exceeding 5 feet (1.5 m) in depth, and with a good snow cover, the river becomes a gateway to everywhere that can be accessed by snow machine, dog sled, or for the truly hearty souls, snowshoes or skis.

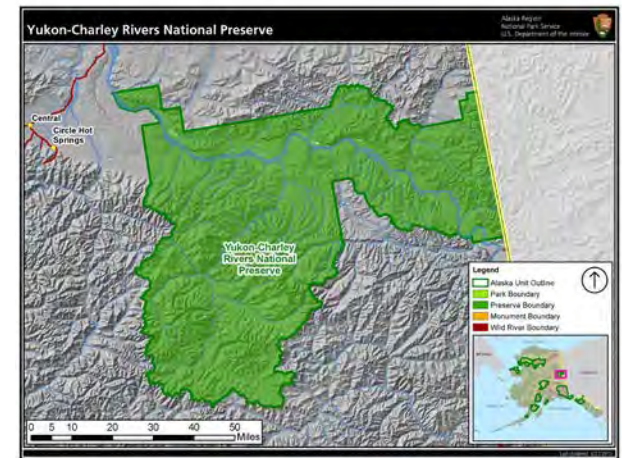


Figure 1. Map of the Yukon-Charley Rivers National Preserve.

The transition seasons interrupt that access as the rivers freeze up in the fall and breakup in the spring. Spring breakup can bring catastrophic floods as the water levels rise and the ice moves, and sometimes jams and stops. During a typical winter in interior Alaska, snow accumulates from October to April and temperatures as low as -60°F (-51°C) keep the snowpack building in depth and water content until April. As the day length starts to rapidly increase in April and May, temperatures rise above freezing, snow begins to melt, and at some point, the river ice begins to move. How it moves downstream determines whether folks living along the river

Yukon River at Eagle looking upstream May 7, 2018. Prior to May 2009, the island in the left foreground was covered with mature trees. Photo courtesy of Scott Lindsey, National Weather Service

breathe a sigh of relief or throw necessities together, pack up their most precious possessions and quickly move to higher ground.

Several factors affect the timing and severity of breakup. Ice thickness and snowpack impact when breakup occurs and the likelihood that ice jams will occur. Temperature typically decreases as elevation increases, so freezing levels determine what proportion of the watershed will contribute snowmelt runoff into the river (e.g., a freezing level at 5,000 feet [1,500 m] means everything below that has a temperature above freezing). Early season rainfall, although rare, can push a significant amount of rainfall runoff into the river. Ice that has a fresh layer of snow with a high albedo (*albedo* is a measure of how much of the sun's energy is reflected rather than absorbed), may be much stronger than ice that is bare of snowcover and has been exposed to the sunshine for days. The level of the river when the ice formed in the fall can also affect the severity of breakup. When rivers freeze at high water levels, ice sheets will extend over the great majority of the river channel, which can translate into ice sheets that don't fracture easily when increased runoff starts to lift them and push them downstream. But the most important factor governing timing and severity of breakup is the temperature pattern from early April to mid-May (Figure 2).

When temperatures begin to rise above freezing and reports of open water and lifted ice on river edges and in river channels begin to arrive at the Alaska-Pacific River Forecast Center (APRFC), it is time to coordinate a launch of a Riverwatch team with the State of Alaska Division of Homeland Security and Emergency Management (DHS&EM). Riverwatch is a collaborative program between DHS&EM and the National Weather Service (NWS) APRFC to monitor the river ice breakup and to assist communities in the event of breakup related flooding. The program, in

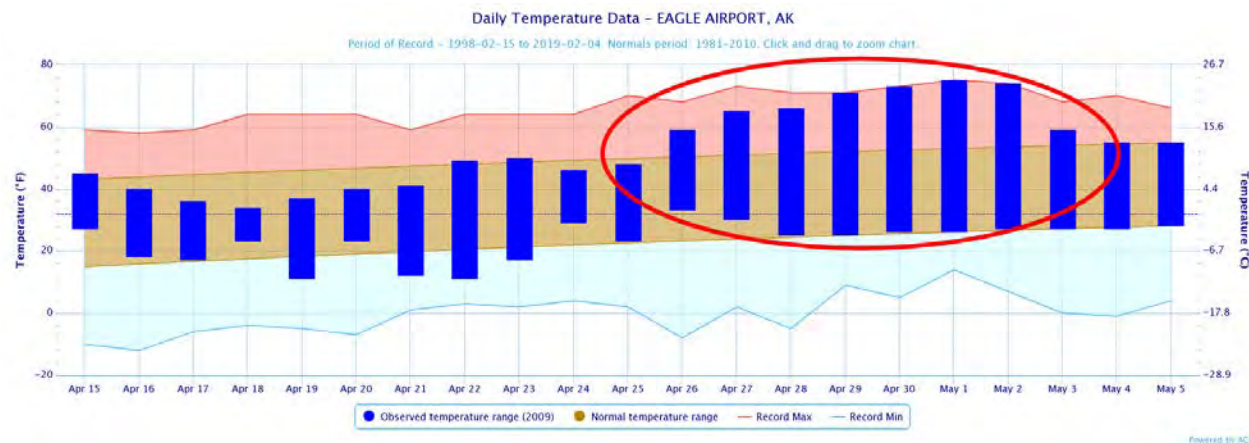


Figure 2. Air temperatures at Eagle Airport, Spring 2009, flooding began on May 3, 2009 following 4 days of record high temperatures. (Data source: <http://xmacis.rcc-acis.org/>)

existence since the 1970s, teams a hydrologist from APRFC with an Emergency Management specialist from DHS&EM in a small, chartered plane. During these flights, the Riverwatch team flies along the river observing ice and breakup conditions and reports pertinent information to the NWS, state officials, and most importantly, residents of the villages and towns along the Kuskokwim and Yukon rivers. The hydrologist determines the potential for flooding, including likely severity, and the team lands in each village or town and talks to community leaders to share their observations of the river, advise them of potential flood threats and ensure that they are properly prepared. NWS Weather Forecast offices disseminate watches and warnings for hazards including flooding from breakup ice jams. When severe flooding occurs that overwhelms the resources of a community, the state's DHS&EM and, in some cases, the federal government through the Federal Emergency Management Agency (FEMA), coordinate the management of various local, state, federal, and tribal efforts to bring relief to the community. The main purpose of Riverwatch is to

keep residents informed of potential threats, let them know where the breakup front is located relative to their town or village, ensure that communities are prepared for potential flooding, and facilitate responses when flooding occurs. In 2009, when flooding began, the state had up-to-date information on the status of Eagle and relief efforts were launched quickly as the need for help became apparent.

Some examples will better explain how breakup factors interrelate and how they can lead to very different outcomes. There are two basic types of breakup processes (Beltaos 2009). The first is called a *thermal breakup* or colloquially, a *mushout*. Various combinations of circumstances can contribute to a thermal breakup. Essentially, ice gets soft and weak before any significant amount of water and ice from upstream arrives to push it. When water levels rise or a local ice run from a tributary reaches that ice, it quickly breaks into very small pieces. A slow transition from cold temperatures to warm temperatures is probably the primary contributor to this type of breakup, but a low snowpack can also

Types of Breakup Processes (most breakups are a blend of these)

Dynamic Breakup

- Ice remains hard and resistant to breaking and moving
- Ice moves when pushed by ice from upstream
- Ice jams form that can cause upstream flooding
- Extreme case are Kenai River in January 1969 and January 2007 and the Yukon River in May 2009 and 2013.

Thermal Breakup

- Ice becomes very rotten (candled) before ice from upstream arrives
- Rotten ice is weak and has less resistance to breaking into very small pieces
- Persistent ice jams are very unlikely to form
- Extreme case would occur with very little snow melt inflow and warm, sunny weather to rot the ice.

lead to a reduction in snowmelt runoff that allows river ice to melt and deteriorate in place. When thermal breakups occur, breakup may begin at a number of different locations on the river, often at nearly the same time, and the ice tends to break up into small pans and chunks and most important, ice jams that persist for a significant length of time are unlikely to form.

The second scenario is often referred to as a *dynamic* or *mechanical breakup*. Typically, this occurs when there is normal to above-normal snowpack and significant ice thickness. When there is a sudden transition from temperatures near freezing to climatological averages or above (interior Alaska temperatures can reach the 60s and 70s in May), a surge of snowmelt enters the river while the ice is still hard and intact, often with a high albedo reflecting much of the sun's energy. Sheets of ice a half mile or more wide and several miles long first float and then start to move as water levels rise (Figure 3). Any type of channel constriction or sharp bend then results in the downstream ice edge being shoved with

considerable force either up onto higher ground or sand bars, or downward into the river bottom. Both options result in a severe restriction of flow through that jam point and water upstream can rise very rapidly.

In 2009, the water level in Eagle rose more than 30 feet (9 m) in 48 hours as a result of an ice jam 10 miles (16 km) downstream. When a jam of this magnitude occurs, a huge volume of ice and water accumulates and when the jam releases, that ice moves downstream until it reaches the next area of solid ice or some type of channel constriction or tight bend. Then the whole cycle repeats. Dynamic breakups tend to march from upstream to downstream and flood multiple areas and communities as it encounters river ice that is not yet ready to move. In 2009, communities on the Yukon River downstream of Eagle including Circle, Stevens Village, and Tanana also experienced major flooding as the breakup front stalled repeatedly while progressing downstream.

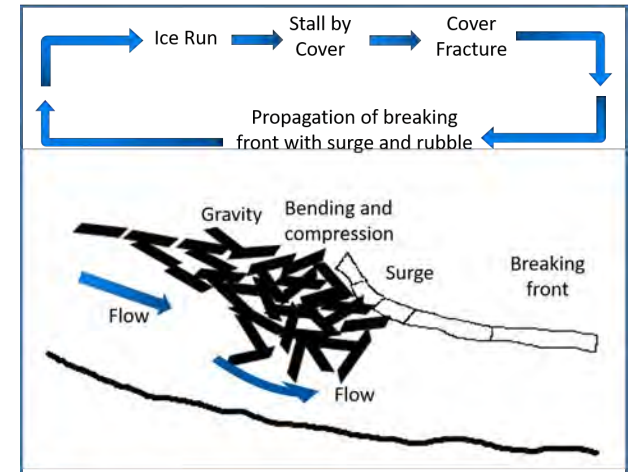


Figure 3. Graphical depiction of what happens at the breakup front during a dynamic breakup of river ice (Shen and Liu 2003).

In addition to the hazard of major flooding, the ice itself can create dangerous situations. Large sheets of ice can be shoved up onto riverbanks and islands and can level everything in the way. An island just in front of Eagle had a mature stand of trees before the 2009 flooding and after the ice went out, the island was barren. Just a short distance upstream of Eagle in Eagle Village, homes and buildings near the river experienced the same treatment and after the ice in the river moved out and the massive chunks of ice stranded on the riverbank melted, there was little evidence of anything left in Eagle Village. Bank erosion can also be accelerated to an extreme level as sheets, pans, and chunks of ice are shoved out of the channel or just move downstream at a fast rate.

Another type of flooding that occurs during spring breakup involves tributaries or smaller streams that enter the main river. When levels on the mainstem, in this case the Yukon River, are very high, water entering from smaller streams tends to back upstream in what is referred to as *backwater*. The level of the ice and water in the mainstem prevent



Thermal breakup at Red Devil on the Kuskokwim River in May of 2005.
Photo courtesy of the National Weather Service



Dynamic breakup in Eagle on the Yukon River in May of 2009.
Photo courtesy of the National Weather Service



Eagle Village, May 5, 2009. When the flooding ended, there was little evidence left of any structures in what had been old Eagle Village.
Photo courtesy of Scott Lindsey, National Weather Service



Tributary entering the Yukon graphically displays backwater flooding as the high levels on the Yukon prevent water in Hess Creek near Rampart from entering the Yukon, causing upstream flooding, May 10, 2009.
Photo courtesy of Scott Lindsey, National Weather Service

normal flow from the tributary into the mainstem and water starts to back up and rise on the tributary until it reaches the same or greater height as the water and ice at the confluence with the mainstem. This can cause flooding on the tributary far upstream of the confluence with the mainstem river.

After the extreme flooding in 2009, it was four years before Eagle saw another significant ice jam flood. In 2013, temperatures around the state were very cool during the month of April and temperature outlooks from the National Oceanic and Atmospheric Administration's (NOAA) Climate Prediction Center showed that trend continuing through mid-May. Although April 1 is typically the date when snowpacks in Alaska reach their peak water equivalent, in 2013 snow kept accumulating in some parts of the interior right through the middle of May. Temperatures then began a quick rise toward normal values (Figure 4), river levels started to rise, but the ice was not ready to move yet. Just a week of temperatures with lows near freezing, highs near normal, and freezing levels near 5,000 feet (1,500 m) was enough to jump start another dynamic breakup. Claude Denver and I were staying in a bed and breakfast right on the bank of the river when ice started moving just after midnight on May 17. By 3 am, the ice had stopped moving and less than an hour later there was 3 feet (1 m) of water in the ground floor of the building we were staying in. Eagle ended up with water levels at 43.9 feet (13 m) or almost 10 feet (3 m) above flood stage for the second-highest flood on record (but well below the 55.7 feet [17 m] level of 2009). In true dynamic breakup fashion, Circle saw moderate flooding, Fort Yukon experienced some minor flooding, and the town of Galena downstream of the confluence with the Tanana River experienced catastrophic flooding.

The first recorded breakup at Eagle occurred on May 10, 1898 and the breakup date has been

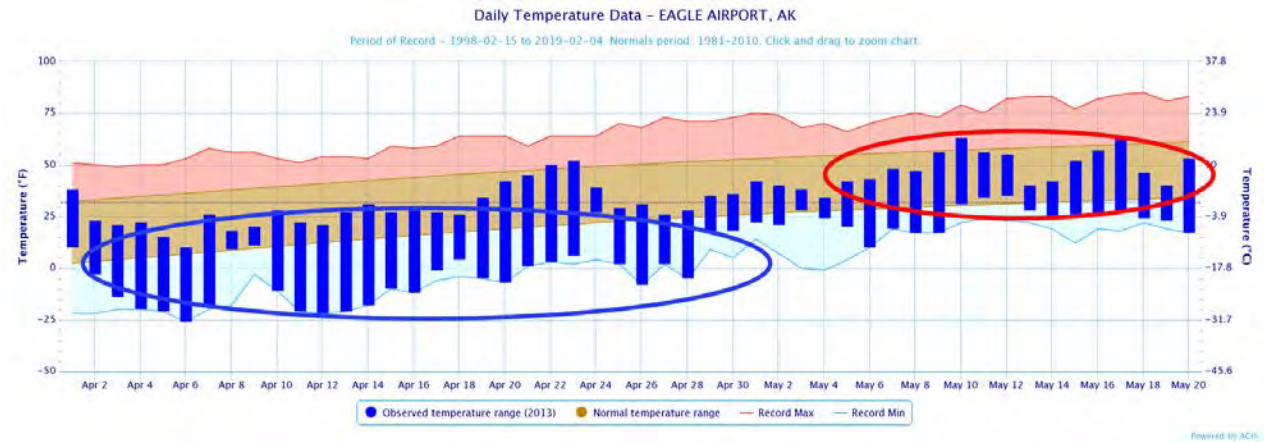


Figure 4. Temperature trace at Eagle Airport in 2013: Note that while temperatures were not significantly above normal, there was a rapid rise from well below normal to normal with overnight lows above freezing. (Data source: <http://xmacis.rcc-acis.org/>).

[documented](#) most years since that time. The U.S. Army Corps of Engineers has an [ice jam database](#) showing locations and dates of river ice jams around the country. The APRFC is located in Anchorage, Alaska and in addition to the Riverwatch program for the Yukon and Kuskokwim rivers, provides detailed information, forecasts, and flood warnings for rivers in the state. In the years since 2013, breakup has been quiet on the upper Yukon River. Generally, spring temperatures have warmed up slowly and uniformly, causing snowmelt to enter the river at a pace that has not created any large waves of runoff moving downstream. Ice has slowly melted and weakened, and although the timing has been different each year (many villages experienced their earliest breakup on record in 2016), the result has been the same, a thermal breakup and no flooding. But there will be another year, maybe in the near future, when snow and ice conditions are right and we have a rapid transition from winter to spring, and the ice will stop.

REFERENCES

[Alaska-Pacific River Forecast Center Breakup Map](#)

Beltaos, S., ed. 2009.

River Ice Breakup. Water Resources Publications, LLC. Highlands Ranch, CO. p. 53, 201-202.

Shen, H. T. and L. Liu. 2003.

Shokotsu River ice jam formation. *Cold Regions Science and Technology* 37(1):35-49.



Coastal Dynamics in Bering Land Bridge National Preserve and Cape Krusenstern National Monument

Louise M. Farquharson, *Geophysical Institute Permafrost Laboratory, Geophysical Institute, University of Alaska Fairbanks*

Richard M. Buzard, *Alaska Department of Natural Resources, Division of Geological and Geophysical Surveys*

Daniel H. Mann, *Department of Geoscience, University of Alaska Fairbanks*

Benjamin M. Jones, *Water and Environmental Research Center, Institute of Northern Engineering, University of Alaska Fairbanks*

Arctic coastlines are changing as a result of warming temperatures and decreasing sea ice extent and duration. An understanding of these changes can contribute to the effective management of coastal habitats and ecosystems, oil-spill response, marine debris collection, and the preservation of cultural artifacts.

Citation:

Farquharson, L. M., R. M. Buzard, D. H. Mann, and B. M. Jones. 2019. Coastal Dynamics in Bering Land Bridge National Preserve and Cape Krusenstern National Monument. *Alaska Park Science* 18(1):76-83.

Coastal areas of Bering Land Bridge National Preserve (NPres) and Cape Krusenstern National Monument (NM) coastline (Figure 1) possess complex geomorphologies (Figure 2) where factors that shape the coastline, like waves and sediment supply, act across many different temporal and spatial scales. Sea ice, Arctic Ocean storm tracks, tides, and constantly changing wave and wind patterns impact ice-rich permafrost lowlands, deltas, lagoons, and barrier islands (Figure 2). This creates a dynamic system with a diverse morphology that is in constant flux. As ice-rich permafrost bluffs erode, the sediment is deposited on sand spits. Barrier island and beach ridge morphology shifts as sea levels rise and storm surges frequently redistribute large volumes of sediment. The diverse morphology and complexity of these coastal systems make accurately predicting future changes a challenge for land managers. The objective of this study was to explore how the coastlines of Bering Land Bridge NPres and Cape Krusenstern NM have changed over the past 60+ years, especially in the context of ongoing sea ice decline.

Climate Change and its Potential Impact on the Coast

The coastlines in Bering Land Bridge NPres and Cape Krusenstern NM extend for over 300 miles (480 km; Figure 1). Arctic coastlines differ from those at lower latitudes because they are influenced by the presence of sea ice and permafrost (ground

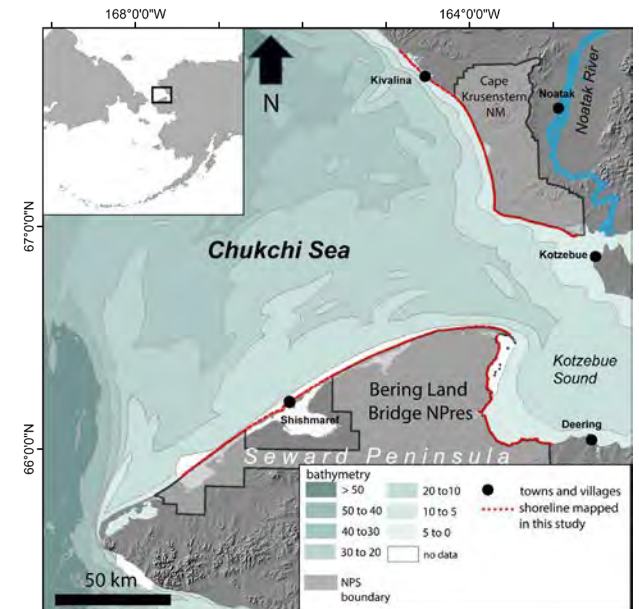


Figure 1. The study region with Bering Land Bridge NPres and Cape Krusenstern NM outlined in grey. Modified from Farquharson et al. 2018.

that stays frozen year-round). Extensive reaches of the coastline in the two parks are characterized by ice-rich permafrost bluffs (Figure 2). Permafrost in the coastal zone influences coastal processes, primarily by facilitating the presence of large volumes of ground ice that support the ground surface and bind together bluff sediment (Figure 3). When this ice melts, the surface subsides and the sediment previously cemented by ice loses strength.



Figure 2. Types of coastline found in Bering Land Bridge NPres and Cape Krusenstern NM. (A) sand dunes along the low laying barrier islands, (B) ice-rich permafrost bluffs, (C) sand dunes on Cape Espenberg Spit, (D) a lagoon and gravel barrier, (E) ice-rich permafrost bluffs fronted by a gravel beach, (F) beach ridge plain. Modified from Farquharson et al. 2018.

As the Arctic warms, rising air and water temperatures are causing permafrost to thaw, which is causing some Arctic coastlines to erode more rapidly (Barnhart et al. 2014, Günther et al. 2015, Jones et al. 2009). Mean annual ground temperatures in Bering Land Bridge NPres are projected to increase by up to 3°C by 2050 (Panda et al. 2016), and this is expected to cause an increase in the rate of thaw and degradation of ice-rich permafrost bluffs. Offshore warming in the ocean is also important. The surface temperature of the Chukchi Sea has risen by 0.5°C per decade since 1982 (Timmermans and Proshutinsky 2015). Warmer ocean water also increases the rate of thaw along ice-rich permafrost bluffs, a process known as *thermoerosion*.

The coastlines of Bering Land Bridge NPres and Cape Krusenstern NM are also closely tied to the dynamics of sea ice, which exerts a crucial control over coastal processes. When sea ice is present, it protects coastal bluffs from wave-driven erosion and inhibits sediment transport along the shore. When sea ice is absent, it leaves the coastline open to erosion and sediment transport. Climate change is now altering the sea-ice regime in the Bering and Chukchi seas quickly and radically. Arctic sea ice extent and thickness has been declining by >10 % per decade since satellite observations began in 1981 (Stroeve et al. 2012). Over the last 40 years in the southern Chukchi Sea, the period of time when ice is frozen to the shore (land-fast sea ice) has declined by approximately one week per decade (Mahoney et al. 2014). The decline of sea ice leaves shorelines exposed to waves and fall storms and increases the window of time that erosion and deposition can occur.

As the impacts of climate change are felt more and more in the Arctic, they are expected to affect numerous park resources. Bering Land Bridge NPres



Figure 3. Photograph showing an exposed ice wedge located close to the Bering Land Bridge NPres coastline. The ice-rich permafrost bluffs of the parks are composed of alternating blocks of frozen silt and massive ice bodies.

and Cape Krusenstern NM are rich in ecological, cultural, and geologic resources. These include unique habitats for Arctic plants and animals, as well as archaeological sites (Darwent et al. 2013, Giddings

1966) and paleoenvironmental archives that can help us unravel the mysteries of the Bering Land Bridge (Jordan and Mason 1999, Mason and Jordan 1993, Wetterich et al. 2012). The landscape also provides crucial subsistence resources for local communities.

Over the coming decades, effective management of park resources will require an understanding of the causes and rates of coastal change. One approach that can help us better assess how the coastline may change in the future is looking at historic rates of change. Using GIS-based tools (Thieler et al. 2009), aerial photographs taken in the 1950s, 1980s, and 2000s can be compared to satellite imagery acquired in the 2010s. We can then look at rates of coastal change and see how factors like sea-ice coverage may influence coastal dynamics. By understanding the behavior of the coastline over recent decades, and exploring the responses of the coastline to different environmental forcing factors, park managers and scientists can attempt to predict how these coasts are likely to change in the future.

Measuring Coastal Change

To understand how they change through time, we mapped shorelines using photographs and satellite images from different observation periods (Jones et al. 2009, Manley and Lestak 2012, Radosavljevic et al. 2016; Figures 4 and 5). Historical aerial images of these parks are available from 1950, 1980, and 2003 (Manley et al. 2007a and b), and we studied these in combination with high-resolution satellite images taken in 2014, thus providing a 64-year record of change. We followed change detection methods that have been successfully applied to previous coastal change studies (Jones et al. 2009, Radosavljevic et al. 2016). We first aligned images using geospatial software and then traced the edge of coastal bluffs along the shore in each image (Figure 4). This provided a set of points that could be compared through

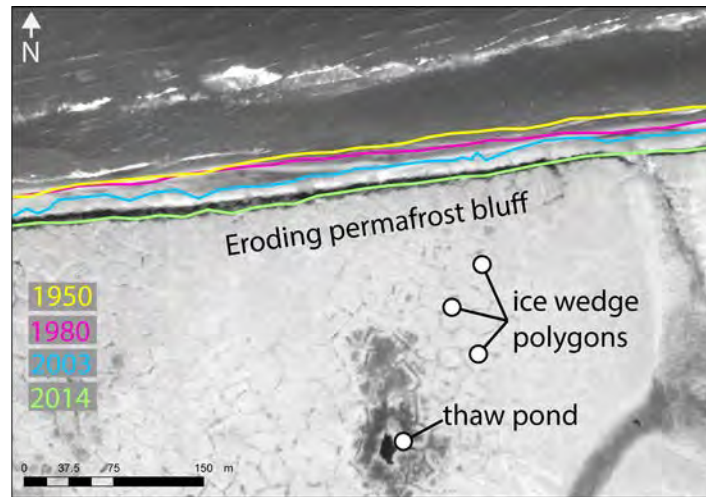


Figure 4. Historic shorelines mapped along a stretch of ice-rich permafrost bluff in Bering Land Bridge NPRES. Digital Globe WorldView2 imagery provided by DigitalGlobe, Inc.

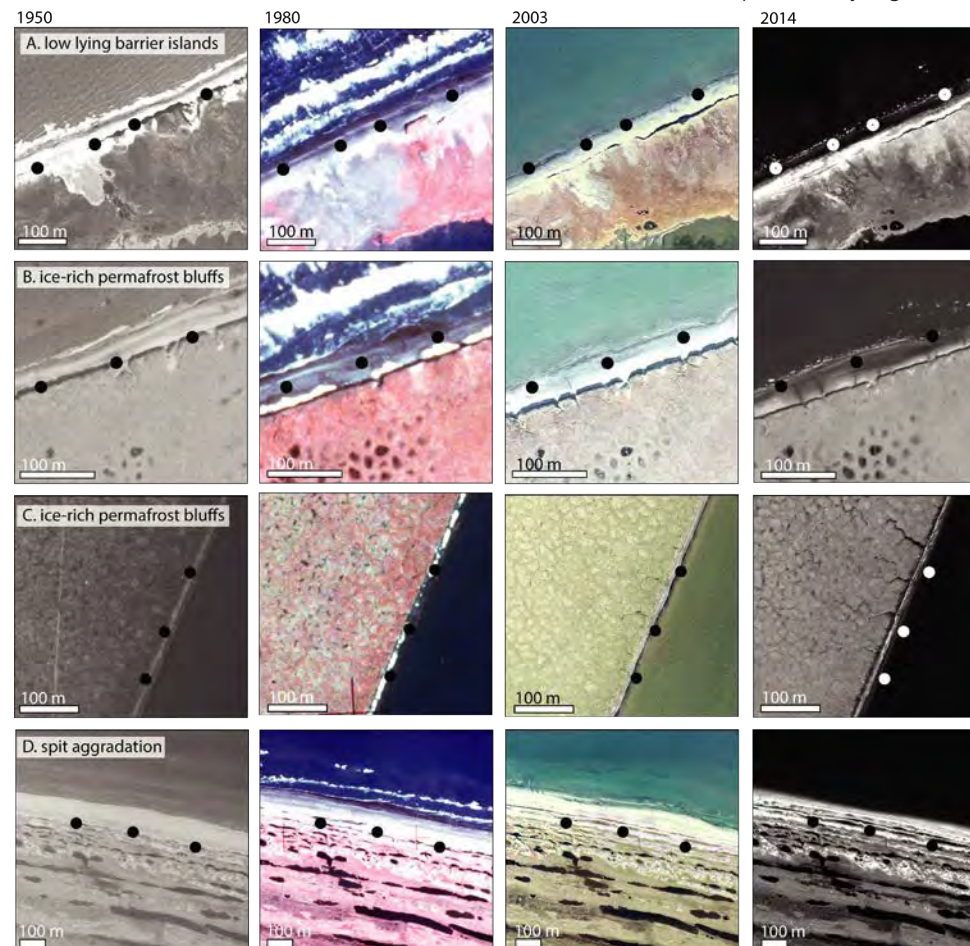


Figure 5. Historical imagery used and examples of coastal change from Bering Land Bridge NPRES. Row A: low-lying barrier islands, Rows B and C: ice-rich permafrost bluffs, Row D: aggradation of Cape Espenberg Spit.

time using the ArcMap Digital Shoreline Analysis System extension (Thieler et al. 2009) and allowed us to explore how much the coastline had changed (Figure 2). Another method used to monitor change is to compare elevation data sets from different time periods. We used high-resolution elevation data sets to measure changes in geomorphology between 2003 and 2016. To make sure the digital measurements were correct, we conducted field surveys at long-term monitoring sites in both parks. At each site, we measured the distance between the permanently installed survey markers and the edge of the permafrost bluff, beach ridge, or foredune, and reported any notable geomorphological changes, such as subsidence.

To understand coastal change in Bering Land Bridge NPRES and Cape Krusenstern NM, it is important to identify when the coast is sea ice free each year because this determines how long the coast is exposed to erosion. To explore how sea ice coverage has changed in the Chukchi Sea adjacent to the parks, we compiled records of sea ice extent and duration from satellite images of sea ice by the [National Snow and Ice Data Center](#) (NSIDC). We then calculated how many days the ocean was ice free and thus exposing the coast to erosion, and how many days the wave fetch (the distance waves travel before encountering land) exceeded 31 miles (50 km). Wave fetch is an important parameter for coastal change because waves gain energy as they travel over longer distances.

Changes in Sea Ice

Our analysis revealed that the ice-free season along the study shores has increased by approximately 10 days per decade since satellite observations began in 1980. This is because sea ice broke up earlier in the spring and formed later in the fall. The change in sea ice duration means that

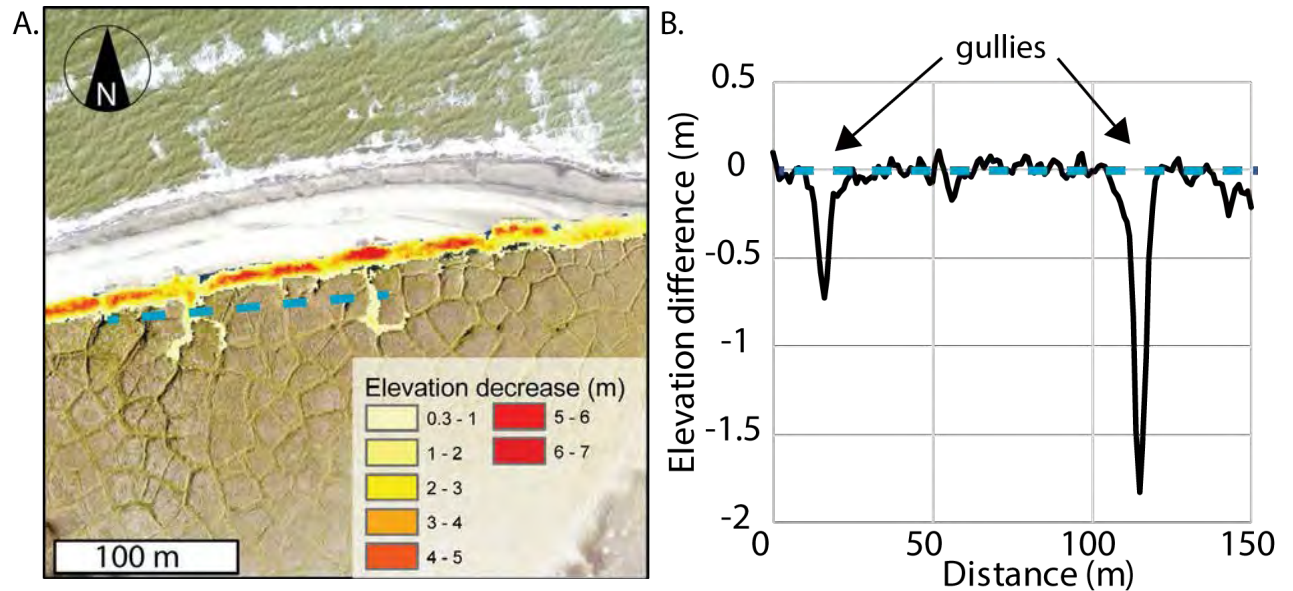


Figure 6. Measurements of surface subsidence due to permafrost degradation and the formation of thermoerosion gullies between 2003 and 2016 in Bering Land Bridge NPRES. Rates of erosion appeared to be more rapid where gullies were present. A. The black line indicates where the topographic profile in B is located. Areas in red indicate more elevation change (up to 7 m). B. A graph showing the change in elevation along the transect. The thermoerosion gullies are nearly 2 m in depth (Farquharson and Jones 2017).

the coastlines of Bering Land Bridge NPRES and Cape Krusenstern NM were exposed to waves and potential storms for, on average, one extra day every year, which over the course of the study period means that more than a month has been added to the erosion season (Farquharson et al. 2018). Sea ice extent during the summer and fall storm season also declined, meaning that waves had a greater distance across which to gain erosive force. As a result, this coastline has experienced more powerful waves over increasingly longer periods each year.

By looking at aerial photographs and satellite images, we can detect several different processes driving coastal change. Along permafrost bluffs, warm air and ocean water melt the ice binding the permafrost soils, causing sediment to slough off bluffs onto the beaches. In addition, the top-down

thaw of ice wedges results in thermoerosion and the formation of gullies (Figure 6), which then exacerbate bluff erosion. On the shoreface, coarser sediment like sand and pebbles is transported alongshore while finer-grained material is pulled offshore into deeper water. We found that the processes driving erosion are different where the coast consists of barrier islands. Longshore-transported sediment builds spits and feeds the downdrift growth of barrier islands. During storm events, when waves have more energy, sand is washed across barrier islands to form overwash fans in lagoons.

We discovered that the rates of coastline change in Bering Land Bridge NPRES and Cape Krusenstern NM have varied over the last 60 years. Although both erosion (sediment loss) and accretion (sediment gain) have taken place, erosion has been the

dominant process (Table 1). In Bering Land Bridge NPres, average rates of change were -2.2 feet/year, -0.8 feet/year, and -2.2 feet/year (-0.68 m/yr, -0.26 m/yr, and -0.68 m/yr) between 1950 and 1980, 1980 and 2003, and 2003 and 2014, respectively (Figure 7). The negative numbers indicate that the shoreline, on average, moved inland. In Cape Krusenstern NM, average rates of change were slower: -1.6 inches/year, -8.7 inches/year, and -5.1 inches/year (-0.04 m/yr, -0.22 m/yr, and -0.13 m/yr) between 1950 and 1980, 1980 and 2003, and 2003 and 2014, respectively (Figure 8). We also found that the rates of change differed along different sections of coastline, such as along barrier islands versus permafrost bluffs. In Bering Land Bridge NPres, the most rapidly changing type of coastline has been the low-lying barrier islands. The mean rate of change for these features was highest between 2003 and 2014, where rates reached up to -5 feet/year (-1.53 m/yr). Ice-rich permafrost bluffs changed much more slowly, with a maximum rate of only -1.7 feet/year (-0.51 m/yr) between 1950 and 1980.

The observed range in rates of change shows just how complicated the coastal systems of Bering Land Bridge NPres and Cape Krusenstern NM are. This variability suggests it is difficult to predict how ongoing sea ice decline will influence overall rates of coastal change. In addition to documenting a wide variability in mean rates of change, we also found that the range of rates (difference between minimum and maximum rates) of change were greatest between 2003 and 2014 in both Bering Land Bridge NPres and Cape Krusenstern NM (Table 1).

Uncertain Futures for the Coastlines

The coasts of Bering Land Bridge NPres and Cape Krusenstern NM have become more dynamic over the last 60+ years (Figures 7 and 8, Table 1), probably due, in part, to an increase in the open-water season.

Table 1. Rates of change between 1950 and 1980, 1980 and 2003, and 2003 and 2014 for Bering Land Bridge NPres and Cape Krusenstern NM. Rates of change are provided in meters per year (m/yr).

	Observation Period		
	1950 to 1980 (m/yr)	1980 to 2003 (m/yr)	2003 to 2014 (m/yr)
Bering Land Bridge National Preserve			
Mean rate of change	-0.7	-0.3	-0.7
Range of change rates	2.6	2.0	4.8
Maximum erosion	-2.6	-2.0	-4.8
Maximum accretion	0.0	0.0	0.0
Cape Krusenstern National Monument			
Mean rate of change	0.0	-0.2	-0.1
Range of change rates	3.3	3.8	6.5
Maximum erosion	-1.1	-3.1	-3.6
Maximum accretion	2.2	0.8	3.0

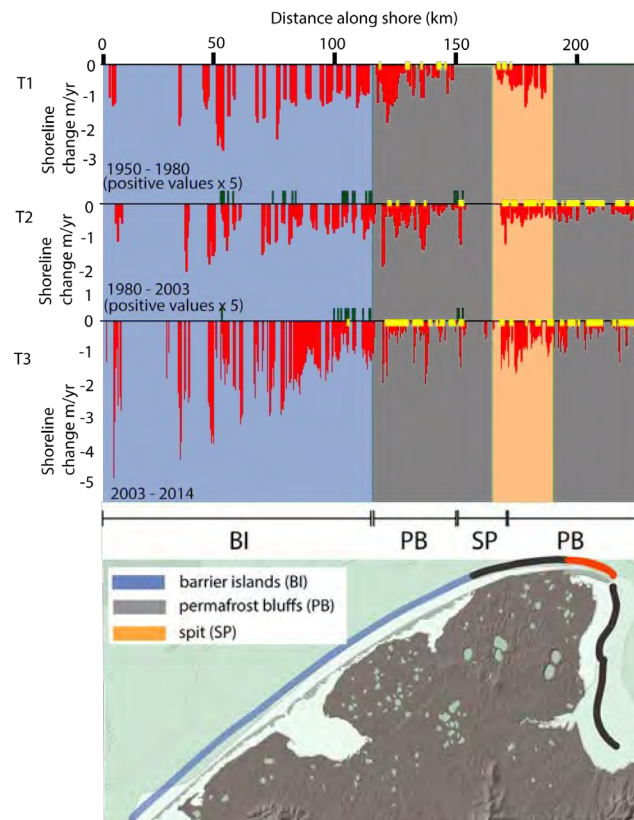


Figure 7. Shoreline changes (m/yr) in Bering Land Bridge NPres during the three study periods: 1950-1980, 1980-2003, and 2003-2014. Each column depicts a transect across the shoreline. Red columns extending below the 1950 baseline represent measured declines; yellow dots represent no change; green bars extending above the baseline represent measured accretion. In T1 and T2 the green bar height is increased by 5x to make them more visible. Yellow dots represent transects that were measured, but where no change was observed. Transects are arranged from southwest to northeast. Background shading corresponds to the color of the main coastal reaches shown on the map: blue = barrier island; grey = permafrost bluff; orange = spit. Modified from Farquharson et al. 2018.

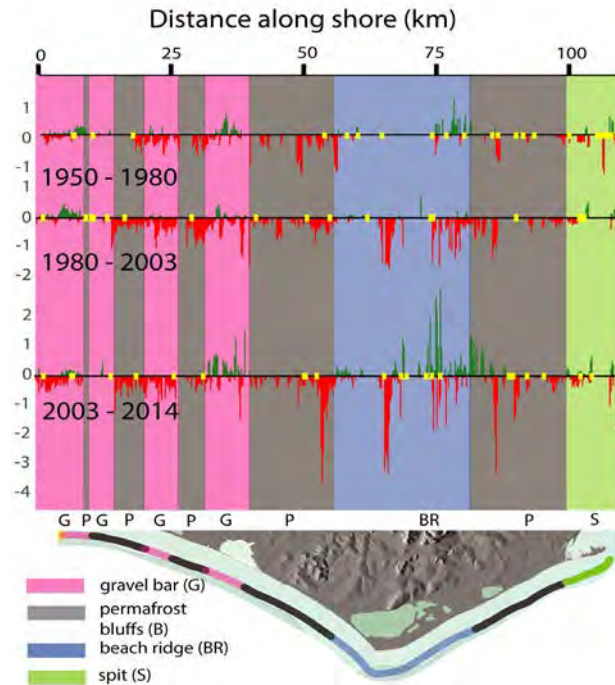


Figure 8. Shoreline change (m/yr) in Cape Krusenstern NM during each of the three study periods: 1950-1980, 1980-2003, and 2003-2014. Red columns extending below the 1950 baseline represent measured declines; yellow dots represent no change; green bars extending above the baseline represent measured accretion. Transects are arranged northwest to southeast. Colors in the background correspond to the main types of coastal geomorphology: pink = gravel bars; grey = permafrost bluffs; blue = welded gravel bars and beach ridges; green = spit. Modified from Farquharson et al. 2018.

Coastal landforms show no sign of being suddenly altered or radically modified by the changing sea ice regime; however, as the open-water season continues to lengthen, and the permafrost in coastal bluffs warms, shoreline geomorphic processes in Bering Land Bridge NPRES and Cape Krusenstern NM may begin to change more rapidly. Shorelines now characterized by erosion may see erosion rates increase, and shorelines now experiencing sediment deposition may accrete more rapidly or convert to a new regime dominated by erosion. Despite such uncertainties, an understanding of how the coastline changed in the past, combined with further monitoring, can contribute to the effective management of coastal habitats and ecosystems, oil-spill response, marine debris collection, and the preservation of cultural artifacts within Bering Land Bridge NPRES and Cape Krusenstern NM.

Acknowledgements

This project was funded by the NPS Climate Change Youth Initiative Fellowship and the NPS Inventory & Monitoring Division in collaboration with NPS ecologist David Swanson. We thank China Kantner and Sara Grocott for field assistance and Arctic Backcountry Flying Service in Kotzebue for safe transport to the field. Additional support provided by the National Science Foundation OPP-1745369 grant. Constructive reviews from Chris Maio and David Swanson greatly improved this article.

REFERENCES

- Barnhart, K. R., R. S. Anderson, I. Overeem, C. Wobus, G. D. Clow, and F. E. Urban. 2014. Modeling erosion of ice-rich permafrost bluffs along the Alaskan Beaufort Sea coast. *J. Geophys. Res. Earth Surf.* 119: 1155-1179. <https://doi.org/10.1002/2013JF002845>
- Darwent, J., O. K. Mason, J. F. Hoffecker, and C. M. Darwent. 2013. 1,000 years of house change at Cape Espenberg, Alaska: A case study in horizontal stratigraphy. *Am. Antiq.* 78: 433-455.
- Farquharson, L. M., D. H. Mann, D. K. Swanson, B. M. Jones, R. M. Buzard, and J. W. Jordan. 2018. Temporal and spatial variability in coastline response to declining sea-ice in northwest Alaska. *Marine Geology* 404: 71-83.
- Farquharson, L. and B. M. Jones. 2017. Changes in coastline elevation along the southern Chukchi Coast between 2004 and 2016, in: American Geophysical Union Fall Meeting 2017.
- Giddings, J. L. 1966. Cross-dating the archeology of northwestern Alaska. *Science* 80(153): 127-135.
- Günther, F., P. P. Overduin, I. A. Yakshina, T. Opel, A. V. Baranskaya, and M. N. Grigoriev. 2015. Observing Muostakh disappear: Permafrost thaw subsidence and erosion of a ground-ice-rich Island in response to arctic summer warming and sea ice reduction. *Cryosphere* 9: 151-178. <https://doi.org/10.5194/tc-9-151-2015>
- Jones, B. M., C. D. Arp, M. T. Jorgenson, K. M. Hinkel, J. A. Schmutz, and P. L. Flint. 2009. Increase in the rate and uniformity of coastline erosion in Arctic Alaska. *Geophys. Res. Lett.* 36(3), L03503. <https://doi.org/10.1029/2008gl036205>

Jordan, J. W. and O. K. Mason. 1999.

A 5,000-year record of intertidal peat stratigraphy and sea level change from northwest Alaska. *Quat. Int.* 60(1): 37-47. [https://doi.org/10.1016/S1040-6182\(99\)00005-1](https://doi.org/10.1016/S1040-6182(99)00005-1)

Mahoney, A. R., H. Eicken, A. G. Gaylord, and R. Gens. 2014.

Landfast sea ice extent in the Chukchi and Beaufort Seas: The annual cycle and decadal variability. *Cold Reg. Sci. Technol.* 103: 41-56. <https://doi.org/10.1016/j.coldregions.2014.03.003>

Manley, W. F. and L. R. Lestak. 2012.

Protocol for high-resolution geospatial analysis of coastal change in the Arctic Network of Parks. National Park Service, Fort Collins, Colorado.

Manley, W. F., D. M. Sanzone, L. R. Lestak, and E. G. Parrish. 2007a.

High-resolution orthorectified imagery from approximately 1980 for the Coastal Areas of Bering Land Bridge NP (BELA) and Cape Krusenstern NM (CAKR), Northwest Alaska, report, Arctic Network Invent. and Monit. Program, Natl. Park Serv., Fairbanks, Alaska.

Manley, W. F., D. M. Sanzone, L. R. Lestak, E. G. Parrish, D. M. Sanzone, and L. R. Lestak. 2007b.

High-resolution orthorectified imagery from approximately 1950 for the coastal areas of Bering Land Bridge NP (BELA) and Cape Krusenstern NM (CAKR), northwest Alaska, report, Arctic Network Invent. and Monit. Program, Natl. Park Serv., Fairbanks, Alaska.

Mason, O. K. and J. W. Jordan. 1993.

Heightened north pacific storminess during synchronous late holocene erosion of northwest Alaska beach ridges. *Quat. Res.* 40: 55-69. <https://doi.org/10.1006/qres.1993.1056>

Panda, S., V. Romanovsky, and S. Marchenko. 2016.

High-resolution permafrost modeling in the Arctic Network National Parks, Preserves, and Monuments. Natural Resource Report NPS/ARC/NRR—2016/1366. National Park Service, Fort Collins, Colorado. <https://doi.org/10.13140/RG.2.2.18127.89767>

Radosavljevic, B., H. Lantuit, W. Pollard, P. Overduin, N. Couture, T. Sachs, V. Helm, and M. Fritz. 2016.

Erosion and Flooding—Threats to Coastal Infrastructure in the Arctic: A Case Study from Herschel Island, Yukon Territory, Canada. *Estuaries and Coasts* 39: 900-915. <https://doi.org/10.1007/s12237-015-0046-0>

Stroeve, J., M. Serreze, M. Holland, J. Kay, J. Malanik, and A. Barrett. 2012.

The Arctic's rapidly shrinking sea ice cover: a research synthesis. *Clim. Change* 110: 1005-1027. <https://doi.org/10.1007/s10584-011-0101-1>

Thieler, E. R., E. A. Himmelstoss, J. L. Zichichi, and A. Ergul. 2009.

The Digital Shoreline Analysis System (DSAS) version 4.0—an ArcGIS extension for calculating shoreline change. U.S. Geological Survey.

Timmermans, M. L. and A. Proshutinsky. 2015.

Sea surface temperature, in: Blunden, J., Arndt, D. (Eds.), State of the Climate in 2014. *Bulletin of the American Meteorological Society* pp. ES1-ES32.

Wetterich, S., G. Grosse, L. Schirrmeister, A. A. Andreev, A. A. Bobrov, F. Kienast, N. H. Bigelow, and M. E. Edwards. 2012.

Late Quaternary environmental and landscape dynamics revealed by a pingo sequence on the northern Seward Peninsula, Alaska. *Quat. Sci. Rev.* 39: 26-44. <https://doi.org/http://dx.doi.org/10.1016/j.quascirev.2012.01.027>

TSUNAMI EVACUATION AREA
IN CASE OF EARTHQUAKE, STAY
ON HIGH GROUND OR INLAND

TSUNAMI
EVACUATION
ROUTE



Penny Hardy

Community Center

13915 Lowell Point Road

BEAR CR

Addressing Earthquake and Tsunami Hazards in Alaska Parks

Michael West, Ian Dickson, and Lea Gardine, Alaska Earthquake Center, Geophysical Institute, University of Alaska

The forces that produce hazards such as earthquakes and tsunamis are as much a part of the parks—and the parks' beauty—as wildlife and glaciers. Engaging visitors in learning about and preparing for these hazards serves the dual functions of increasing park safety while also enriching the visitor experience.

Citation:

West, M. I. Dickson, and L. Gardine. 2019. Addressing earthquake and tsunami hazards in Alaska parks. *Alaska Park Science* 18(1):84-91.

Alaskans who lived through the 1964 magnitude 9.2 Great Alaska earthquake described shaking so fierce that it felt like being tossed in a boat on the sea. This shaking triggered landslides, avalanches, and ground failures all across southern Alaska. The tsunamis that ensued were responsible for more than one hundred casualties. This pattern of violent earthquakes followed by deadly tsunamis has been a constant throughout Alaska's historical record (Lander 1996). Diaries from the Russian period describe canoes full of men lost and villages washed away by tsunamis after strong earthquakes. Many older stories passed down by Alaska Native groups contain themes of violent ground shaking and waves washing people into the ocean.

An event comparable to 1964 would play out differently now (West et al. 2014). Alaska is far more populated and has infrastructure and critical facilities only dreamed of fifty years ago. But the earthquake remains a useful case study for Alaska's national parks. Away from the coast, many visitors and employees are likely to be outside or in relatively modest structures where most should be fairly safe, even though park infrastructure might be severely damaged. In coastal parks, the opposite is true. Alaska's fjords, beaches, and bays—the very features that draw visitors—are some of the most dangerous places a person could be when a major quake strikes.

This illustrates two points about earthquake hazards in Alaska's national parks. First, the parks'

hazards are as different as the parks themselves. Second, earthquake hazards are inseparable from what makes the parks valuable in the first place. Southeast's dramatic coastline and the Denali Massif's incredible relief are products of the forces that shaped and continue to shape the parks. Earthquakes and tsunamis are as much a part of what makes the parks wild as bears and wolves. Just like dangerous wildlife, the perspective of park managers should include not only how to keep people safe, but also how to convey awe for the powerful role that these forces play in the park.

In this article, we will offer a brief outline of Alaska's earthquake activity as it relates to the national parks, followed by a discussion of preparedness for earthquake and tsunami disasters. We will also point to some resources that can help park managers to plan, and we will describe an approach to contextualize the hazards that we feel might connect with visitors.

Earthquakes in Alaska

To understand earthquakes in Alaska's parks, start by looking at the landscape itself (Koehler 2013). On a map of Glacier Bay National Park and Preserve, you will see the Fairweather Fault marked by a deep trough that parallels the coast and separates the coastal foothills from the Fairweather Range. Looking at this feature, it is easy to imagine the tectonic plate under the Pacific Ocean sliding north beside Alaska's panhandle. Motion along this

Tsunami evacuation signs at Lowell Point, near Kenai Fjords National Park. In steep fjords, where landslide-generated tsunamis can strike within minutes of an earthquake, public education and marked evacuation routes are critical to survival. Photo courtesy of Alaska Earthquake Center

fault is quite fast, about two inches per year, so the Queen Charlotte-Fairweather Fault system regularly produces major strike-slip earthquakes in the magnitude 8 range. To give an idea of how active this fault is, the 2013 magnitude 7.5 earthquake near Craig re-ruptured a part of the fault that had previously ruptured as recently as 1949, in a magnitude 8.1 earthquake (Holtkamp and Ruppert 2015).

To the north, the intersecting mountain ranges in Wrangell-St. Elias National Park and Preserve reveal the complex interactions of this plate impinging on southcentral Alaska. This interaction is complicated by the so-called Yakutat block—a piece of ocean crust carried northward along the Fairweather Fault that is being slowly scraped off onto North America. In 1899, this collision produced two magnitude 8 earthquakes near Yakutat Bay, triggering tsunamis and causing as much as 45 feet (13 m) of permanent uplift. The entire area is extremely active seismically, and even small earthquakes there can trigger huge landslides capable of setting off megatsunamis in the region's narrow fjords and bays.

Continuing north, the Yakutat block collision plays a role in driving the Denali Fault that connects Wrangell-St. Elias to Denali National Park and Preserve in a great mountainous arc. One-hundred-ninety miles (306 km) of the central part of the fault ruptured in 2002 together with segments of neighboring faults. The combined magnitude 7.9 earthquake caused heavy damage to sections of the Richardson Highway and Tok Cutoff and triggered numerous landslides and avalanches, but caused no major injuries. The western end of the fault, which runs through Denali National Park and Preserve, did not rupture in 2002 but can be expected to produce a comparable earthquake in the future.

So far, our tour of Alaska tectonics has skirted around the best-known hazard. From just north

of the panhandle all of the way west to Attu Island, every southern and coastal National Park Service location is at risk from great earthquakes along the megathrust fault where the Pacific Plate subducts under the North American Plate. These earthquakes can exceed magnitude 9 and generate devastating, Pacific-wide tsunamis. In addition to these infrequent events, the subduction zone generates many strong, shallow earthquakes along crustal faults as well as deeper earthquakes within the subducting slab. The 2018 magnitude 7.1 Anchorage earthquake is a recent example of the latter.

Elsewhere in the state earthquakes occur in places where many Alaskans might not expect them (Koehler et al. 2018). Over the last century, magnitude seven earthquakes have struck across the Fairbanks region, and another magnitude seven struck near Huslia (Davis 1960), south of Kobuk Valley National Park and Gates of the Arctic National Park and Preserve. Magnitude six earthquakes have occurred on the Seward Peninsula and the Norton Sound coast. In 2014, a vigorous swarm roughly between Noatak National Preserve and Red Dog Mine persisted for months and produced five magnitude 5.8 earthquakes. These proved to be more of a nuisance than a danger, but the initial quakes did cause minor structural damage in Noatak.

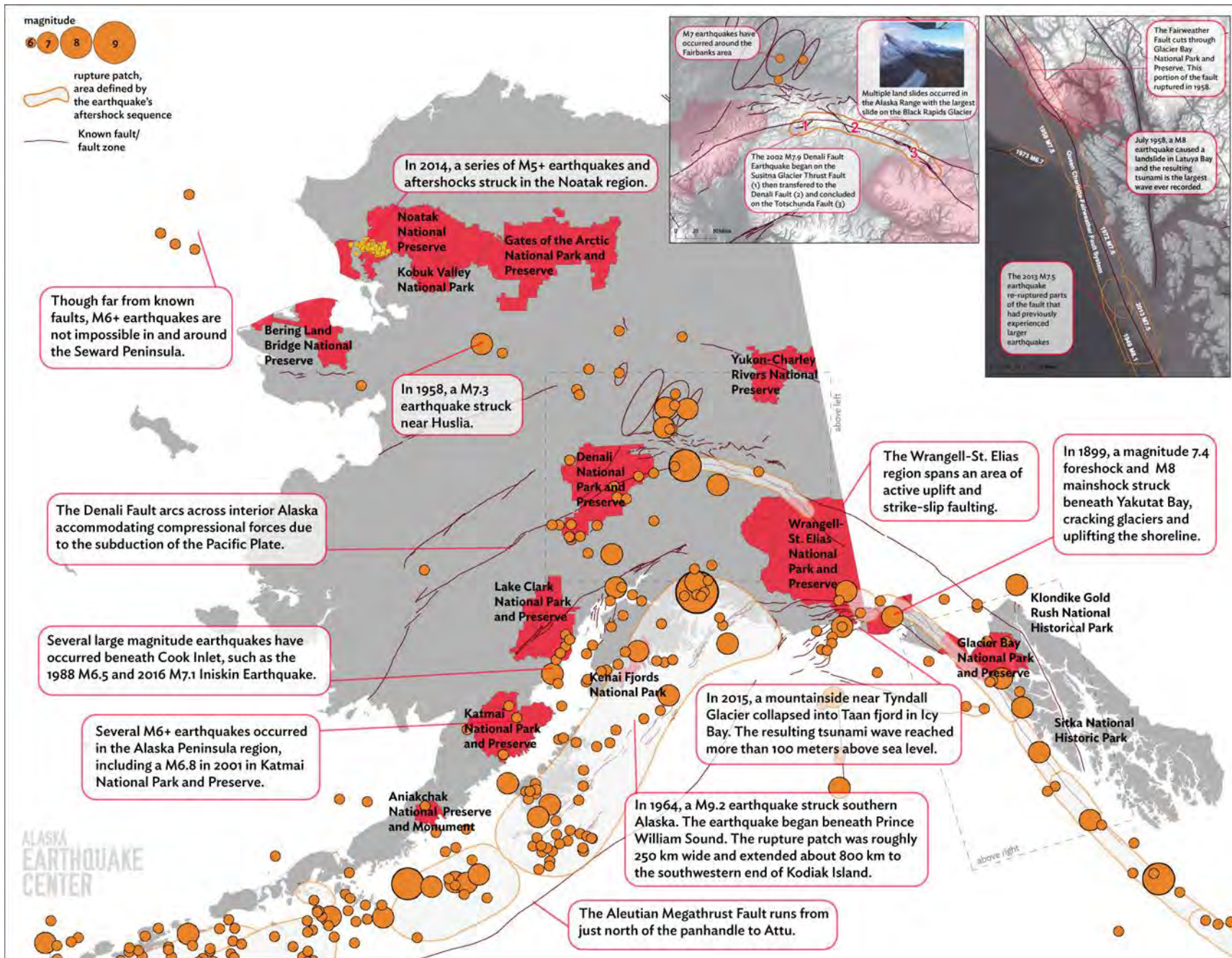
Despite this history, there are large gaps in our knowledge of seismic hazard, especially in western and northern Alaska. Because they are more sparsely populated and less seismically active than southern Alaska, the scientific community has historically put far less effort and resources into researching and monitoring them—though that has been changing recently. Researchers continue to investigate and assess the hazards in each of these regions. But the earth continues to surprise us as well with events that were not previously on our radar.

Preparing for Earthquakes in the Parks

Not only can damaging earthquakes happen at any time, but they do, and frequently. In the half century following 1964, Alaska has been generally lucky. Recent offshore magnitude 7.9 events have not generated deadly tsunamis. The 2002 Denali fault earthquake caused damage but no loss of life, and the magnitude 7.5 Craig earthquake occurred far enough offshore that it had only modest impact. The most impactful earthquake in recent time is unquestionable the 30 November 2018 earthquake north of Anchorage. Despite considerable damage, Alaska fared comparatively well considering the strength of shaking. There are clear demonstrations from this event about the important role of building codes and public education campaigns over the years prior to the earthquake. The impact was also lessened by the location of the earthquake which was nearly 31 miles (50 km) below the surface. Any of these earthquakes could have been devastating if they had happened closer to towns or cities or had they triggered tsunamis. In the middle of the last century, earthquakes in 1946, 1958, and 1964 all caused loss of life in or outside of Alaska.

Given this frequency, park managers should understand that there is a realistic chance they will be part of a disaster response during their careers. Its strikes us as prudent to include this specifically in staff training.

There are a lot of buzz words in emergency management, but the concepts are straightforward and can be lumped into two categories: (i) reducing the risks before disasters occur, and (ii) building resilience to respond and bounce back when they do. By far, the lowest hanging fruit is identifying and reducing vulnerabilities. For parks, this means assessing facilities for dangers they might pose to occupants and seeking ways to reduce damage to



A sample of earthquake history and features relevant to National Parks in Alaska. See legend for details. Data sources include the Alaska Earthquake Center historical catalog of earthquakes and the Alaska Division of Geological and Geophysical Surveys quaternary fold and fold database (Koehler 2013).



Kageet Point in Wrangell-St Elias National Park and Preserve was largely stripped of trees by the 2015 Taan Fiord megatsunami. These events may be happening more often as retreating glaciers destabilize steep mountain slopes. Photo courtesy of Chris Larsen, University of Alaska Fairbanks Geophysical Institute

those facilities. This includes buildings, bridges, docks, and any type of precariously perched, or aerial, infrastructure. While close inspection can at

times turn up significant structural short-comings, more frequently the fixes will be easy and economical such as buttressing fuel containers, securing building frames to their foundation, or anchoring cabinets, shelving, and computers in place. Administrative facilities, though perhaps less glamorous than other National Park Service (NPS) assets, should not be overlooked. These facilities play essential roles during the response effort, but only if they weather the strong shaking and retain their core

capabilities—electricity, heat, water, phone, internet, transportation, etc. Managers should be particularly attuned to the secondary impacts of strong shaking. Soil failure, slumping, landslides and avalanches are common risk multipliers during earthquakes. These factors may be particularly acute for some NPS facilities located in remote and dramatic settings.

The Federal Emergency Management Agency (FEMA) promotes an economical method for evaluating buildings called Rapid Visual Screening (RVS). The RVS approach looks at factors such as age and type of construction to identify vulnerabilities and prioritize improvements. Rapid Visual Screening does not eliminate the need for more in-depth assessment, but it acts as a sort of triage for determining which facilities should be prioritized. RVS results can also provide strong arguments when seeking funding to upgrade or retrofit facilities. Under the leadership of the Alaska Seismic Hazards Safety Commission, many of Alaska's schools have been assessed in the last few years using the RVS method, at a cost of under \$1,000 per building (State of Alaska 2019).

Many different activities can help build resilience. Developing written plans for responding to earthquakes, creating inspection checklists, training staff, and educating visitors are all excellent steps toward building resilience. Realistic planning requires imagining what scenarios are likely. What if an earthquake renders park roads impassable for days? What happens when a park's administrative offices lose power or become unsafe? Consider distant earthquakes as well. For example, extensive damage in Southcentral could disrupt deliveries and leave visitors stranded at parks that were otherwise unaffected by an earthquake. Envision as many plausible scenarios as possible. Earthquakes consistently surprise us. In 1964, nobody anticipated that Alaska would experience the second largest

earthquake ever recorded. But the strength of the magnitude 7.9 Denali fault earthquake 16 years ago was a surprise too, as was the January 2018 magnitude 7.9 offshore Kodiak. One fact we can almost certainly count on is that the next big earthquake will be different from what we have seen historically.

In a significant disaster response, NPS personnel would presumably fall under the interagency coordination defined by FEMA's Incident Command System (ICS). The numerous ICS certification courses available, both on-line and in-person, give managers an easy way to provide professional development opportunities for staff while simultaneously enhancing NPS's earthquake planning and response.

No disaster response is perfect, and even the best planning will need to be augmented by considerable improvisation. Painful as these lessons can be, building resilience is an iterative process in which the lessons of each disaster (or disaster averted) help us to build and plan more effectively for the next one.

Preparing for Tsunamis in the Parks

The first step is to recognize that most, though not all, tsunamis will come as part of the aftermath of an earthquake. Many people's ability to respond to a tsunami may be greatly hampered by the earthquake itself. This might include computers broken on the floor, inoperable phone lines, or essential staff who left to go check on family. As 1964 demonstrated so clearly, earthquakes and tsunamis are often part of the same bad day.

On paper, the process of identifying tsunami hazards is relatively clear. People and facilities are either located within a tsunami hazard zone, or they are not. Risk reduction is largely accomplished by minimizing the permanent assets inside a tsunami hazard zone. One exception to this is

the construction of so-called vertical evacuation structures. These structures can provide good alternatives to evacuation in places where there are significant numbers of people and less-than-ideal evacuation routes.

Investing in response efforts is particularly valuable for tsunamis. Unlike many hazards, in some cases we are aware of tsunamis minutes to hours before they strike. While there are not many response activities that can protect buildings and facilities, there is considerable potential to save lives if response plans can be executed rapidly. Response efforts should be two-pronged. In some situations there may be a formal tsunami warning notice distributed by the National Oceanic and Atmospheric Administration (NOAA). If so, it is imperative that managers have pre-determined plans that can be put into motion immediately. But many tsunami incidents may not be preceded by an official warning. The second prong of the response is to teach staff as well as visitors the warning signs of potential tsunamis in advance (e.g., ground shaking that is "strong and long," waters receding or advancing very quickly, loud rumbles.)

Maritime traffic may be where response pays off the most for many Alaska parks. Narrow fjords, inlets, and channels can amplify ocean currents created by passing tsunamis. Though the waves may not be high, the currents they create can far exceed anything occurring from tides or storms. For kayakers, fisherman, day-tours, and cruise ships, even modest advance notice might be the difference between being in a safe location, and being subjected to powerful destructive currents. Marine-band radio provides some good options. As remote communications become increasingly common, even in the backcountry, NPS would do well to consider how to ensure tsunami warnings are disseminated and received as widely as possible.

Earthquake Resources

There are dozens of good resources and publications that could be valuable in developing park strategies for earthquakes and tsunamis. Most can be accessed through the portals below.

Alaska Seismic Hazards Safety Commission

People and references to connect with Alaska-specific resources.

<http://seismic.alaska.gov>

U.S. Geological Survey seismic hazard map

The seismic hazard map estimates the probability of strong ground shaking and underpins most building codes. Though currently lagging behind the lower 48, the 2007 effort is slated for update in the next few years.

<https://earthquake.usgs.gov/hazards/hazmaps>

Alaska tsunami hazard maps and publications

Published as a joint effort between several state and federal entities, these products details potential tsunami hazards in most coastal Alaska communities—though notably most of the parks are not included.

<http://dggs.alaska.gov/pubs/keyword/tsunami>

Alaska Earthquake Center

Up-to-the-minute reporting of current earthquakes, and information about historical events, and interactive tsunami hazard maps.

<https://earthquake.alaska.edu>

FEMA earthquake resources

Starting point for developing risk mitigation plans, rapid visual screening, and grant opportunities.

<https://www.fema.gov/earthquake>

One caveat to consider is that, to date, most of Alaska's tsunami hazard mapping efforts have focused on communities, not parks. However, the state has well-developed procedures and professionals who can work with managers to determine local needs and then execute advanced modeling to assess the particular tsunami hazards.

A second important caveat is that most tsunami resources, including warning systems and mapped hazard zones, have been developed for a range of well-understood scenarios generated by earthquakes and submarine landslides. Massive so-called mega-tsunamis, such as the 1,700-foot (518-m) Lituya Bay wave in 1958, or the Taan Fjord landslide and tsunami in 2016 are currently outside the scope of any systematic hazard assessment. It is tempting to treat these as "black swan" events that are so unique and rare that, like meteor impacts, we simply cannot plan for them. At some point, however, Alaska will need to come to terms with these mega-tsunami events. Alaska's coastal history makes quite clear that they are not rare, and there is some suggestion that the frequency of these events may be increasing as climate change and receding glaciers destabilize coastal terranes.

Engaging Park Visitors

NPS is unusually well-acquainted with operating facilities in hazardous environmental conditions. NPS is also experienced with how to educate and manage visitors exposed to environmental risks—extreme weather, limited emergency facilities, wildlife, etc. The authors presume that NPS is better positioned than most to approach earthquakes and tsunamis in a responsible, yet realistic, way. No amount of preparation can make these risks go away. They are just as inherently a part of the parks as glaciers, foxes, and lupine. Nearly every interpretive center in the parks addresses the profound role of

geology. Though we frequently describe geology as a set of slow inexorable processes, much of the landscape that underpins the parks has been created in short bursts of geologic activity manifest as earthquakes, tsunamis and their sibling hazards of landslides, avalanches, and volcanic eruptions.

These events are, arguably, part of the core value and beauty of most of Alaska's parks. NPS is perhaps uniquely positioned to educate people on the sharp distinction between natural hazards and natural disasters. Natural hazards are inexorable forces of nature that cannot be diverted or controlled, while natural disasters are a wholly human creation that result from our co-existence, and at times lack of respect, for the hazards. People, including park managers and park visitors, have the ability to keep natural hazards from becoming natural disasters. One example is the urgency of teaching people to self-evacuate from coastal areas when they feel strong shaking. Nothing people do will change the innate hazard of a tsunami. Yet they have considerable control over whether or not it becomes a disaster. In the hands of skilled interpretive staff, that simple message is full of teaching potential.

Most park visitors will never experience these events firsthand, just as most will never come face-to-face with a bear. Yet these hazards have the potential to be an important part of the park experience. The unmatched power displayed by earthquakes and tsunamis can captivate visitors like few other phenomena. Proactively engaging visitors in learning about and preparing for these hazards serves the dual functions of increasing park safety while also enriching the visitor experience. Knowing that these hazards exist, learning about their role in the ecosystem, and learning how to plan for and live amongst them, seems in perfect alignment with the mission of the National Park Service.

REFERENCES

Davis, T. N. 1960.

A field report on the Alaska earthquakes of April 7, 1958. *Bull. Seis. Soc. Am.* 50(4): 489-510

Holtkamp, S. and N. A. Ruppert. 2015.

A high-resolution aftershock catalog of the magnitude 7.5 Craig, Alaska, earthquake on 5 January 2013. *Bull. Seism. Soc. Am.* 105(2B). doi: 10.1785/0120140179

Koehler, R. D., G. A. Carver, and Alaska Seismic Hazards Safety Commission. 2018.

Active faults and seismic hazards in Alaska: Alaska Division of Geological & Geophysical Surveys Miscellaneous Publication 160, 59 p. Available at: <http://doi.org/10.14509/29705> (accessed 20 May 2019)

Koehler, R. D. 2013.

Quaternary Faults and Folds (QFF): Alaska Division of Geological & Geophysical Surveys Digital Data Series 3. Available at: <http://doi.org/10.14509/qff> (accessed 20 May 2019)

Lander, J. 1996.

Tsunamis affecting Alaska, 1737-1996. Boulder, CO. NOAA. Available at: <https://www.hsdll.org/?view&did=762299> (accessed 20 May 2019)

State of Alaska. 2019.

Alaska Seismic Hazards Safety Commission (listed by school district under 2015-2017). Available at: http://seismic.alaska.gov/presentations_reports.php (accessed 20 May 2019)

West, M. E., P. J. Haeussler, N. A. Ruppert, and J. T. Freymueller. 2014.

Why the 1964 Great Alaska Earthquake Matters 50 Years Later. *Seismological Research Letters* 85(2): 245–251, doi:10.1785/0220140020



An Earthquake Center seismic station and communications hub on MacColl Ridge in Wrangell-St. Elias National Park and Preserve. The park seismic network not only monitors earthquakes and helps forecast tsunamis, it can detect large landslides and glacial calving events. Photo courtesy of Chris Bruton, Alaska Earthquake Center



List of Contributors

Douglas A. Anderson, Engineering Geologist, Western Federal Lands Highway Division, Federal Highways Administration

Erin K. Bessette-Kirton, Physical Scientist, Geologic Hazards Science Center, U.S. Geological Survey

Eric Bilderback, Geomorphologist, Geologic Hazards and Disturbed Land, National Park Service

Richard M. Buzard, National Oceanic and Atmospheric Administration Digital Coast Fellow, Division of Geological and Geophysical Surveys, Alaska Department of Natural Resources

Cheryl Cameron, Geologist, Division of Geological and Geophysical Surveys, Alaska Volcano Observatory, Alaska Department of Natural Resources

Denny Capps, Geologist, Denali National Park and Preserve, National Park Service

Jeffrey A. Coe, Research Geologist, Geologic Hazards Science Center, U.S. Geological Survey

Ian Dickson, Communications Specialist, Alaska Earthquake Center, Geophysical Institute, University of Alaska Fairbanks

Anja Dufresne, Assistant Professor, Rheinisch-Westfälische Technische Hochschule Aachen University, Germany

Louise M. Farquharson, Graduate Research Assistant, Permafrost Laboratory, Geophysical Institute, University of Alaska Fairbanks

Lea Gardine, Outreach Coordinator, Alaska Earthquake Center, Geophysical Institute, University of Alaska Fairbanks

Marten Geertsema, Adjunct Professor, Ecosystem Science and Management, University of Northern British Columbia, Canada

Bretwood Higman, Executive Director and Co-Founder, Ground Truth Trekking

Chad A. Hults, Alaska Regional Geologist, National Park Service

Mylène Jacquemart, Geological Sciences Doctoral Candidate, University of Colorado Boulder

Benjamin M. Jones, Research Assistant Professor, Water and Environmental Research Center, Institute of Northern Engineering, University of Alaska Fairbanks

Debra Kurtz, Physical Science Programs Manager, Kenai Fjords National Park, National Park Service

Scott Lindsey, Alaska Regional Hydrologist, River Forecast Center, National Weather Service, National Oceanic and Atmospheric Administration

Michael Loso, Geologist, Wrangell-St Elias National Park and Preserve, National Park Service

Patrick Lynett, Professor of Civil and Environmental Engineering, Viterbi School of Engineering, University of Southern California

Daniel H. Mann, Associate Professor, Department of Geoscience, University of Alaska Fairbanks

Molly McKinley, Outdoor Recreation Planner, Denali National Park and Preserve, National Park Service

Katherine Mulliken, Geologist, Division of Geological and Geophysical Surveys, Alaska Volcano Observatory, Alaska Department of Natural Resources

Robert G. Schmitt, Geographer, Geologic Hazards Science Center, U.S. Geological Survey

Hans Schwaiger, Research Geologist, Alaska Volcano Observatory, U.S. Geological Survey

Dan Shugar, Assistant Professor of Geoscience, University of Washington and Director of the Water Sediment Hazards and Earth-surface Dynamics (waterSHED) Lab

Kristi Wallace, Research Geologist, Alaska Volcano Observatory, U.S. Geological Survey

Chris Waythomas, Research Geologist, Alaska Volcano Observatory, U.S. Geological Survey

Michael West, State Seismologist and Director, Alaska Earthquake Center, Geophysical Institute, University of Alaska Fairbanks

Gabriel Wolken, Geologist, Division of Geological and Geophysical Surveys, Alaska Department of Natural Resources

Alaska Park Science

ALASKA REGIONAL OFFICE
240 WEST 5TH AVENUE
ANCHORAGE, ALASKA 99501

akr_alaska_park_science@nps.gov
www.nps.gov/subjects/alaskaparkscience/index.htm

